Energy Harvesting from Slender FRP Pedestrian Bridges

Master Thesis

Rob Linssen
4014464

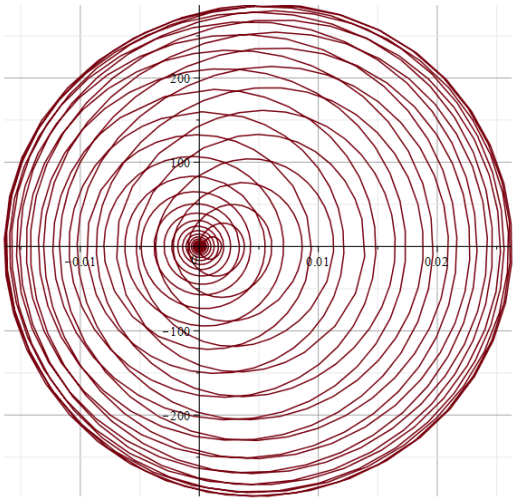

Delft University of Technology
Faculty of Civil Engineering and Geosciences
Structural Engineering
April 19, 2020

Thesis committee:
dr. F. van der Meer (chair)
dr. M. Pavlovic
dr. B. Sluys
ir. W.D. Schutte

Contents

List of Figures

List of Tables

Preface

Dear reader,

Before you lie the fruits of my labour over the past year: the Master thesis for my degree in Structural Engineering, specialization Structural Mechanics, at the Delft University of Technology. The research was carried out based on a proposal by the Rotterdam municipality's Engineering Office.

I am grateful to have been given the opportunity to work on a subject I found both challenging and intriguing: the dynamics of structures. To me, this field has always felt like a clear, visible manifestation of the fundamental laws and mathematics that usually remain hidden.

I feel like this project has taught me a lot, and I will gladly take with me this knowledge to the (uncertain, yet exciting) times that lie ahead in the 'real world' of jobs, mortgages and (possibly) suits. Hopefully, it will come in handy.

Writing this thesis - and, indeed, finishing my degree - has been a rather bumpy road from time to time. Despite that, or maybe because of that, it has been very rewarding, and I am very glad to have stuck with it over the years.

I do hope that this thesis is able to convey some of the beauty and wonder that lies within the realm of structural dynamics.

Rob Linssen
Utrecht
April 19, 2020

Abstract

The Rotterdam municipality is constantly busy replacing old footbridges that have reached their lifetime. Lately, this is done using modern materials, such as fibre-reinforced polymers (FRP). FRP is a relatively light-weight material that has a high yield strength, which allows for aesthetically pleasing, very slender designs. Governing for such designs is often the dynamic behaviour of the bridge: its eigenfrequency may very well lie within the 'critical range' of common footfall frequencies. If the step frequency of a pedestrian crossing the bridge lies near the eigenfrequency, a high dynamic amplification factor occurs: high vertical acceleration values for the bridge deck will occur, which means discomfort for the pedestrians.

In this thesis, a sustainable solution to that problem was sought. Rather than using pile foundations to clamp the bridgeheads (and thereby increase the eigenfrequency out of the critical range), it was investigated whether the kinetic energy can be harvested from the bridge. Ideally, this both dampens the vibrations and provides free, sustainable energy.

Several theoretical models were developed to describe the behaviour of an existing footbridge for which data is available. Adaptations to these models were made in the form of either extra dashpots or a tuned mass damper (TMD). In both cases, the dampers are regenerative, i.e. able to harvest energy.

It was shown that adding a TMD provides the best energy harvesting performance. From a practical perspective, it has some advantages as well, such as universal applicability. The parameters in the single degree of freedom (SDOF) model were optimized for maximum energy harvesting while still

keeping the vertical deck acceleration at reasonable levels. Finite element analysis largely confirmed these design choices, and showed that reducing the vibration levels is certainly possible with only a relatively small TMD. For a single person crossing at near-resonant footfall frequency only leads to a vertical acceleration of about 1.5 m/s.

The amount of energy that can be harvested in such a way is small but non-negligible: about 26 Joules worth of energy is estimated to be gained by an 'average' person crossing the bridge. This is taking into account system efficiency as well.

A literature study concerning real-world energy harvesting systems was performed, and showed the possibility to closely emulate the theoretical behaviour that was assumed for the regenerative dashpots. This can be done using electromagnetic dampers in combination with proper power electronics design.

Chapter 1

Introduction

This chapter starts off with a description of the current situation regarding the bridges in Rotterdam, including the problem statement. Secondly, both primary and secondary functions of footbridges are defined. Thirdly, two current solutions to fulfil those functions are briefly discussed, as well as a rough description of the desired novel solution. Next, the research question of this thesis is posed, along with a description of the approach that has been followed to answer this question. After that, the scope of the thesis is defined - what will, and what will *not* be investigated? Finally, a quick overview is given of all the models that were developed during this thesis, and where to find them in this report.

1.1 Current Situation and Problem Statement

The city of Rotterdam is well known for its multitude of small canals, as well as the large Maas river meandering through its center. Consequently, it is home to a plethora of bridges ranging from small ones that span only a couple of meters to the famous Erasmus-bridge, which has a main span of 278 meters.

There are hundreds of small bridges intended solely for pedestrians. Many

of those have been around for quite a while; they are often solid, simple, old-fashioned, and sturdy. An example of this is pictured in figure 1.1.

Now that many older pedestrian bridges approach the end of their lifespan, an opportunity for innovation arises. Using modern design methods and materials when replacing those bridges, solutions can be found that are both aesthetically pleasing and sustainable.

The Rotterdam municipality has expressed their interest in the possibilities offered by using fibre-reinforced polymer (FRP) bridges. Because of FRP's high strength, very slender constructions are possible. This is beneficial for both the aesthetics and the sustainability - less material is required. Furthermore, FRP bridges have a long lifespan and require hardly any maintenance during their lifetime.

Figure 1.1: The Burgemeester Roosbrug, Rotterdam, which was built in 1896. [1]

There is, however, a significant downside to designing slender bridges using FRP. Because of the slenderness, the beam stiffness will be relatively low. This causes the natural frequency of the bridge to decrease. If this frequency becomes low enough, resonance may occur in the dynamic range of pedestrians using the bridge. Resonance does not necessarily lead to failure, but it increases the vibration amplitude, which may cause discomfort and anxiety for anyone on the bridge deck.

Another thing to consider is that because FRP has a lower density than

steel, and because the bridge design is so slender, the self weight of the bridge becomes quite small. This leads to a high ratio between live load and dead load, which means that the vibration amplitude increases - again. [10]

The combination of these two effects makes the design of a slender FRP pedestrian bridge a more complex undertaking. The dynamic behaviour is not simple, and cannot be neglected.

1.2 Bridge requirements

In order to design a bridge, a primary set of requirements need to be identified. For a relatively small pedestrian bridge, those are the following:

- The bridge should allow for comfortable crossing; for example, vertical accelerations of the deck due to vibrations should not become too large
- The strength of the material should not be exceeded (no fracture should occur)
- The bridge should not be too steep, otherwise not everyone will be able to cross (e.g. elderly people using a walker)
- The approach area should not be too large, otherwise the bridge may not fit into the existing surroundings
- Sufficient space should be left open underneath the bridge, for inspection and maintenance purposes

Additionally, we can list some of the *desired* qualities of a bridge, which are not mandatory but optional. These are:

- The bridge should be as low-maintenance as possible
- The bridge should be aesthetically pleasing
- The bridge should be relatively cheap

- The bridge should be sustainable

All of the above points are quite straightforward, except for the desire for sustainability; some extra explanation is warranted there. It should be noted that sustainability is not a binary thing, but rather a continuous scale. The following points all *improve* the sustainability performance, and should therefore be strived for:

- Using little material
- Using material with a low environmental impact
- Proper design-for-lifetime; no 'over-designing'
- Recyclable at the end-of-life
- Minimal hindrance for local residents during construction

1.3 Possible bridge lay-outs

Now that both the strict requirements and the desirable qualities of a pedestrian bridge have been established, we should look at several possibilities to achieve those goals.

1.3.1 Regular layout

The go-to option for a pedestrian bridge is a classic, not-very-slender design, made of conventional materials like steel, timber or concrete. It is built with a shallow foundation, which has no foundation piles ('fundering op staal'). An example can be seen in figure 1.2. This bridge type looks like a simply supported beam or truss structure, but the 'hinges' on both supports actually act like rotational springs. Since the beam is not clamped, it needs to be non-slender in order for the eigenfrequency to be sufficiently high (i.e. outside the

Figure 1.2: Typical non-slender bridge with shallow foundation [2]

range of common pedestrian step frequencies). A more thorough explanation of this reasoning is given in Chapter 2.

A bridge like this can meet all the primary requirements. As for the secondary (desired) requirements, it may not perform as well. The bridge will be cheap, but it is not particularly sustainable, nor does it have a very long, maintenance-free lifetime. It may be designed with aesthetics in mind, but the design is always limited by the thick bridge deck required for conventional materials. Summarizing, it gets the job done, but it does not stand out in areas besides simplicity and cost-effectiveness.

1.3.2 Slender bridge on pile foundation

A more novel approach is the one employed when designing and building the so-called Exercitie-bridge, which is located in Rotterdam. This bridge is made out of FRP, with a span of about 19 meters, and was designed as a collaborative effort between the Rotterdam municipality's Engineering Office, and FiberCore Europe. It features a very slender FRP deck, using the InfraCore technology, with custom-designed parapets. A picture and a

technical drawing can be seen in figures 1.3 and 1.4.

This design is innovative in the way it deals with dynamic loading. Because of the pile foundation, the bridge will respond like it is clamped on both sides - at least for dynamic loading conditions. This leads to a higher eigenfrequency and also to a lower maximum deflection compared to a simply supported system.

While this type of bridge fulfils all primary requirements, it also has significant downsides due to the required foundation piles. The construction process will take longer; during pile driving there will be noise hindrance; this type of foundation is more expensive than a shallow foundation; and more material is needed for the piles, making it less sustainable.

Figure 1.3: The Exercitie-bridge, Rotterdam

1.3.3 Desired solution

Ideally, the Rotterdam municipality's Engineering Office would like a slender bridge that is constructed out of FRP. This choice of material guarantees a long lifetime during which only minimal maintenance is necessary. This ideal bridge should have a shallow foundation, much like the foundation used in the standard bridges described earlier. Of course, all primary requirements must still be met. This means that despite the shallow (i.e. non-clamped) foundation and the slender design, the deck acceleration when vibrating should be

kept at an acceptable level. What is defined as 'acceptable' will be discussed later on.

The solution that will be investigated in this thesis is based on the Exercitie-bridge. The major difference will be that while the Exercitie-bridge relies on its foundation piles to meet all requirements regarding dynamical behaviour, the ideal bridge will employ *energy harvesting*. This has - in theory - the twofold benefit of keeping the vibration amplitudes at an acceptable level, while at the same time regaining some of the energy that is expended when someone crosses it.

Successfully harvesting some of the energy from the vibrating bridge would increase its sustainability - energy that is otherwise lost (i.e. dissipated as heat to the environment) could be used for something useful like lighting up the bridge at night. It could also raise awareness for the possibilities of green energy. Finally, it could be a proof-of-concept that can be expanded to other structures as well.

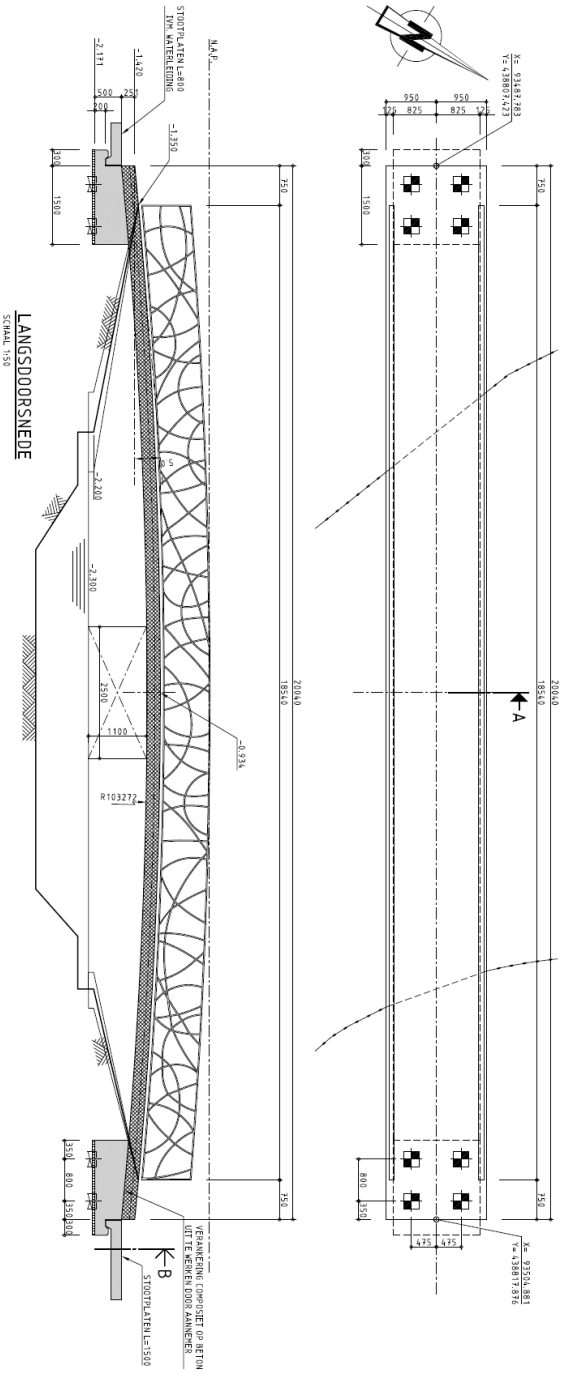

Figure 1.4: Technical drawing of the Exercitie-bridge

1.4 Research question and approach

In this thesis, the following main research question will be answered.

Would it be feasible to build a properly functioning, slender FRP pedestrian bridge that uses energy harvesting techniques to dampen its vibrations?

In order to find the answer to this question, a clear approach has to be chosen. The first part of this project will be a literature and background study. Part of this is gathering 'general' knowledge, such as the dynamic behaviour of beams under harmonic loading, or the different models that exist to model pedestrian loads. Most of this information can be found in engineering textbooks and readers. Another part consists of more specialized knowledge regarding energy harvesting and FRP bridges. For this part scientific papers are required, as these are developing fields on which no comprehensive textbooks exist as of yet. Reference to these papers will be made throughout this report. A third part is the most specific, in a way. It involves investigating the available data and documentation concerning the specific bridge that will be used as a reference (the Exercitie-bridge), as well as the thoughts, ideas and desires of the Rotterdam municipality's engineering office about this project.

Next, several analytical models of the bridge have to be developed. This includes both a single-degree-of-freedom system (SDOF), featuring a mass supported by a spring and a dashpot, and a distributed parameter system. For both models, first the bridge as it is has to be modelled, so that its behaviour can be determined. Next, adaptations can be made in the models, such as adding dampers or extra mass elements. This will allow for investigation of the effects of each structural adaptation. For example, how would adding a certain dashpot affect the bridge's maximum acceleration? Also included in these models is a way to find the energy that can be harvested under certain conditions. More on these models and this analysis can be found in Chapters 2 and 3.

Next, a numerical model will be made of the bridge. This model should be able to correctly represent both the static and the dynamic response of the bridge. Once this is achieved, theoretical modifications can be made, just as for the analytical solution. The same load cases as for the analytical models

will be employed here. The finite element software that has been used is DIANA FEA. The finite element models are be discussed in Chapter 4.

Once a 'theoretical solution' is found (e.g. a couple of dashpots in strategic locations), we have to translate these theoretical springs into real-world objects, such as electromagnetic generators. Several options will be investigated, and their pros and cons weighed.

The next question is one of feasibility and practical aspects. An energy harvesting system is more than just the harvester: it might also includes energy storage, motion amplification, and electronics such as rectifiers. How much does it cost to outfit a bridge with the energy harvester? Will there be a lot of extra maintenance required? Will the bridge still be aesthetically pleasing? What sort of things could be done with the harvested power?

Finally, we can draw conclusion about the project as a whole. While doing so, we have to keep in mind that the aim is to come up with a proof-of-concept, rather than a product that is in itself useful or profitable enough to compete in a free market.

1.5 Scope

Based on both the limited time available for this project, and the fact that this is but a single-person endeavour, some limits have to be set from the get-go. These are not limits in the sense that they should not be exceeded, but rather guidelines to ensure a measure of simplicity, and to define what would count as 'sufficiently detailed'. These limitations are:

- Only pedestrian bridges are considered, to limit the dynamic loading range and allow optimization in that regard.
- Only FRP bridges are considered, no other materials. Different types of FRP *could* be considered, if needed.
- The components and subsystems should be available off-the-shelf as much as possible; if not possible, fabrication should be relatively simple.

- What is to be done with the electrical output (i.e. the harvested energy) should not be given too much attention.

1.6 Model Overview and Verification Procedure

As mentioned earlier in this chapter, quite a few different models of the bridge will be developed. In table 1.1, a preview of the most important characteristics of each model can be found. A more detailed explanation can be found in the relevant chapter, which is also indicated in the table.

Table 1.1: Preview of all models to be used

Model	Type	Description	Software used	Chapter
1	SDOF; analytical	Basic bridge deck	Maple	2
2	SDOF; analytical	Deck + extra dashpot	Maple	2
3	2-DOF; numerical	Deck + TMD	MATLAB	2
4	Continuous; analytical	Deck + extra dashpots	Maple	3
5	Continuous; FEM	Deck + extra dashpots	DIANA	4
6	Continuous; FEM	Deck + TMD at midspan	DIANA	4

All of these different models will have to be checked as well as possible, to ensure that there are no errors. Unfortunately, the amount of available experimental data is quite limited. Because of this, the best available option was to check these models against themselves. Simply put: if two different models give the same results, it is very likely that they are both correct. This approach has been used throughout this thesis to verify every model. An overview of the most important verification results can be found in Appendix A. Reference to this appendix will be made where necessary, so that most of the verification process can be kept out of the main body of this report. For now, suffice it to say that all of the aforementioned models have been properly checked, and found to behave as expected.

Chapter 2

Analytical Model - SDOF Variants

In this chapter, the most basic dynamic model of a vibrating system is introduced: the single-degree-of-freedom system (SDOF). First, some general information and equations are given for SDOF models. In the second section, the data that is available from experiments on the Exercitie-bridge is discussed. The third section collects all relevant system parameters that are available for the bridge deck, and shows how to apply those to the analytical model. In section 2.4 a proper loading function is developed to emulate a pedestrian crossing the bridge.

Once all these preliminaries are taken care of, the rest of the chapter is dedicated to introducing and analysing the first three models of the Exercitie-bridge. First, the response of the most basic model - Model 1 - is shown, and a comparison is made with the available experimental data. This serves mostly as validation of the theory. Next, two adapted models - Model 2 and Model 3 - are proposed, and their responses analysed. This includes not only the expected response of the bridge deck, but also an estimate of the amount of energy that can be harvested.

2.1 SDOF Model Theory

A single-degree-of-freedom (SDOF) model is both the most basic and the most commonly used tool for analytically modelling the dynamic response of structural elements. The idea is that - in this case - a beam, which is a continuous system, is represented as a mass supported by a spring and a dashpot, possibly with a load acting on it. An example, with sign conventions and notation as opted for throughout this thesis, is shown in figure 2.1. Note that the green arrows represent the forces exerted on the mass by the spring and the dashpot, respectively. Also note that for both the displacement w and the external force, downwards is considered positive. When all parameter values are chosen properly, monitoring the single degree of freedom in the model should correspond quite closely to the point of interest in the actual beam that was chosen. Monitoring this point not only allows us to keep track of its displacement over time, but also to determine its speed and acceleration - which are the first and second derivatives of the displacement, respectively. Usually, the point that is modelled and thus monitored is either the mid-span point, a point that is suspected to be critical to the design, or a point directly underneath the load that acts on the beam. In this case, this mid-span of the bridge will be considered, since the displacement and its time-derivatives (i.e. velocity and acceleration) will have maximum values there under symmetrical vibration conditions.

It should be noted that the force exerted by/on the spring is proportional to the displacement, while the force exerted by/on the dashpot is proportional to the velocity, i.e. the first derivative of the displacement. The governing equation for this SDOF system, as can be seen in equation 2.1, is a second-order differential equation. To derive this equation, simply consider Newton's second law in w-direction, as can be found in any textbook on vibrations.

$$m\ddot{w} + c\dot{w} + kw = F(t) \tag{2.1}$$

It can be shown that the *undamped* eigenfrequency of the system is set by:

$$\omega_n = \sqrt{k/m} \tag{2.2}$$

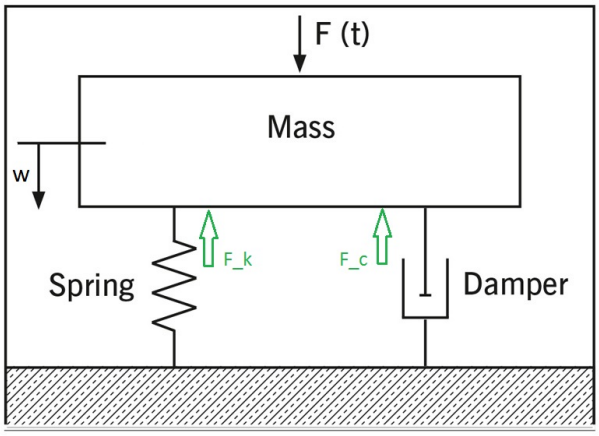

Figure 2.1: A simple SDOF model with the proper notation and sign convention. Picture adapted from [3]

Also, for convenience, we introduce the dimensionless *damping ratio*, ζ:

$$\zeta = \frac{\text{actual damping coefficient}}{\text{critical damping coefficient}} = \frac{c}{c_{crit}} = \frac{c}{2\sqrt{km}} \tag{2.3}$$

The so-called critical damping c_{crit} is the value that c would need to have to prevent *any* oscillations in the system. In other words, a critically damped system with some initial conditions would very smoothly return to its equilibrium position, without ever crossing it. An example of the effect of the damping ratio can be seen in the figure below. For a beam such as the bridge deck, we expect that $0 < \zeta < 1$, i.e. the system is 'underdamped'.

Using the definitions of the natural frequency and the damping ratio from equations 2.2 and 2.3, we can rewrite equation 2.1 in the following commonly used form:

$$\ddot{w} + 2\zeta\omega_n\dot{w} + {\omega_n}^2 w = \frac{F(t)}{m} \tag{2.4}$$

The next two sections will explain what data are available, and how the data can be used to find the parameters in the SDOF model such that it properly

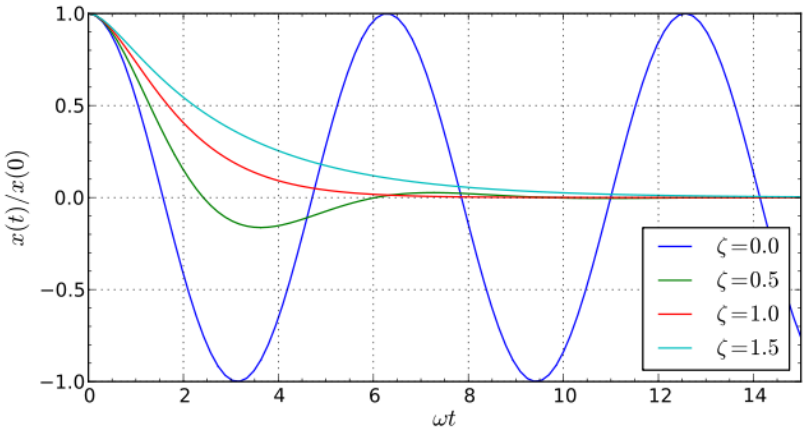

Figure 2.2: The effect of the damping ratio ζ on the behaviour of a simple system [4]

models the desired structure.

2.2 Available Data

As mentioned in Chapter 1, the Exercitie-bridge will be used as a reference case. At several moments during the manufacturing process, both static and dynamic tests were performed by Schutte and Blom [11]. Reports on these tests are available on the municipality intranet servers.

To summarize, the tests were performed first on *just* the bridge deck, then on the bridge deck including the railing, and finally on-site after installation and attachment to the foundation piles. The first two instants were tested with the bridge lying on metal tubes to emulate the theoretical simply supported situation as well as possible.

Since the goal of this thesis is to find a solution that is as generally applicable as possible, the focus will be on the first set of tests, concerning just the bridge deck. A solution that suffices for this situation will very likely be able to cope with any similar pedestrian bridge that will be designed in the future. No stiffening railing or elaborate pile foundation should be needed to satisfy all requirements.

The first series of tests was performed using several distances between the supports, thereby emulating several spans. The tests on the span closest to the actual in-situ span will be considered, and used to validate the analytical and numerical models. Another reason for this choice is that a simply supported beam with parts of the beam 'sticking out' on both ends is not the same as a simply supported beam from span to span. Especially in dynamic analysis, the free ends could have a significant - yet unrealistic - influence.

Within the context of testing just the bridge deck with a span closest to the actual span, several experiments were performed. The most important of these are:

- Static deflection test
- Heel test (impact test) at several locations along the bridge
- Walking test, with test subject traversing the bridge

- Intentional excitation test, both whilst standing on the bridge and while standing next to it

For all tests, acceleration data over time was recorded using a smartphone app developed by dr. Blom, called 'Vxacc', which uses the phone's built-in acceleration sensors, and outputs a text file. A smartphone running this app was placed upon the bridge deck. Furthermore, camera footage and a piece of software was used to determine the deflection at mid-span over time. The raw data is either available on the intranet servers, or has been provided by dr. Blom.

From the static test, the stiffness (EI) of the bridge deck can be obtained using the basic deflection formula for a simply supported beam. The heel test at mid-span can be used to find the first and second eigenfrequency of the deck, using Fourier analysis. The dynamic walking test is useful because it emulates 'normal use' of the bridge as closely as possible. Finally, the intentional excitation test had to be performed to make sure the bridge would be able to withstand vandal loads - or simply children playing around with it. For each of the performed dynamic tests, the damping coefficient ζ of the deck can be determined as well.

Finally, more psychological aspects were investigated as well: how does it *feel* to stand or walk on a bridge that is vibrating with a magnitude way higher than what one is used to in conventional bridges? Does it feel safe? Does it feel comfortable? These tests are obviously not quite as technically rigorous, but they do provide some real-world insight that cannot be obtained through theory alone.

As for the lay-out and build-up of the Exercitie-bridge, for both the deck and the finished bridge, detailed technical drawings are available, including all relevant measures. The material properties that were used by FibreCore in the design process of the InfraCore deck are available as well, to be used for modelling.

Finally, something that is lacking in the experimental data has to be addressed: the exact loading for the dynamic tests. Only the weight of the test subject has been recorded, not the step frequency nor the walking speed. Furthermore, the force exerted on the bridge is not known exactly as a function

of time. To deal with these limitations, some assumptions will be made later on concerning the step frequency; a model will be adopted for the footfall-force as a function of time; and the walking velocity will be estimated based on the span and the observable different 'parts' of the time-response that was recorded. All in all, this should provide a fair approximation of the tests that were performed as input for the analytical and numerical models.

2.3 Bridge Deck Properties

As explained in Chapter 1, some tests have been performed during the building process of the Exercitie-bridge. Based on this, we can determine the proper parameters to use in the SDOF system. These are m, k, and either c or ζ. As explained in Chapter 1, we are interested in just the bridge deck, tested with a span (L) of 19.04 meters. Our point of interest is at mid-span.

2.3.1 Spring stiffness

The simplest parameter to determine is the spring stiffness, k. A static deflection test was performed, in which a person with a mass of 95 kg stood in the middle of the simply supported bridge deck. The deflection was measured to be 5.2 mm. As a check, the beam stiffness, EI, can be determined by making use of the following standard beam deflection formula:

$$w_{static} = \frac{1}{48}\frac{FL^3}{EI} \tag{2.5}$$

According to this formula, the actual beam stiffness EI is $2.58 \cdot 10^7\, N \cdot m^2$. This is quite close to the design stiffness, which was $2.47 \cdot 10^7\, N \cdot m^2$. The spring stiffness in the model can be calculated as follows:

$$k = \frac{F}{w_{static}} = \frac{48EI}{L^3} = 1.79 \cdot 10^5\,\mathrm{N/m} \tag{2.6}$$

2.3.2 Equivalent mass

Since the SDOF model is - of course - a simplification of reality, not everything that can be physically measured 'adds up'. Specifically, the mass that will be used in the SDOF model (the 'equivalent mass') *cannot* simply be taken equal to the actual mass of the beam in between the supports. Doing so would lead to an eigenfrequency in the model that is *lower* than the actual eigenfrequency. Rather, we base the equivalent mass on the measured value of the first natural eigenfrequency of the beam.

This first eigenfrequency (f_n), corresponding to the first (sine-shaped) eigenmode, was determined using a heel test. The test subject stamps his foot down on the bridge deck to create a pulse loading, and then the free response is monitored. The first peak in a Fourier analysis of the response (i.e. the first peak in the frequency-response domain) corresponds to the eigenfrequency we are looking for.

It should be noted that this measured eigenfrequency is in fact the *damped* eigenfrequency, since *some* damping is present in the bridge deck. However, this difference is negligible in case of just the bridge deck, as will be shown in the next subsection.

According to the JRC Guidelines, step frequencies between 1.25 and 2.3 Hz are most common [12]. Alternatively, Bachmann states that the step frequency is normally distributed with a mean of 2 Hz and a standard deviation of 0.175 Hz, which would mean that "95% of pedestrians walk at rates between 1.65 and 2.35 Hz". [13]

From the experiment, the measured eigenfrequency of the bridge deck was 1.68 Hz. Normally when designing a structure, resonance should be avoided if possible. However, for an energy-harvesting bridge, there might be benefits to a loading frequency close to the eigenfrequency. This will be investigated in more detail later on in this chapter.

Now that the first eigenfrequency and the spring stiffness have been determined, we can set the equivalent mass of the model as follows:

$$m_{equiv} = \frac{k}{2\pi {f_n}^2} = 1608\,\mathrm{kg} \tag{2.7}$$

This is indeed quite a bit lower than the actual mass of the beam in between the supports. The total deck has a length of 20 meters, and is not perfectly prismatic: extra steel beams are present near both ends. The total mass is about 4600 kg; the actual mass in between the supports for the 19.04 meter test would be about 4136 kg, as explained in the experiment report by Schutte and Blom. This means that the equivalent mass is a factor of 2.6 lower than the actual mass. This sounds reasonable - theory states that the equivalent mass for a perfectly prismatic beam with no ends 'sticking out' over the support would be lower than the actual mass by a factor 2. [14]

2.3.3 Damping

The value for c that is inherent in the bridge deck is determined via a quantity called the logarithmic decrement [15]. Using the measured acceleration data, the formula below can be filled in to find this quantity.

$$\delta = \frac{1}{n} \ln \left(\frac{\ddot{w}(t)}{\ddot{w}(t + nT)} \right) \tag{2.8}$$

In this formula, T is the oscillation's period, and n is the number of periods that are considered. In theory, every value of n should give the same value for δ; in practice, a larger value of n might be beneficial to get the 'average' logarithmic decrement. This quantity can than be used to determine the damping ratio ζ, using the following formula:

$$\zeta = \frac{\delta}{\sqrt{4\pi^2 + \delta^2}} \tag{2.9}$$

Using equation 2.3, while replacing m by m_{equiv}, allows us to calculate the value for c.

It should be noted that, while the above holds in theory, there is a practical issue here. During testing, it became apparent that the damping ratio *decreased* over the course of the day. This is most likely due to the setting of the glue and laminate, and the opening up of initial micro-crack. This only happens after the bridge has been loaded and unloaded a sufficient number of times. The tests we are most interested in, however, were performed early on in the day: the tests on a span of 19.04 meters were performed first. As a result, we cannot be sure of the value of ζ; it ranges from 0.6% to 4.0%. For our analytical model, a value of 1% will be assumed. In the most basic case (Model 1), where the only damping present is the inherent damping of the deck, this does influence the behaviour. As other sources of damping get added, the influence becomes smaller, as will be shown later on in this report.

When doing the calculations with our value of $\zeta = 1\%$, we find that $c_{deck} = 340\ \frac{kg}{s}$.

One other formula that should be discussed in this subsection is the damped eigenfrequency ω_d. Because there is a non-zero value of ζ, the eigenfrequency of the structure will in reality be slightly *lower* than the undamped (natural) eigenfrequency $omega_n$. The following formula described this relation.

$$\omega_d = \omega_n \sqrt{1 - \zeta^2} \tag{2.10}$$

The bridge deck's ζ value of 1% will barely cause a difference between ω_n and ω_d. Care should be taken, however, when extra damping is added to the structure (Model 2 and onwards).

2.4 Loading Conditions

In order to obtain a realistic response of the bridge model, a realistic loading function has to be defined. For now, only the pedestrian load for one person walking across the bridge will be considered - a very common use case.

Loading models for pedestrian traffic make up an entire field of study on their

own. For the purposes of this thesis, the conclusions regarding pedestrian loading as drawn in M. Sousamli's Master thesis will be adopted [16]: the Bachmann loading model was deemed to be the most suitable model for application to footbridges [13]. Like most pedestrian load models, we start out with the following general formula.

$$F(t) = G_0(1 + \sum_{n=1}^{k} a_n sin(2\pi n f_{step} t - \phi_n) \tag{2.11}$$

According to Bachmann [13], the following constants should be used when modelling someone walking:

$$\begin{aligned} &k = 3; \\ &a_1 = 0.4;\ a_2 = 0.1;\ a_3 = 0.1; \\ &\phi_1 = 0;\ \phi_2 = \pi/2;\ \phi_3 = \pi/2; \end{aligned} \tag{2.12}$$

When using those values, as well as a step frequency of 1.63 Hz and a static weight G_0 of $9.81 \cdot 75 = 737\,N$, we can obtain the following loading graph.

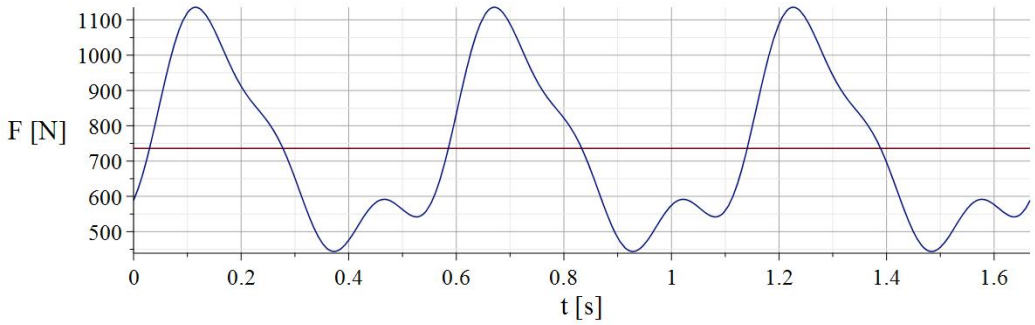

Figure 2.3: Three periods of the load-versus-time plot according to the Bachmann pedestrian loading model

For the SDOF model, this load cannot be applied directly. A certain force acting near the midspan would have a stronger influence on the midspan deflection than that same force acting near one of the supports. A person

walking over the bridge is, of course, a moving load. Since an SDOF model does not take this into account (all loads are applied at the midspan point), a correction factor γ has to be adopted.

My suggestion for this correction factor would be to define it as a function of time. Assuming a person is walking along the bridge at a constant pace, starting at $t = 0$, his location is always uniquely determined by the time. At the midspan, the load predicted by the model is indeed present there in real life, so the correction function should have a value of 1 when the pedestrian passes the midspan point. When the pedestrian crosses either of the supports (i.e. when he steps *onto* or *off* the bridge), the effect of the loading on the midspan is negligible. Therefore, the function should have a value of 0 at the end-points of the bridge.

For now, a simple half-sine function is used to specify γ. Using the walking velocity v and the bridge span L, we find the following correction formula:

$$\gamma(t) = \sin\left(\frac{\pi v t}{L}\right) \tag{2.13}$$

In order to properly emulate a person crossing the bridge, we use the following product of loading function, correction function, and two Heaviside functions. A graphical representation can be seen in figure 2.4.

$$F_{Bachmann\,crossing}(t) = \gamma(t) \cdot F_{Bachmann}(t) \cdot \left(H(t) - H\left(t - \frac{L}{v}\right)\right) \tag{2.14}$$

Where v is the pedestrian's walking speed, and $F_{Bachmann}(t)$ is the result of filling in equation 2.11 using the coefficients from equation 2.12, as well as an assumed static load G_0 of 75 kg.

One should keep in mind that in order to arrive at the proposed load model above, the following assumptions were made:

- A single pedestrian (assumed mass of 75 kg) crosses the bridge

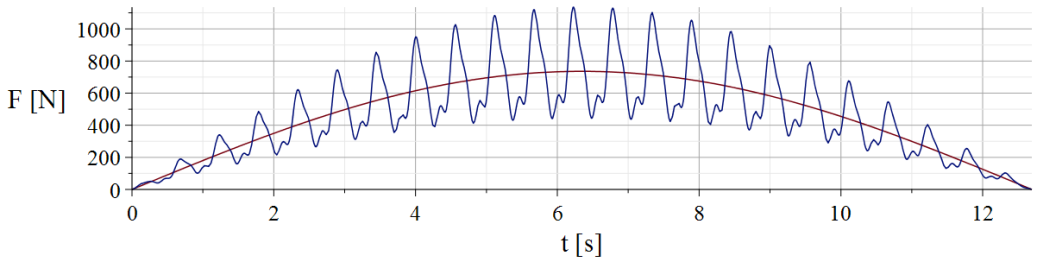

Figure 2.4: The corrected load-versus-time model of a person crossing the bridge, using the Bachmann model

- The pedestrian walks with a constant velocity and a constant step frequency
- The footfall load is modelled using the method proposed by Bachmann
- The correction function is a simple half-sine

For any other scenario, the loading function would have to be adapted.

2.5 Model 1 - SDOF basic bridge deck

Now that we have both the equation of motion and the proper loading function for the SDOF model, the response for Model 1 can be found analytically using Maple. The 'response', in this case, consists of the displacement at mid-span $w(t)$, the midspan velocity $\dot{w}(t)$ and the midspan acceleration $\ddot{w}(t)$.

Before we can calculate the response, though, values have to be assigned to the walking velocity v, the step frequency f_{step}, and the mass of the pedestrian crossing the bridge. For now, these values are picked to match the testing conditions as accurately as possible. This requires some reverse engineering based on the experimental data. The acceleration data for the relevant test are plotted in figure 2.5.

In this figure, we can observe that the time between stepping onto the bridge and the acceleration amplitude decaying exponentially (free response, i.e. the

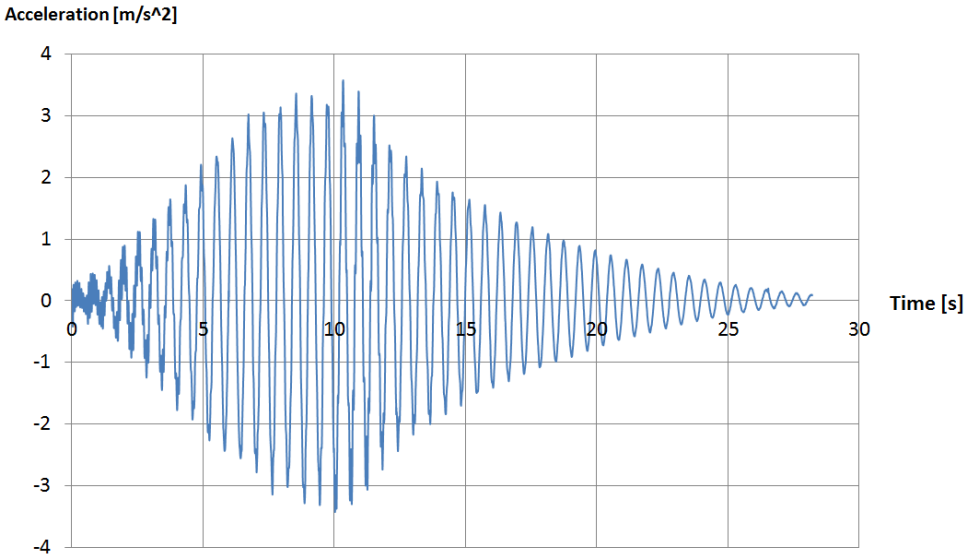

Figure 2.5: The experimental acceleration data for test 'Walk 1'

test subject has stepped off the bridge) is approximately 13 seconds. This is the crossing time. Given that the length is known to be 19.04 meters, the walking velocity can be calculated to be about 1.5 m/s, or slightly above 5 km/h. The mass of the test subject is known to be 95 kg, rather than the 75 kg mentioned earlier. So, for comparison's sake, in this section we will use a mass of 95 kg. Outside of this section, the 75 kg will be used since it is a more realistic estimate of the *average* pedestrian. Finally, the step frequency has to be estimated. This is done quite roughly, according to [17]. Considering the test subject was a tall male, this leads to a value of about 1.75 Hz. Using these values, we can obtain the following response plots.

When comparing figures 2.5 and 2.7, we can see that both the order of magnitude and the overall shape of the graphs match up quite well. Interestingly, both in reality and in Model 1, the response amplitude starts to decrease *before* the crossing time has passed. This is caused by the diminishing influence of the load on the midspan response as the load gets further away from midspan.

There are two notable differences that should be considered. The first one

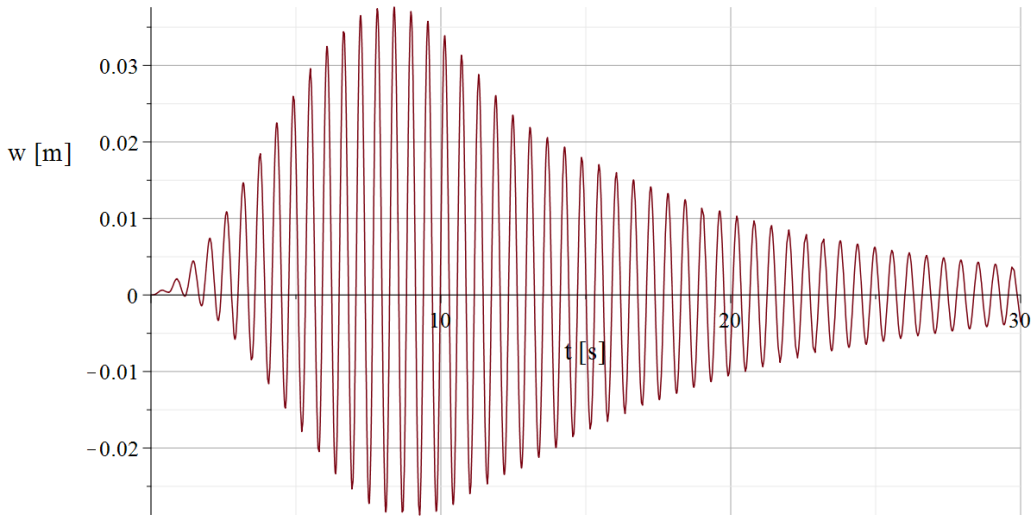

Figure 2.6: Displacement response of Model 1 to a load function emulating a person crossing the bridge

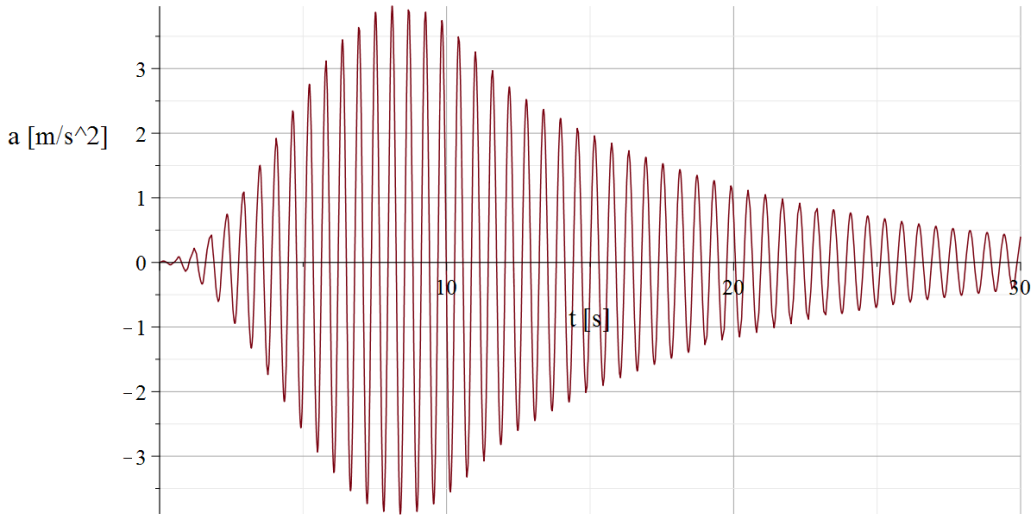

Figure 2.7: Acceleration response of Model 1 to a load function emulating a person crossing the bridge

is the presence of small-amplitude, high-frequency oscillations on top of the larger sine function in the experimental data. These are the higher-order modes that are present in reality. The SDOF model has (by definition) only

one eigenmode, and does not have these smaller fluctuations. The second difference is the rate of decay once the test person has stepped off the bridge. In reality, acceleration values decrease quicker than in Model 1. This is because - as mentioned earlier - this experiment was performed before all micro-cracks and imperfections had set properly. In other words: the experiment shows a higher ζ than used in Model 1, because it was one of the first experiments that was performed.

Both these differences between Model 1 and the experimental results are acceptable. It seems as if Model 1 described the regular use case of a person walking over the bridge deck quite accurately. Now that this validation check has been passed, we can adapt Model 1 to include the energy harvesting device. Note that from now on, a pedestrian mass of 75 kg will be assumed.

2.6 Model 2 - SDOF bridge deck with extra viscous damping

The first proposed change to Model 1 - which then becomes known as Model 2 - is to add an extra damping term, $c_{harvester}$, to the EoM from equation 2.1. This term represent the component of the energy harvesting system that takes energy from the bridge deck and transforms it into electrical energy. The corresponding EoM can be written as:

$$m\ddot{w} + (c_{deck} + c_{harvester})\dot{w} + kw = F(t) \tag{2.15}$$

Once again, the analytical mathematics on this differential equation was performed using Maple.

2.6.1 Influence of the amount of extra damping

Adding this extra damping term alters the response of the bridge to the applied loading. The higher the $c_{harvester}$, the lower the maximum displacement,

velocity and acceleration. This can be understood intuitively, and matches the theory on this topic.

Quantitatively, the effect of $c_{harvester}$ on the maximum absolute value of the response is shown in figures 2.8 and 2.9. Note that again, the same loading conditions are used as for Model 1 in the previous section (a single pedestrian crossing the bridge). This time, the walking speed is again kept at $v = 1.5$ m/s and two different step frequencies are compared, namely $f_{step} = 1.75\,\text{Hz}$ and $f_{step} = 2.20\,\text{Hz}$. The first frequency is rather close to the bridge's eigenfrequency (which is 1.68 Hz), while the second is on the high end of the pedestrian step frequency spectrum, and thus quite far away from resonance. Again, note that a pedestrian mass of 75 kg is assumed, rather than the 95 kg that was used to validate Model 1.

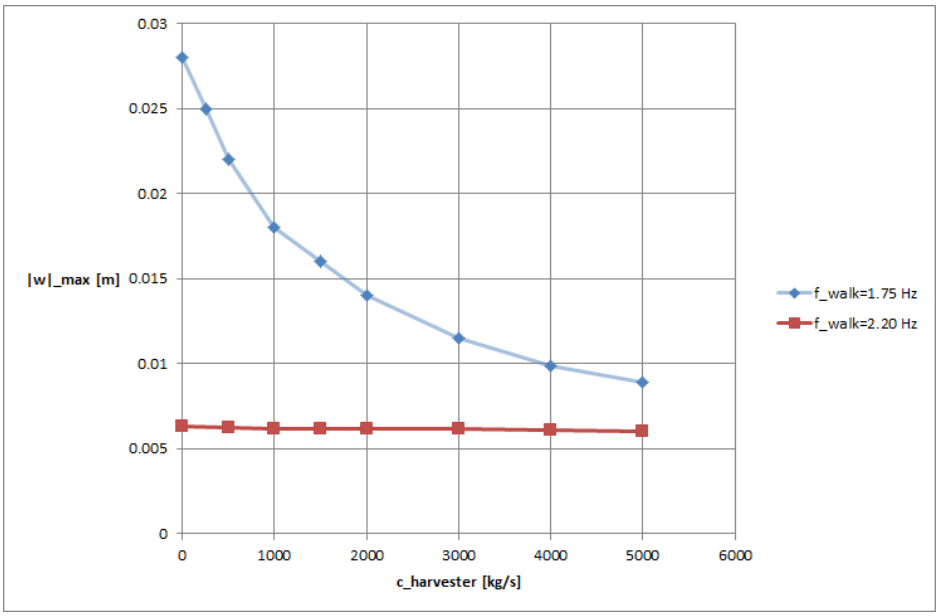

Figure 2.8: Maximum occuring absolute displacement response of Model 2 as a function of $c_{harvester}$

From these figures, it becomes clear that when loaded with a step frequency close to the eigenfrequency, the bridge's response amplitude decreases exponentially. It should be noted that for all investigated values, the damped eigenfrequency stays within 1% of the natural (undamped) eigenfrequency. This is important to note, because an overly large value of $c_{harvester}$ could

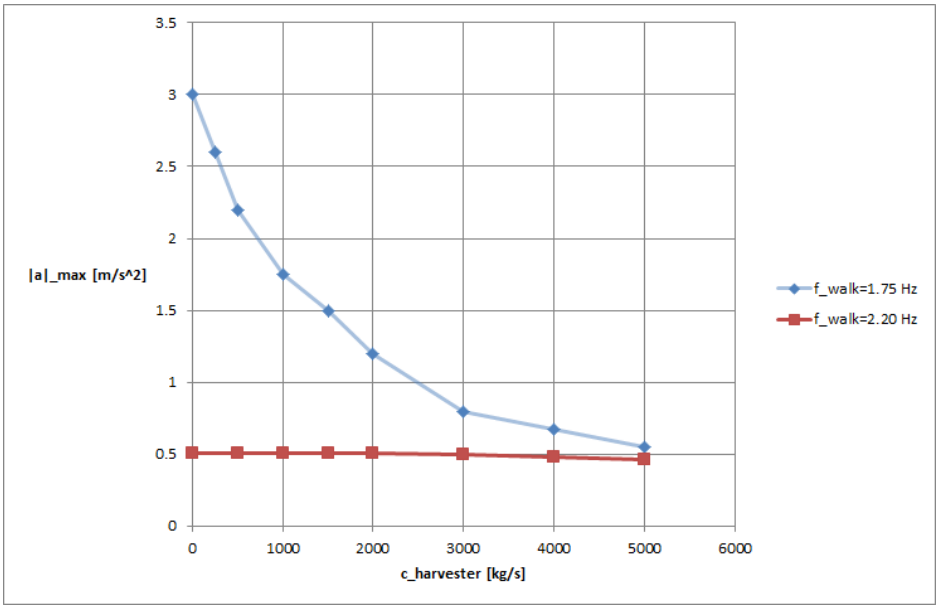

Figure 2.9: Maximum occurring absolute acceleration response of Model 2 as a function of $c_{harvester}$

cause extra resonance by lowering the damped eigenfrequency to the applied step frequency. In figures 2.8 and 2.9, this effect does *not* play a role.

Another conclusion that can be drawn based on these figures is that when the step frequency is relatively far away from resonance, the damping value of the harvester barely has influence on the response amplitude. This is because for non-resonance, the response amplitudes are governed by the bridge deck's static deflection, which is indeed independent of loading frequency.

The reduction in response amplitude could be an argument in favor of designing for a large $c_{harvester}$ value. However, we have to keep in mind that the goal of this project is not to dampen the vibrations as much as possible, but rather to harvest the most energy possible. Therefore, the effect of $c_{harvester}$ on the harvested energy has to be investigated.

2.6.2 Energy considerations

The energy analysis can be visualized using a so-called hysteresis plot: a parametric plot of the force exerted by the component in question versus the displacement at the relevant point. In more specific terms: a plot of $c_{harvester} \cdot \dot{w}(t)$ versus $w(t)$. The graph starts out at $(0, 0)$, assuming the initial conditions are zero. From there, it 'spirals' outward until the (more-or-less) steady-state solution is reached. A perfect steady-state solution would be represented by an ellipse being repeated over and over again. A decline in response amplitude can be seen by the plot spiralling back inwards, towards the new equilibrium state. In this case, once the pedestrian leaves the bridge, the equilibrium state is again $(0, 0)$. For this specific SDOF model, with an example value of $c_{harvester} = 1000\ \frac{kg}{s}$, the hysteresis plot shown in figure 2.10 can be obtained.

The area enclosed by this graph corresponds to the work done by the harvester. This makes sense intuitively when considering the formula for work ($W = Fs$). For each oscillation, a circle or spiral section of 360° is added to this graph. It should be emphasized that an area that is enclosed multiple time also *counts* multiple times towards the total work done.

In a vibrating system, there is a constant interchange between potential energy and kinetic energy. A simple, idealized spring being loaded and unloaded without loss of energy would show up as straight line in a hysteresis-plot (back and forth over the same trajectory). To get an idea of how much of the energy being interchanged is 'lost' to damping, we can also obtain a hysteresis plot which includes all forces acting on the mass. Such a plot can be seen in figure 2.11. It is clear that the idealized spring has the most influence on the shape of this plot; only the relatively slight deviation from a straight, back-and-forth line shows the presence of a damper.

To quantify the amount of energy, we still want to obtain the area enclosed by these hysteresis plots. In practice, it is easier to determine the work done by the harvester (i.e. the gross harvested energy) by taking note of the following formulas [18].

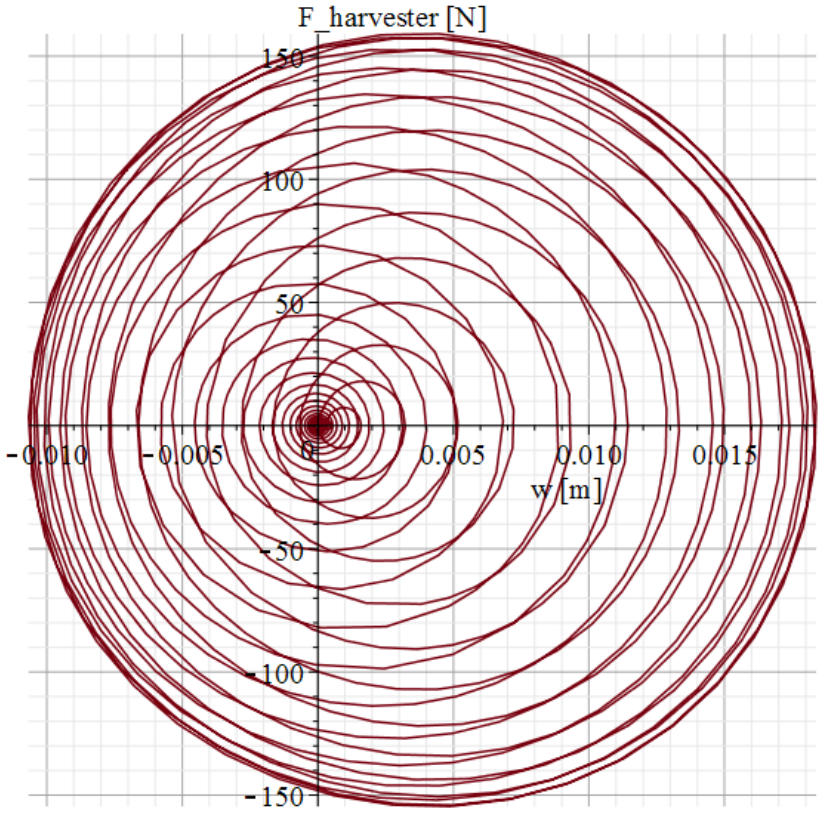

Figure 2.10: Hysteresis plot of the adapted SDOF model, using $c_{harvester} = 1000\,\frac{kg}{s}$ as an example

$$E_{harvested} = \oint F_d \, dw \tag{2.16}$$

$$\dot{w} = \frac{dw}{dt} \rightarrow dw = \dot{w}\, dt \tag{2.17}$$

$$F_{harvester} = c_{harvester} \dot{w} \tag{2.18}$$

Combining these equations leads to the following formulas for the gross harvested energy:

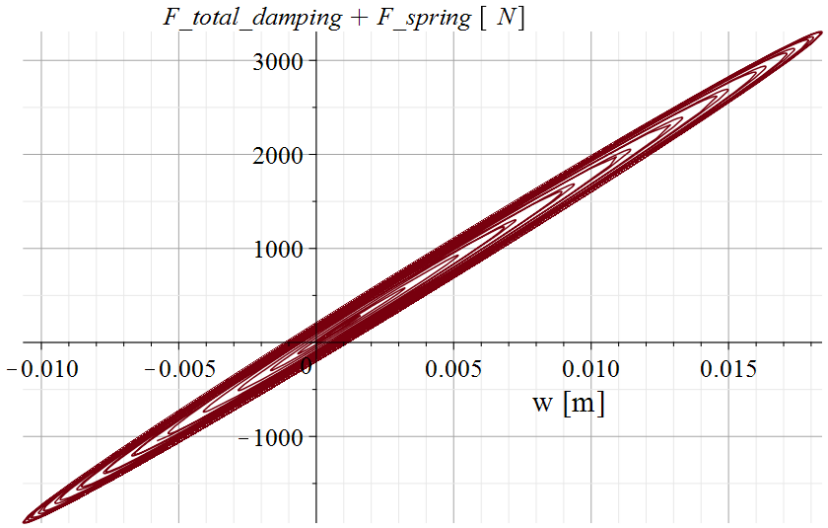

Figure 2.11: Hysteresis plot of the adapted SDOF model, using $c_{harvester} = 1000\,\frac{kg}{s}$ as an example. All forces are included.

$$\begin{aligned} E_{harvested} &= \int c_{harvester}\dot{w}^2 dt \\ &\approx \int_0^{2\frac{L}{v}} c_{harvester}\dot{w}^2 dt \end{aligned} \tag{2.19}$$

Using equation 2.19, the gross harvested energy can be investigated for varying $c_{harvester}$ and f_{step}. The results of this analysis is shown in figure 2.12.

From this figure, we can see that there is an optimum value for the harvester's damping value, such that the maximum amount of energy can be harvested - at least for step frequencies near resonance. For step frequencies far away from the bridge's eigenfrequency, a higher damping value seems to be slightly better. However, for non-resonance the amount of energy harvested remains much lower than for near-resonance.

In order to optimize the energy harvesting, the bridge has to be designed such that its eigenfrequency lies within the typical range of walking frequencies; also, the harvester should be designed to have a damping value that

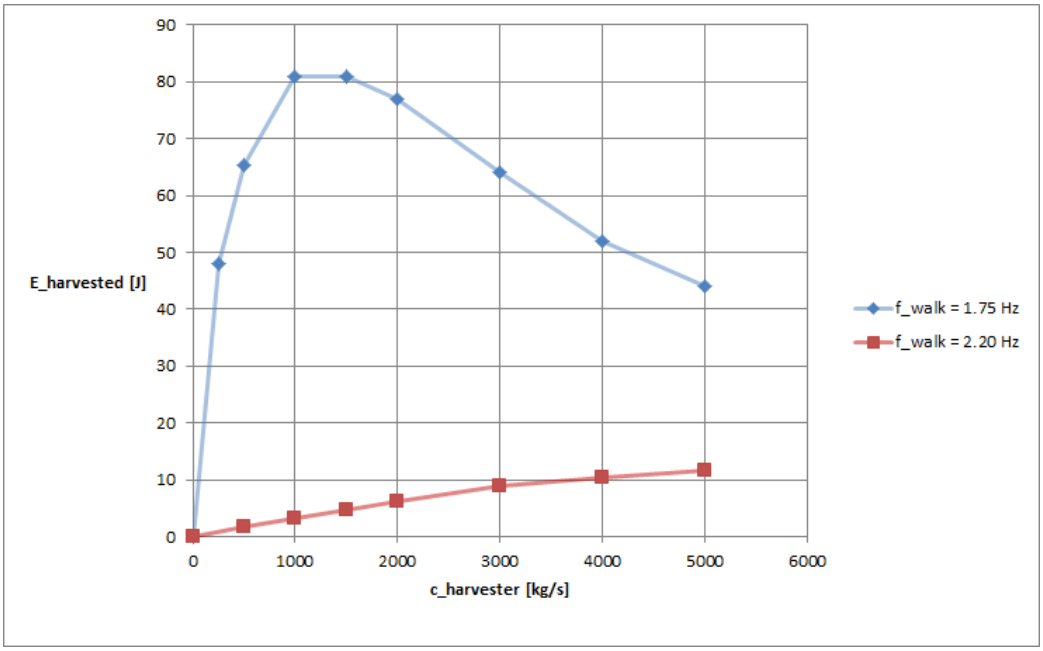

Figure 2.12: Gross harvested energy for Model 2 for a single pedestrian crossing the bridge

corresponds to a peak in the near-resonance line in figure 2.19.

It should be noted that this - as of yet - theoretical dashpot is assumed to act at the point of interest for which this SDOF system was calibrated: the bridge midspan. This means that if in reality a dashpot with the 'optimal' value would be placed in another location, like on land near the supports, it might underperform.

Another characteristic of the system is that only a small fraction (order of magnitude 1 to 2%) of the gross harvested energy is harvested from the freely-vibrating bridge after the pedestrian has stepped off. In other words: as soon as the energy sources ceases to put energy into the system, the energy output of the system decreases very rapidly.

2.7 Model 3 - SDOF bridge deck with TMD

The next adaptation that will be investigated makes use of a so-called tuned mass damper (TMD). TMDs consist of an auxiliary mass that is attached to the main structure by means of a spring and a dashpot. A representation of such a model, including the notation and sign convention that will be used in this thesis, can be seen in figure 2.13. Again, we are considering the bridge deck as a SDOF system, but the inclusion of a TMD adds another degree of freedom, making it a two-degree-of-freedom system (TDOF). Together, however, it can be analysed as two coupled SDOF systems, with coupled equations of motion. The mathematics and concepts remain the same, that is why Model 3 is included in the SDOF chapter.

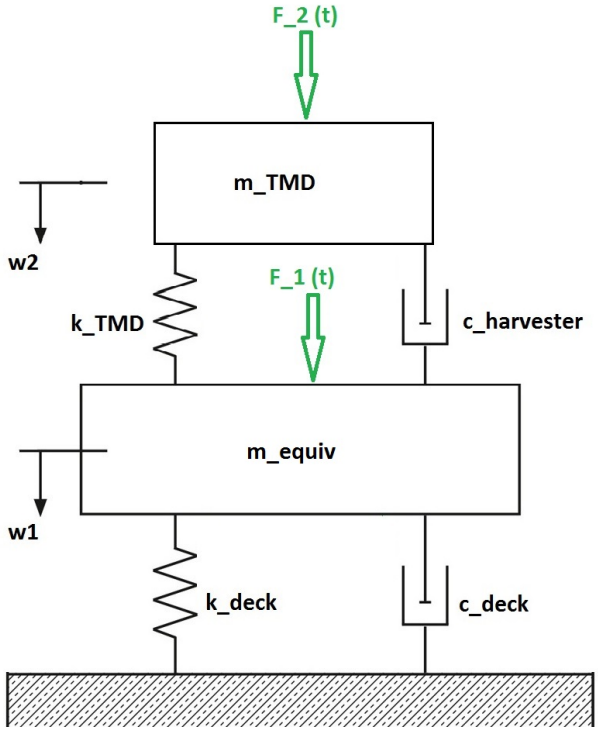

Figure 2.13: TDOF system consisting of the bridge deck and a TMD. Figure adapted from [3]

A clear and concise description of the idea behind TMDs is given by [19]:

"A tuned mass damper (TMD) is a device consisting of a mass, a spring, and a damper that is attached to a structure in order to reduce the dynamic response of the structure. The frequency of the damper is tuned to a particular structural frequency so that when that frequency is excited, the damper will resonate out of phase with the structural motion."

In our case, a TMD will be able to decrease the maximum occurring acceleration quite easily, which will increase the comfort of pedestrians. The big question that we need to answer, however, is whether placing the harvester-dashpot in between the bridge deck and the auxiliary mass will increase or decrease the amount of energy that can be harvested from the system, when compared with Model 2.

In this section, the 'near-optimal' approach will be used [19], in which the eigenfrequency of the TMD is equal to that of the main system. Since this is a preliminary investigation, near-optimal should suffice.

Another limitation to the scope of this section is that only *passive* TMDs will be considered. An active TMD would require an extra actuator that exerts a force on the TMD, thereby increasing its effectiveness in damping the motion of the bridge. This would require not only a more complicated system, but also energy to drive the actuator - which would nullify the point of energy-harvesting.

When considering the dynamics of the system, two coupled differential equations can be derived. Note that for clarity, the subscripts d and h indicate the deck and the harvester, respectively.

$$m_{equiv}\ddot{w}_1 + (c_d + c_h)\dot{w}_1 - c_h\dot{w}_2 + (k_d + k_h)w_1 - k_h w_2 = F_1(t) \quad (2.20)$$

$$m_{TMD}\ddot{w}_2 + c_h(\dot{w}_2 - \dot{w}_1) + k_h(w_2 - w_1) = F_2(t) = 0 \quad (2.21)$$

In matrix-vector format, this can be written as:

$$\mathbf{M\ddot{u}} + \mathbf{C\dot{u}} + \mathbf{Ku} = \mathbf{F}(t) \tag{2.22}$$

Where the following matrices and vectors are used:

$$\mathbf{u} = \begin{bmatrix} w_1 \\ w_2 \end{bmatrix} \tag{2.23}$$

$$\mathbf{F} = \begin{bmatrix} F_1(t) \\ F_2(t) \end{bmatrix} \tag{2.24}$$

$$\mathbf{M} = \begin{bmatrix} m_{equiv} & 0 \\ 0 & m_{TMD} \end{bmatrix} \tag{2.25}$$

$$\mathbf{C} = \begin{bmatrix} c_d + c_h & -c_h \\ -c_h & c_h \end{bmatrix} \tag{2.26}$$

$$\mathbf{K} = \begin{bmatrix} k_d + k_h & -k_h \\ -k_h & k_h \end{bmatrix} \tag{2.27}$$

In theory, this system can be solved analytically . However, if we want to retain the rather complicated loading function that was derived for Model 1, this is not very practical. Even parametric software like Maple runs into practical limitations on computing time and computing power.

Instead, a numerical approach is taken to investigate this system: a state-space representation. According to [20]:

"In control engineering, a state-space representation is a mathematical model of a physical system as a set of input, output and state variables related by first-order differential equations or difference equations. State variables are variables whose values evolve through time in a way that depends on the values they have at any given time and also depends on the externally imposed values of input variables. Output variables' values depend on the values of the state variables."

In its most general form, this can be written as:

$$\dot{\mathbf{x}}(t) = \mathbf{A}(t)\mathbf{x}(t) + \mathbf{B}(t)\mathbf{u}(t) \tag{2.28}$$
$$\mathbf{y}(t) = \mathbf{C}(t)\mathbf{x}(t) + \mathbf{D}(t)\mathbf{u}(t) \tag{2.29}$$

Here, $\mathbf{x}$ and $\mathbf{y}$ are the state vector and the output vector, respectively. Note that while this approach requires such a formulation, the vector $\mathbf{y}$ will not be needed: all the information of interest can be found in the time history of the state vector $\mathbf{x}$. The vector $\mathbf{u}$ is the input vector - not to be confused with the displacement vector $\mathbf{u}$ from equation 2.23.

In our case, we deal with a linear time-invariant system (LTI), meaning that the matrices $\mathbf{A}$ through $\mathbf{D}$ are not dependent on time. They are fixed, and can be determined from the system's equations of motion.

We define the state vector $\mathbf{x}$ as follows:

$$\mathbf{x}(t) = \begin{bmatrix} w_1 \\ w_2 \\ \dot{w}_1 \\ \dot{w}_2 \end{bmatrix} \tag{2.30}$$

The input vector $\mathbf{u}$ is defined in equation 2.31. Note that while there is the option of applying a force both at the bridge deck (F_1) and at the TMD (F_2), the pedestrian load is in fact only applied at the bridge deck, and F_2 is set to zero.

$$\mathbf{u}(t) = \begin{bmatrix} F_1(t) \\ F_2(t) \end{bmatrix} \tag{2.31}$$

The matrices are defined as follows:

$$\mathbf{A} = \begin{bmatrix} 0 & 0 & 1 & 0 \\ 0 & 0 & 0 & 1 \\ \frac{-(k_d+k_h)}{m_{equiv}} & \frac{k_h}{m_{equiv}} & \frac{-(c_d+c_h)}{m_{equiv}} & \frac{c_h}{m_{equiv}} \\ \frac{k_h}{m_{TMD}} & \frac{-k_h}{m_{TMD}} & \frac{c_h}{m_{TMD}} & \frac{-c_h}{m_{TMD}} \end{bmatrix} \tag{2.32}$$

$$\mathbf{B} = \begin{bmatrix} 0 & 0 \\ 0 & 0 \\ \frac{1}{m_{equiv}} & 0 \\ 0 & \frac{1}{m_{TMD}} \end{bmatrix} \tag{2.33}$$

$$\mathbf{C} = \begin{bmatrix} 1 & 0 & 0 & 0 \\ 0 & 1 & 0 & 0 \end{bmatrix} \tag{2.34}$$

$$\mathbf{D} = \begin{bmatrix} 0 & 0 \\ 0 & 0 \end{bmatrix} \tag{2.35}$$

Note the similarities between matrix $\mathbf{A}$ and the matrices $\mathbf{K}$ and $\mathbf{C}$ introduced earlier: it is still the same physical system. This state-space system can be analysed using functionality already present in MATLAB (the `lsim` function).

Before MATLAB can determine the response of the system, numerical values have to be chosen for all variables. These variables are the mass, the spring stiffness, and the damping coefficients for both the bridge deck and the TMD (harvester). For the bridge deck, the same values are used as in Model 1. We define a mass ratio $\bar{m}$ as follows:

$$\bar{m} = \frac{m_{TMD}}{m_{equiv}} \Rightarrow m_{TMD} = \bar{m}\, m_{equiv} \tag{2.36}$$

In order for the TMD to be effective, it should have an eigenfrequency equal to (or very near) that of just the bridge deck. This requires the following to hold as well.

$$k_h = \bar{m} k_d \tag{2.37}$$

This means that once all the bridge deck properties have been determined (as they have), there are only two variables in this model: $\bar{m}$ and c_h. In order to optimize these two variables, nested for-loops can be used to investigate the

system's response to the same loading function that Model 2 was subjected to (equation 2.14, again assuming a pedestrian mass of 75 kg). Connor [19] mentions that a mass ratio of 0.02 is usually a reasonable order of magnitude, so that gives us an idea of the order of magnitude that can be expected to function well.

The key response characteristics of the system are as follows:

- The absolute maximum value of $\ddot{w}_1$, which determines pedestrian comfort levels
- The peak value of $|w_2 - w_1|$, which governs how much relative movement the TMD dashpot and spring should be able to facilitate
- The total energy harvested after a person has crossed (assuming full efficiency, for now)

Analysis of the state-space system using the `lsim` function with input as described above yields the following results when varying over the two parameters $\bar{m}$ and c_h. Note that this analysis has to be performed for each step frequency separately. Also note that the maximum TMD acceleration is included as well, even though it is not governing - this is just to get a feeling of how it behaves.

In order to draw conclusions about the design point (the optimal combination of $\bar{m}$ and c_h), some boundaries have to be defined. This will be done is Chapter 5.

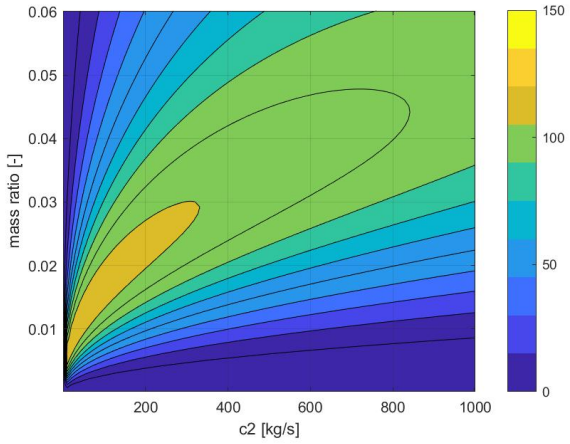

(a) Energy harvested [J]

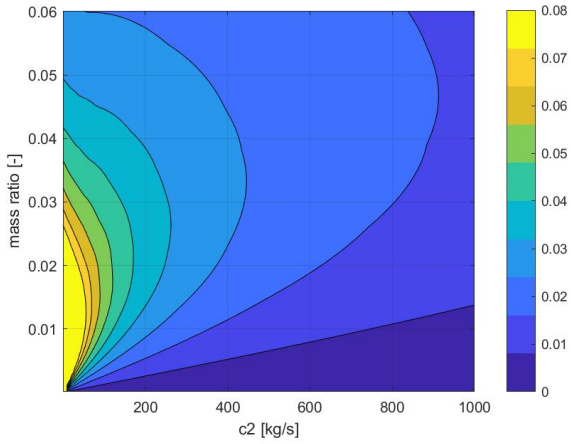

(b) Maximum occurring $|w2 - w1|$ [m]

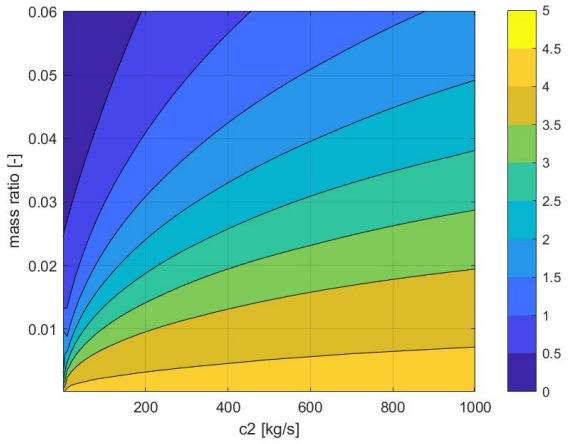

(c) Maximum deck acceleration $[m/s^2]$

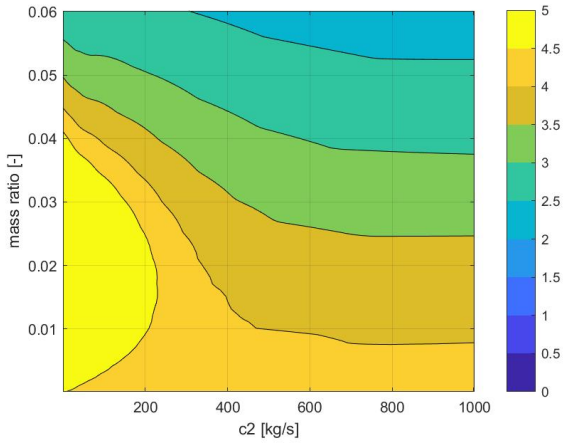

(d) Maximum TMD acceleration $[m/s^2]$

Figure 2.14: Model 3 response to a pedestrian crossing the bridge - $f_{step} = 1.68$ Hz

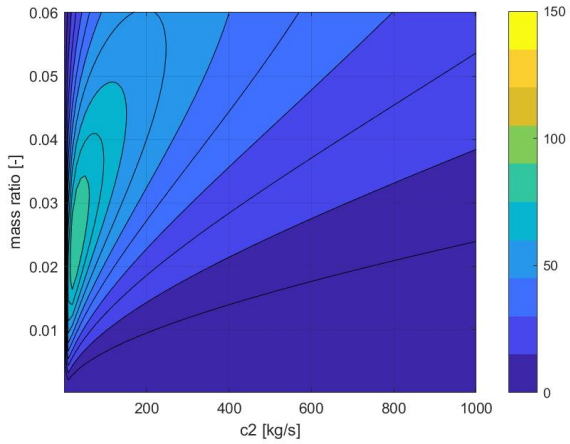

(a) Energy harvested [J]

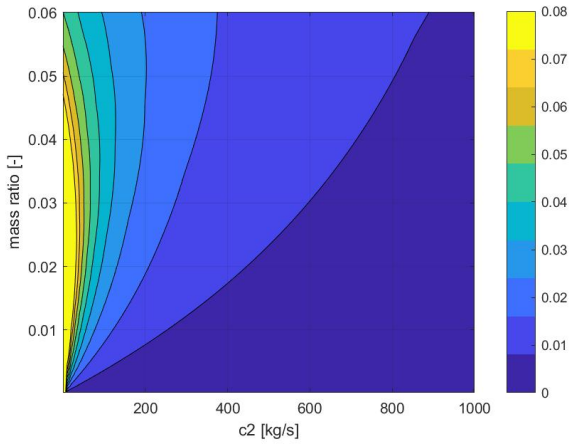

(b) Maximum occurring $|w2 - w1|$ [m]

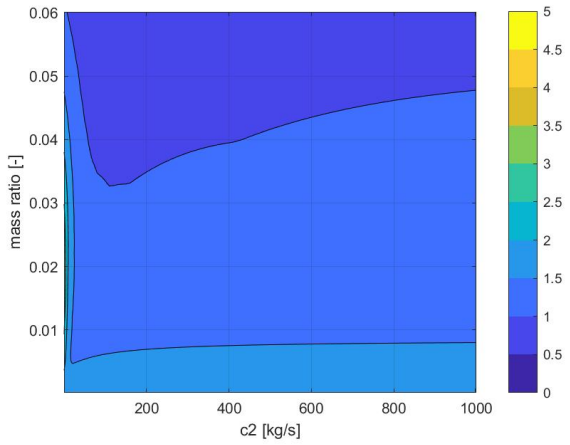

(c) Maximum deck acceleration $[m/s^2]$

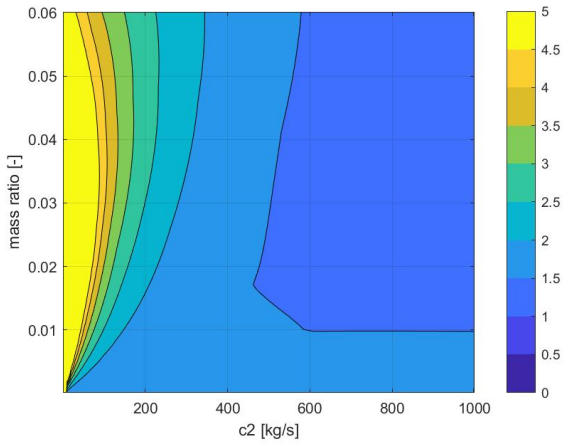

(d) Maximum TMD acceleration $[m/s^2]$

Figure 2.15: Model 3 response to a pedestrian crossing the bridge - $f_{step} =$ 1.80 Hz

Chapter 3

Analytical Model - Continuous Variant

In this chapter, an alternative to representing structures as SDOF (or TDOF) systems is presented: continuous beam theory. Using this more complicated method, we will investigate the validity and limitations of representing a bridge as an SDOF system.

The advantages of the SDOF representation are (relative) simplicity and free choice of loading function. However, is this representation still accurate enough if the system to be represented becomes more complex? More specifically, can the bridge deck with added energy harvesting dashpots on both sides be reasonably approximated by Model 2 from the previous chapter? Or is a continuous model (Model 4) required?

3.1 Continuous Model Theory

In order to analyse a beam as a continuous system, rather than as an SDOF system, the following fourth-order differential equation is needed. For a derivation, see (for example) [14]. Note that a prismatic beam is assumed, i.e. the structural properties do not vary with x.

$$\rho A \frac{\partial^2 w(x,t)}{\partial t^2} + EI \frac{\partial^4 w(x,t)}{\partial x^4} = q(x,t) \tag{3.1}$$

This equation is most commonly used in its static form, i.e. without the leftmost term. For this application, however, the dynamic term is kept: we are dealing with vibrations, after all. A valid simplification that can be made in this case is that the right-hand side is equal to zero: no body forces are present. The only force is the point load due to a pedestrian, which is included as a boundary condition.

It should be noted that because a point load has to be included as a boundary condition, multiple 'fields' are necessary to fully describe the bridge, each with its own fourth-order DE and boundary conditions. Linking these fields properly (e.g. no sudden change in slope) requires appropriate interface conditions.

To simplify the analysis, only half of the bridge will be considered, with the pedestrian load always applying in the middle. The situation that will be modelled can be seen in figure 3.1. In this figure, *x0* indicates the location of the dashpot with respect to the left support. Note that because of symmetry (symmetric bridge under symmetric loading), the slope in the middle will always be zero. This is shown in the figure, and will also be seen later on when defining the system's boundary conditions.

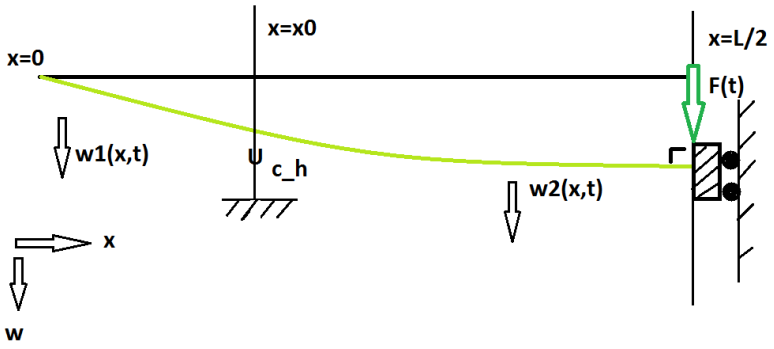

Figure 3.1: The continuous representation of the bridge that will be considered

The main limitation to this approach is that only a simple sine load (with

angular velocity ω) allows us to solve the DE analytically:

$$F(t) = G_0 \sin(\omega t) = G_0 \sin(2\pi f t) \tag{3.2}$$

Another limitation is that only the steady-state solution can be found, *not* the transient response. Furthermore, neither shear deformation nor rotational inertia are taken into account. This is justifiable, however, for slender beams vibrating at a low frequency [14]. Another limitation that is specific to continuous beam theory is that the inherent damping in the bridge deck is not accounted for.

So, what exactly does this type of analysis offer? The main advantage over the earlier SDOF models is the ability to investigate the influence of the location of the dashpot ($x0$). If an SDOF model yields a certain optimal value for c_h, how would that translate to an actual dashpot at a certain position? The aim of this analysis is to find relation between the 'actual' damping coefficient at a certain position, and the 'idealised' damping coefficient in the corresponding SDOF system. Another advantage of Model 4 with respect to Model 2 is that it allows for the fact that the velocity of the dampers is not quite the same as the velocity of the bridge deck at midspan. This influences the amount of energy that can be harvested, as well as the overall system response.

Using separation of variables, it can be shown that for each field i, the steady-state solution is given as [14]:

$$w_i(x) = A_i \cosh(\beta x) + B_i \sinh(\beta x) + C_i \cos(\beta x) + D_i \sin(\beta x) \tag{3.3}$$

Where β has been defined as follows:

$$\beta^4 = \frac{\rho A \omega^2}{EI} \tag{3.4}$$

Before we can find the values of the coefficients above, proper boundary and interface conditions have to be defined. The specific BC's and IC's that

were applied are discussed in the next section. It should be noted that in order to calculate β, the following values were used: $\rho A = 182$ kg/m and $EI = 2.58 \cdot 10^7 N \cdot m^2$. These values were taken from [11].

3.2 Model 4 - bridge deck with added dashpots, continuous representation

In order to find the analytical steady-state solution for the bridge deck after adding an additional dashpot (as was done for Model 2), the following boundary conditions were applied. Note that in equation 3.6, only *half* the static weight G_0 of a pedestrian is used. This is because only half the bridge is being modelled, as explained earlier.

$$x = 0 \begin{cases} w_1 = 0 \\ \frac{\partial^2 w_1}{\partial x^2} = 0 \end{cases} \tag{3.5}$$

$$x = \frac{L}{2} \begin{cases} \frac{\partial w_2}{\partial x} = 0 \\ EI \frac{\partial^3 w_2}{\partial x^3} = -\frac{G_0}{2} \end{cases} \tag{3.6}$$

At the location of the dashpot ($x0$), the following interface conditions have to be imposed to ensure the correct connectivity between the two fields:

$$x = x0 \begin{cases} w_1 = w_2 \\ \frac{\partial w_1}{\partial x} = \frac{\partial w_2}{\partial x} \\ \frac{\partial^2 w_1}{\partial x^2} = \frac{\partial^2 w_2}{\partial x^2} \\ EI \frac{\partial^3 w_1}{\partial x^3} - EI \frac{\partial^3 w_2}{\partial x^3} + c_h \frac{\partial w_1}{\partial t} \end{cases} \tag{3.7}$$

In total, this comes down to 8 equations (BC's and IC's) and 8 unknowns (the coefficients from equation 3.3 for both fields), which means the system can be solved. Once again, Maple was used to analyse this system.

The relevant parameters to monitor are the harvested energy, as well as the maximum acceleration that occurs in the bridge deck. Both are dependent on the chosen location for the dashpot ($x0$), the excitation frequency (ω), and the damping coefficient of the harvester (c_h). It should be noted since we are no longer using a realistic loading function, these results do not represent the bridge's predicted behavior in practice. Rather, the *influence* of the dashpot location on harvested energy and maximum deck acceleration will be investigated.

In order to obtain the harvested energy, the same method as before is followed (equation 2.19). In this case, we have:

$$E_{harvested} = 2 \int_0^{\frac{L}{v}} c_{harvester} \left(\dot{w}(x0)\right)^2 dt \tag{3.8}$$

The multiplication by two in front of the integral is due to the fact that only half the bridge was modelled, with only one energy harvester. In reality, the bridge (obviously) consists of two halves, with two dashpots.

It should be noted that by evaluating this integral, the harvested energy during a period equal to the 'crossing time' is obtained, when the bridge is subjected to a simple sine load. This does not represent reality very well, and should not be interpreted as if it does.

3.3 Response to a sine load with $f = 1.75$ Hz

First, the frequency of the sine load that is present at $x = L/2$ is set to 1.75 Hz, such that a comparison with Model 2 can be made. For several values of x0 (i.e. several locations for the added dashpots), a graph can be found that relates the damping coefficient of the harvester to the energy that is harvested. For consistency, the harvested energy from $t = 0$ up till $t = L/v_{walk}$ is considered, i.e. the so-called crossing time. The results of this investigation are shown in the following figures, where x0 is varied from 1 to 9 meters.

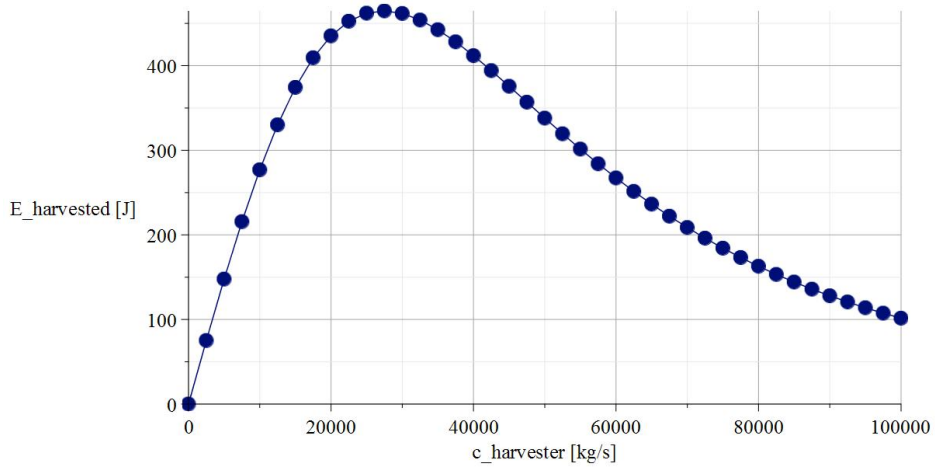

Figure 3.2: The total harvested energy versus the dashpot damping coefficient for $x0 = 1$ m and $f_{step} = 1.75$ Hz

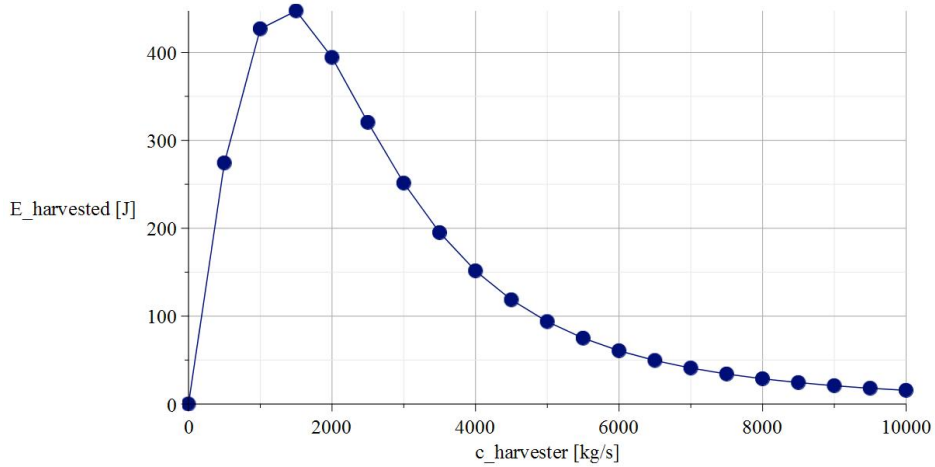

Figure 3.3: The total harvested energy versus the dashpot damping coefficient for $x0 = 3$ m and $f_{step} = 1.75$ Hz

Interestingly, for every $x0$, the shape in the E-c graph is similar. The peak value for the energy that can be harvested is almost constant as well. The optimal value of the harvester's damping coefficient, however, changes with its location $x0$. To further investigate this relation, a plot can be made showing the optimal value of $c_{harvester}$ versus the corresponding value for x0. This plot is shown in figure 3.7.

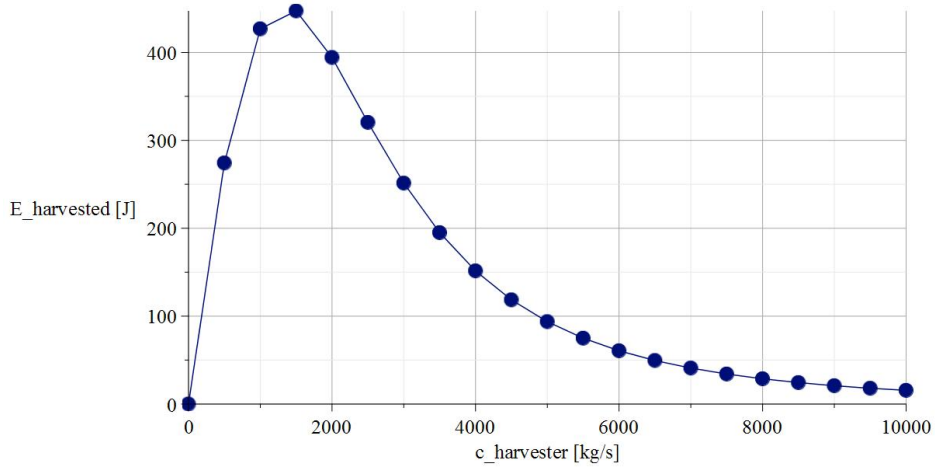

Figure 3.4: The total harvested energy versus the dashpot damping coefficient for $x0 = 5$ m and $f_{step} = 1.75$ Hz

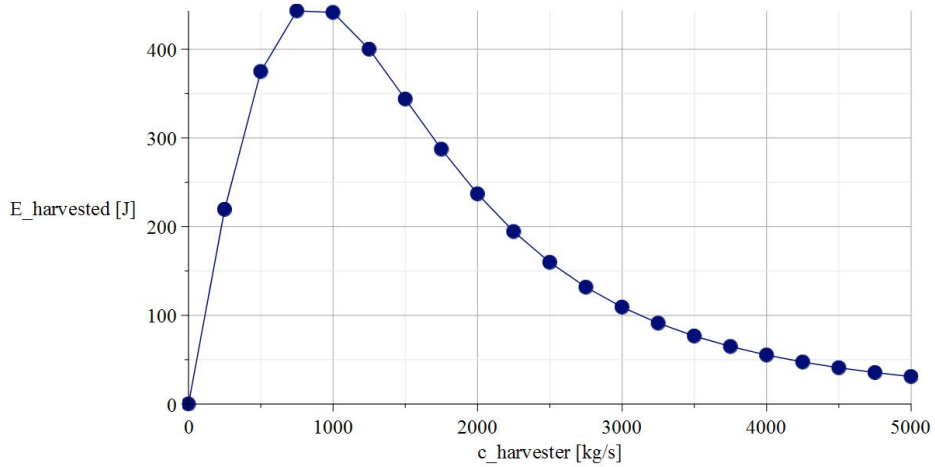

Figure 3.5: The total harvested energy versus the dashpot damping coefficient for $x0 = 7$ m and $f_{step} = 1.75$ Hz

Apparently, the further the dashpot is away from the middle of the bridge (for which $x = \frac{L}{2} = 9.52$ m), the higher the damping coefficient needs to be to allow optimal harvesting of energy.

This conclusion points towards an important practical limitation. When placing the dashpots within a couple of meters from the edge of the bridge,

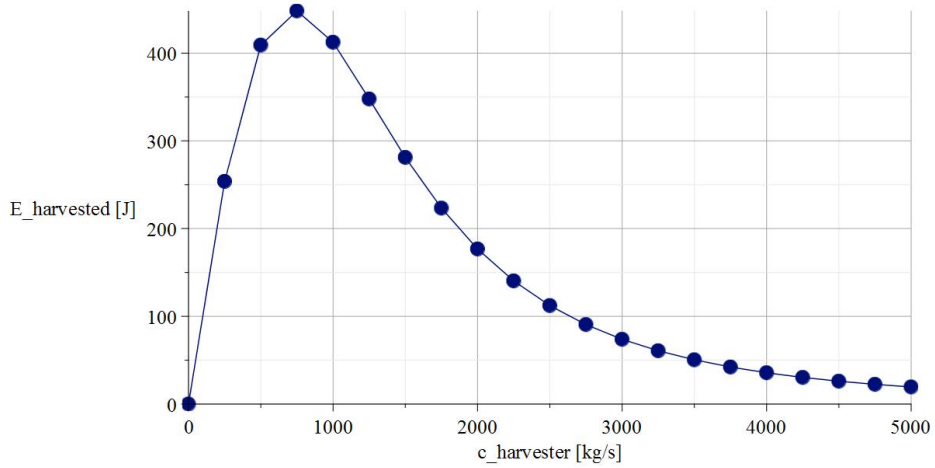

Figure 3.6: The total harvested energy versus the dashpot damping coefficient for $x0 = 9$ m and $f_{step} = 1.75$ Hz

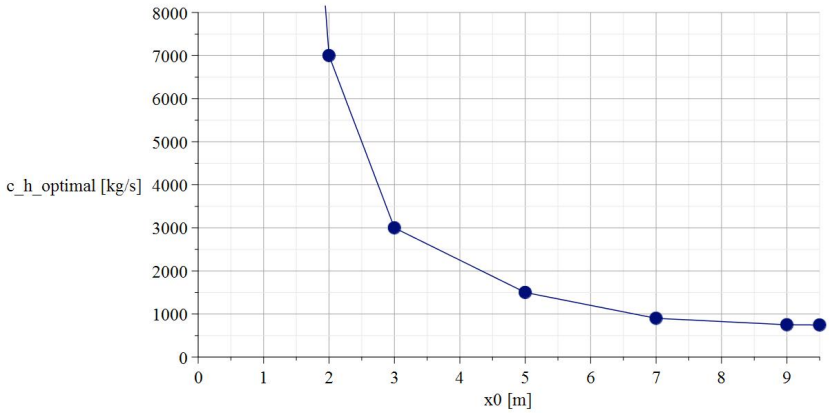

Figure 3.7: Optimal value for c_h vs the dashpot location x0, for Model 4 subjected to a sine load with frequency 1.75 Hz

such that they can be conveniently supported by the ground on either side of the water, a very high value of c_h is required to optimize the harvesting of energy.

If, on the other hand, a value of, say, x0=5m were chosen, the dashpot could no longer be supported from below. This means that either some column-like structure has to be added below the bridge, or a beam-like structure has

to be suspended alongside it, in turn supporting the dashpot. Both these options are far from ideal.

An interesting conclusion that revealed itself while analysing Model 4 is that the mid-span acceleration of the bridge deck - and thus $|a_{max}|$ - is constant for every value of x0, as long as the appropriate optimal c_h value is chosen. The value of x0 will not have any influence on the bridge's comfort levels, according to this model. This is somewhat problematic: it would be preferable to be able to objectively determine which values of x0 are more desirable than others.

3.4 Comparison between Models 2 and 4

Now that the response of Model 4 has been investigated, a parallel can be drawn with Model 2. The similarity is that both models described the basic bridge deck with added dashpots on either side of the middle. There are some key differences as well. First of all, Model 2 was subjected to the loading function that corresponds to a person walking across the bridge. Model 4, on the other hand, can only be analysed for a simple sine load. The second difference is that Model 2 does not specify the position of the dashpots, nor their actual value: only an optimum *effective* value was obtained. This difference is similar to the difference between the actual mass of the bridge deck and the effective (equivalent) mass that one uses in an SDOF representation.

To overcome these differences, Model 2 can be slightly altered to allow for better comparison with Model 4. First, the inherent damping of the deck will be assumed to be non-existent. Second, the load that the bridge is subjected to is chosen to be the same simple sine load as used for Model 4.

For Model 2, a plot of the harvested energy versus the damping coefficient of the harvester can be obtained after applying those adaptations, similar to figure 2.12. This figure is shown below.

The first thing one might notice is that the simple sine loading function (with an amplitude of $G_0 = 737\,N$) allows for far more energy to be harvested than the more realistic loading function considered in chapter 2. This is as

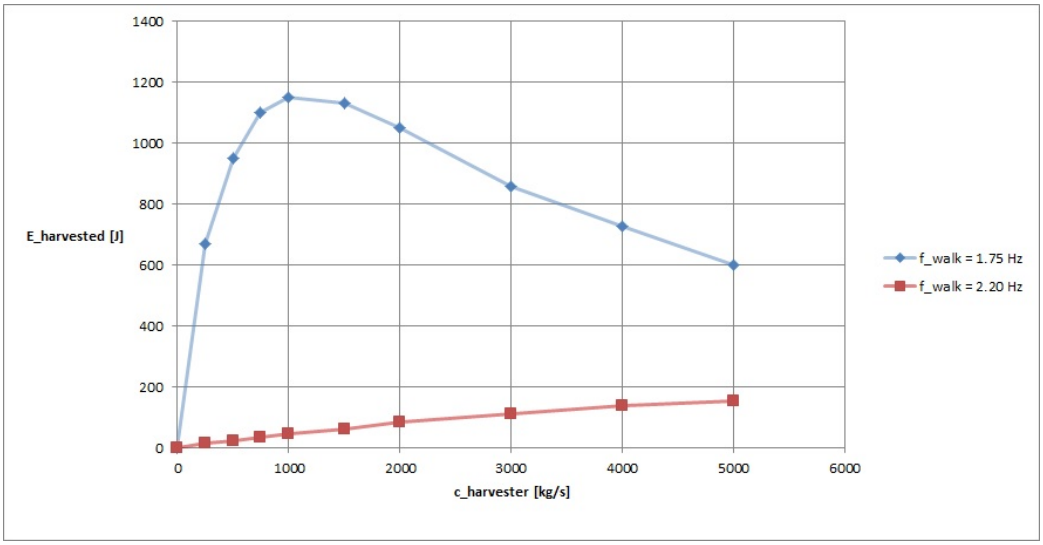

Figure 3.8: Gross harvested energy versus damping coefficient for Model 2, adapted for comparison with Model 4

expected.

As for the optimal dashpot damping coefficient for a step frequency of 1.75 Hz, this is about 1150 kg/s. Looking back to figure 3.7, this value is in fact about 20% higher than the optimum value that c_h approaches as $x0 \rightarrow \frac{L}{2}$.

When comparing the amount of energy harvested, the adapted Model 2 predicts 2 to 3 times more energy to be harvested than what is predicted by Model 4 (for a step frequency of 1.75 Hz). A possible cause for this difference is differing natural frequencies for both models. While determining the natural eigenfrequency for Model 2 is simple (as explained in chapter 2, that is not the case for Model 4. If both models would have a slightly different eigenfrequency, comparing the energy that can be harvested for a load with a set frequency might not be entirely fair. Specifically: it is possible that the eigenfrequency of Model 4 is somewhat higher than 1.68 Hz, thus causing the load with a frequency of 1.75 Hz to be closer to resonance.

3.5 SDOF vs Continuous Modelling - conclusions

After having applied dynamic continuous beam theory to the energy harvesting bridge, some clear downsides of this approach have been identified. These are as follows:

- Only a simple sine loading function could be used, which is not very realistic
- The inherent damping (and thus, the energy dissipation) of the bridge deck cannot be taken into account
- The fact that only the steady-state response can be found is a significant limitation; a relatively large part of the time in reality, the deck will behave as if in its transient regime
- The mid-span acceleration of the bridge deck does not depend on the value of x0, given optimal c_h
- No one-on-one relation between Model 2 and Model 4 could be established, even when fixing a certain value for x0

Because of these downsides, the continuous beam approach seems to have limited value in predicting a real-life structure's dynamic behavior under real-life loading.

What it does offer, however, is a better quantitative understanding of the influence of the dashpot location (x0) on the response. Overall, the analysis of Model 4 seems to indicate some potential problems when relying on the 'two-dashpot design' from Model 2: an SDOF representation is not linked one-on-one to the practical situation if such a design were to be implemented. This indicates the need for finite element modelling to check any design that is arrived at using the SDOF modelling. The next chapter is dedicated to such FE models. A more complete discussion of the merits and drawbacks of the 'two-dashpot design' will be given in section 5.2.1.

Chapter 4

FEM Models

Now that both SDOF and continuous analytical models have been discussed, the logical next step is to use the finite element method (FEM). FEM provides maximal options in what we can model (e.g. geometry-wise), but making changes in the models is quite cumbersome and labour-intensive. That is why design choices are made, and parameter-studies are performed, using the models shown in the previous chapters. Once a design has been arrived at, it can be modelled using FEM in order to validate and further analyse it. For this thesis, DIANA FEA 10.2 will be used.

In this chapter, first the approach taken to building the models is discussed. This includes (amongst others) obtaining properties for the model, deciding upon element types, and choosing the proper analysis options. Next up, Models 5 and 6 are introduced as being the FEM-equivalent of Models 2 and 3, respectively. Preliminary values will be selected to 'try out' these models, and the corresponding preliminary results will be presented.

4.1 Approach and approximations

The finite element method is a very flexible, powerful tool which enables the modelling of almost any kind of structure. It is, however, also a sensitive tool

that should be used with care. Modelling a structure can be done in many different ways, all with their own pros and cons. In this section, the most important modelling choices that were made in this thesis are discussed.

4.1.1 Element types

The first choice - as is often the case when modelling - is whether a 2- or 3-dimensional model will be created. We are interested in the in-plane vibration behaviour of the bridge. Out-of-plane effects, like wind loading from the side, will be ignored in this analysis, as their effect is only minor compared to the main source of vibration (i.e. in-plane pedestrian loading). A major advantage to this simplification is that we will not need full 3D solid elements to model the bridge; solid elements are notoriously computationally expensive.

This brings us to the second choice: what kind of elements do we use to accurately model the bridge's behaviour? A major consideration is that the bridge deck is far from uniform throughout its cross-section: rather, it contains a non-isotropic box-like structure. Even more advanced 2D elements, such as plane stress elements, might not even be able to accurately represent the non-uniformity in the cross-section properly. Rather than attempting this, a choice for 2D beam elements is made, i.e. an 'averaged' homogeneous representation of the non-homogeneous cross-section is used. Specifically, the L6BEN element will be used [5]. A picture of this element can be seen in figure 4.1.

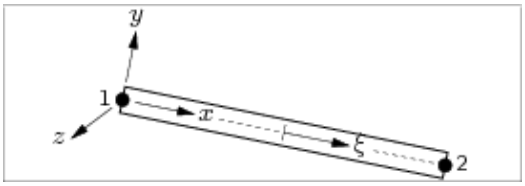

Figure 4.1: The L6BEN element: straight, 2 nodes, 2D [5]

The L6BEN elements is a so-called class-I beam element. This means that it is based on the Bernoulli beam theory, which does not take into account shear deformation. For relatively small loads, that easily remain under ULS

conditions, this seems acceptable. As for the element size, about 0.25 meters will be used. This means that the ratio of element size over bridge length is about 1/40.

Besides the bridge deck, we want to be able to model springs, dashpots and point masses as well. This would allow not just representing the deck as is, but also applying the possible adaptations already investigated in earlier chapters. In DIANA, there are specific elements that can be used for this purpose. The 2D spring and/or dashpot element that will be used is SP2TR, a two-node translational element, which is shown in figure 4.2.

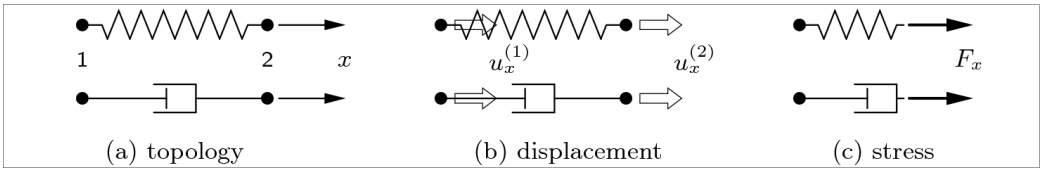

Figure 4.2: The SP2TR element: 2 node translational spring/dashpot [6]

Finally, a tuned mass damper can be represented by a point mass, which requires the PT3T element. [21]. This element allows specifying the mass and damping for each direction. For this application, the mass is considered to be the same in all directions. The damping of the PT3T is set to zero, as it is already accounted for by other elements.

4.1.2 Analysis options

The main analysis that will be performed by DIANA is a 'Structural Non-linear' analysis. For such an analysis, the types of non-linearity that will be taken into account have to be specified. In this case, there is no physically non-linear behaviour, since no fracture (nor plasticity) occurs. All non-linearity stems from physical movement as time progresses: geometric non-linearity. Another option that has to be specified for a dynamic analysis (where momentum and velocity of each element play a role as well) is the option for 'Transient Effects'. Turning this option on - as well as the 'Dynamic Effects' option within - ensures that both the mass and the damping matrices are taken into account in the equations of motion. The Rayleigh damping - if specified as a material property - is also included by doing so.

It should be noted that this 'Structural Nonlinear' analysis is not just an eigenvalue analysis that determines the eigenfrequencies and eigenmodes of the structure. Rather, the actual movement of all points within the structure - as well as all relevant velocities, stresses, etcetera - is tracked throughout time. This is especially useful because we are not dealing with a simply periodic loading, to which there would be a steady-state solution. Transient effects cannot be ignored.

As for the loading that will be considered: there is not really a feasible way to incorporate a moving load into a DIANA model when using beam elements. Therefore, the same correction function $\gamma(t)$ as before will be used, and the corrected load will be applied in the middle of the bridge.

Another thing that has to be specified when running a FEM analysis, is the desired output. In this case, we are mainly interested in the time-history of the location, velocity and acceleration of each node. With that information, the bridge's dynamic behaviour is fully described, and we are able to obtain the harvested energy using the same methods as before. Possible outputs such as the stresses could be easily obtained too, of course, but do not offer additional insight.

All analysis settings are contained in a 'command file' (`.dcf`), which DIANA can output. The contents of this file can be found in Appendix B.

4.1.3 Geometry and material properties

Before any of the analyses mentioned above can be performed, all the relevant parameters have to be specified. For the L6BEN element that will be used for the bridge deck, DIANA asks for the cross-sectional area and the moment of inertia (around the out-of-plane z-axis). These are element geometry properties. Other defining characteristics of the bridge deck - material density, E-modulus, Poisson's ratio, and (if required) Rayleigh damping parameters - are all specified as material properties.

Note that once again, the bridge deck will be modelled as being prismatic, i.e. constant properties along the beam.

What we know about the bridge deck properties is listed below:

- The length of the deck is 19.04 m
- The mass per meter of the deck is assumed to be 182 kg/m [11]
- $EI = 2.58 \cdot 10^7\,\mathrm{Nm}^2$ [11]

At this point, we run into a problem. The finite element model asks for material properties for the beam element, while in reality the bridge deck is a sandwich-like structure made up of a highly orthotropic composite material. Therefore, no exact material properties can be derived for the finite element representation. At best, a more or less 'average' value can be chosen for E, ρ, and ν. However, they can be picked such that the 'combined' properties, such as EI and the mass per meter (which is ρ times the area A), are kept as determined earlier. The following values were assumed :

- The Young's modulus E of the bridge deck is assumed to be 40 GPa [22]
- The density of the deck is assumed to be 1670 kg/m^3 [23]
- The Poisson's ratio ν of the deck is assumed to be 0.2 [23]

Having made the above assumptions, the following parameters can be derived from the known 'combined' properties mentioned above.

- $A = 0.109\,m^2$
- $I = 6.45 \cdot 10^{-4}\,m^4$

However, when the eigenfrequency of a system with these parameters is checked in DIANA (by means of an eigenvalue analysis), we find that $f_0 =$ 1.62 Hz. This is lower than the 1.68 Hz that followed from experimental data. The easiest way to fix this issue is to change the element geometry of the bridge deck. Since the model's eigenfrequency is 3.6% lower than it should be, the cross-sectional area of the bridge deck has to be multiplied by a factor

$(1 - 0.036)^2 = 0.93$. This leads to a corrected value: $A = 0.1014\,m^2$. A new eigenvalue analysis shows that after applying this correction, $f_0 = 1.68$ Hz, as it should be.

The internal structural damping of the bridge deck can be incorporated into the finite element model as well, by making use of Rayleigh damping. Rayleigh damping assumes a damping matrix that is a linear combination of the mass matrix and the stiffness matrix:

$$\mathbf{C} = a\mathbf{M} + b\mathbf{K} \tag{4.1}$$

The values for a and b are calculated as follows. An eigenvalue analysis provides the first two eigenfrequencies, f_0 and f_1. Multiplying by 2π gives us ω_0 and ω_1. The natural damping ratio of the bridge deck (ζ_{deck}) is still assumed to be 1%, as explained in section 2.3.3. Then, the following formulas can be filled in:

$$\alpha = \frac{\omega_0}{\omega_1} \tag{4.2}$$

$$\beta = \frac{(1 - \alpha)\zeta_{deck}}{\omega_1 - \alpha\omega_0} \tag{4.3}$$

$$a = 2\omega_0\omega_1\beta \tag{4.4}$$

$$b = 2\beta \tag{4.5}$$

In DIANA, the Rayleigh coefficients a and b can be specified as material properties. In this case, we find:

- $a = 0.163\,s^{-1}$
- $b = 3.92 \cdot 10^{-4}\,s$

Finally, the parameters of the proposed adaptations to just the bridge deck have to be determined. Since those elements are not made up of a material in the traditional sense, their only input is the spring stiffness and the damping coefficient, or simply the mass in case of the TMD element. How those parameters are determined is discussed in sections 4.2 and 4.3, respectively.

All the parameters mentioned in this section, as well as the overall shape of the bridge deck and more, are defined in the DIANA input file (`.dat`). The contents of this file can be found in Appendix C.

4.2 Model 5 - FEM model with extra dashpots

The first finite element model that will be discussed is a continuous version of the SDOF Model 2. It is very similar to Model 4, which is also continuous, but analytical. However, with the FEM model there are fewer restrictions on the loading. The main geometrical difference between Models 4 and 5 is the fact that Model 5 includes the curvature of the bridge. The Exercitiebridge does not have a very high curvature, as can be seen in figures 1.3 and 1.4, but it is there nonetheless, and it might influence the vibration behaviour of the system. Being able to incorporate such 'details' is a clear advantage of FEM over analytical methods.

The parameters specific to this Model 5 are the dashpot damping coefficients, and the location at which the dashpots are attached to the bridge deck. As in the chapter 3, these parameters will be referred to as c_h and $x0$, respectively.

As discussed in chapter 3, it was not possible to arrive at a (realistic) optimal design point using Model 4. As a starting point for this FEM analysis, a desirable value for $x0$ will be chosen, and the value of c_h will then be tweaked to ensure an acceptable maximum acceleration level at mid-span.

For $x0$, I have opted to use a value of 3 meters. Less than that will most likely lead to the issues discussed in Chapter 3. More than that would impose a rather stringent requirement on the available ground area underneath the bridge, and would detract from the system's universal applicability.

Based on figure 3.3, a preliminary value of 1500 kg/s was chosen for c_h. This might not be fully optimized, but it should give a good first impression of this model's behaviour.

Running DIANA using the preliminary values mentioned above, and analysing the program's output, we find that $|a_{deck,\,max}| = 1.77\,m/s^2$, and $E_{harvested} =$ 77 J. Again, this value of the harvested energy is the *gross energy per crossing*. The full response of Model 5 can be seen in figure 4.3. As expected, the vibrations at $x = x0$ and at $x = L/x$ are fully in-phase.

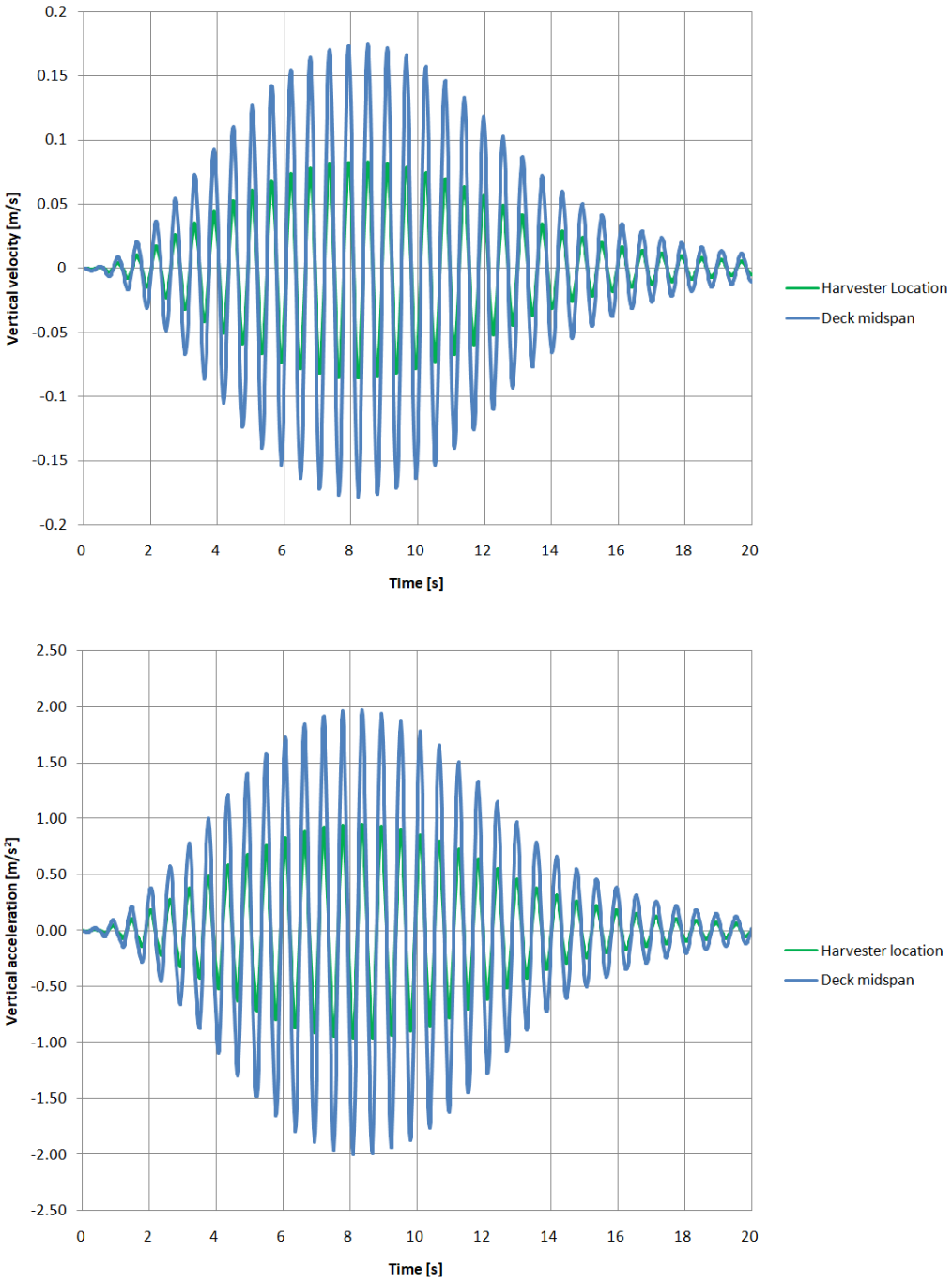

Figure 4.3: The results for Model 5, using $x0$=3 m and $c_h = 1500$ kg/s

4.3 Model 6 - FEM model with TMD

The second finite element model corresponds to Model 3, which was a 2-DOF system that was analysed using a state-space representation in MATLAB. It consists of the bridge deck and a TMD at midspan.

Just as for Model 3, the parameters to be determined are the dashpot damping coefficient c_h and the mass ratio $\bar{m}$. Again, from the chosen mass ratio, we can easily determine the spring stiffness for the TMD-spring, and the mass of the TMD itself. These will be referred to as k_{TMD} and m_{TMD}, respectively.

Based on the figures in section 2.7, the following values were chosen for preliminary investigation using DIANA:

- $m_{bar} = 0.02$
- $c_h = 100$ kg/s

Note that these values are a *preliminary* choice; they should provide a rough idea of what the final design will look like and how it will behave, but these values are not optimally fine-tuned as of yet. The resultant behavior of the optimized system will be shown in Chapter 5, after all design choices that need to be made have been discussed and implemented into this model.

The mass of the tuned mass damper (m_{TMD}) is equal to the chosen mass ratio multiplied by the modal mass. The modal mass can be found in the `.out` file that DIANA provides after running an eigenvalue analysis of just the bridge deck. In this case, the modal mass was found to be 1626 kg.

After running the analysis with the aforementioned preliminary parameters, and analysing the output, we find that $|a_{deck,\,max}| = 1.62\,m/s^2$, and $E_{harvested} = 83$ J. Note that the harvested energy is for one person crossing the bridge, and assuming 100% energy conversion efficiency for the energy harvester - let us call this outcome the gross harvested energy per crossing. In chapter 6, a more realistic estimate for the overall system efficiency will be given. The graphs corresponding to the analysis can be seen in figure 4.4. As expected for a tuned mass damper, the vibrations at of the bridge deck and the TMD's mass are out of phase.

Figure 4.5 shows the outcomes from Model 3 that were obtained using the same design values. As for the maximum deck acceleration and the harvested energy, MATLAB gives $|a_{deck,\,max}| = 1.52\,m/s^2$, and $E_{harvested} = 74$ J.

When comparing these models, it is clear that the 2-DOF model (Model 3) approximates the continuous case (Model 6) very well. This is due to the fact that the only adaptation that was made to the bridge deck - adding the TMD - was *exactly at midspan*, i.e. at the point that is being modelled in the 2-DOF approach.

Finally, it should be mentioned how exactly the amount of energy harvested was calculated for Model 6. In principle, we apply the integral from equation 2.19 again; this time, however, we are dealing with a numerical solution, so a Riemann sum was used to evaluate this integral. The figure 4.6 shows the data points for the squared relative velocity for the first few seconds. It is clear that the time steps ($\Delta t = 0.02\,s$) are sufficiently small for this Riemann approximation to be valid.

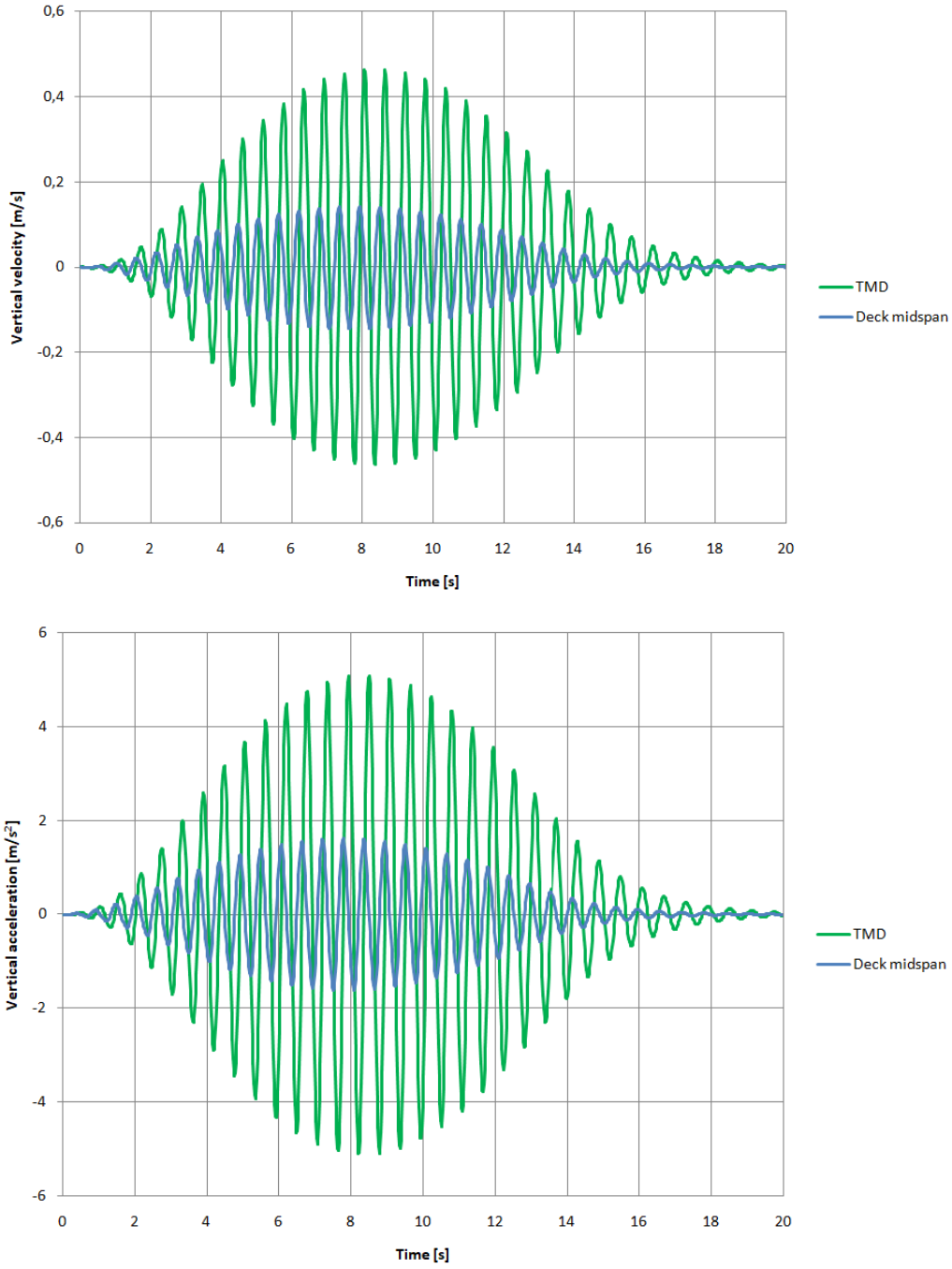

Figure 4.4: The results for Model 6, using $m_{bar} = 0.02$ and $c_h = 100$ kg/s

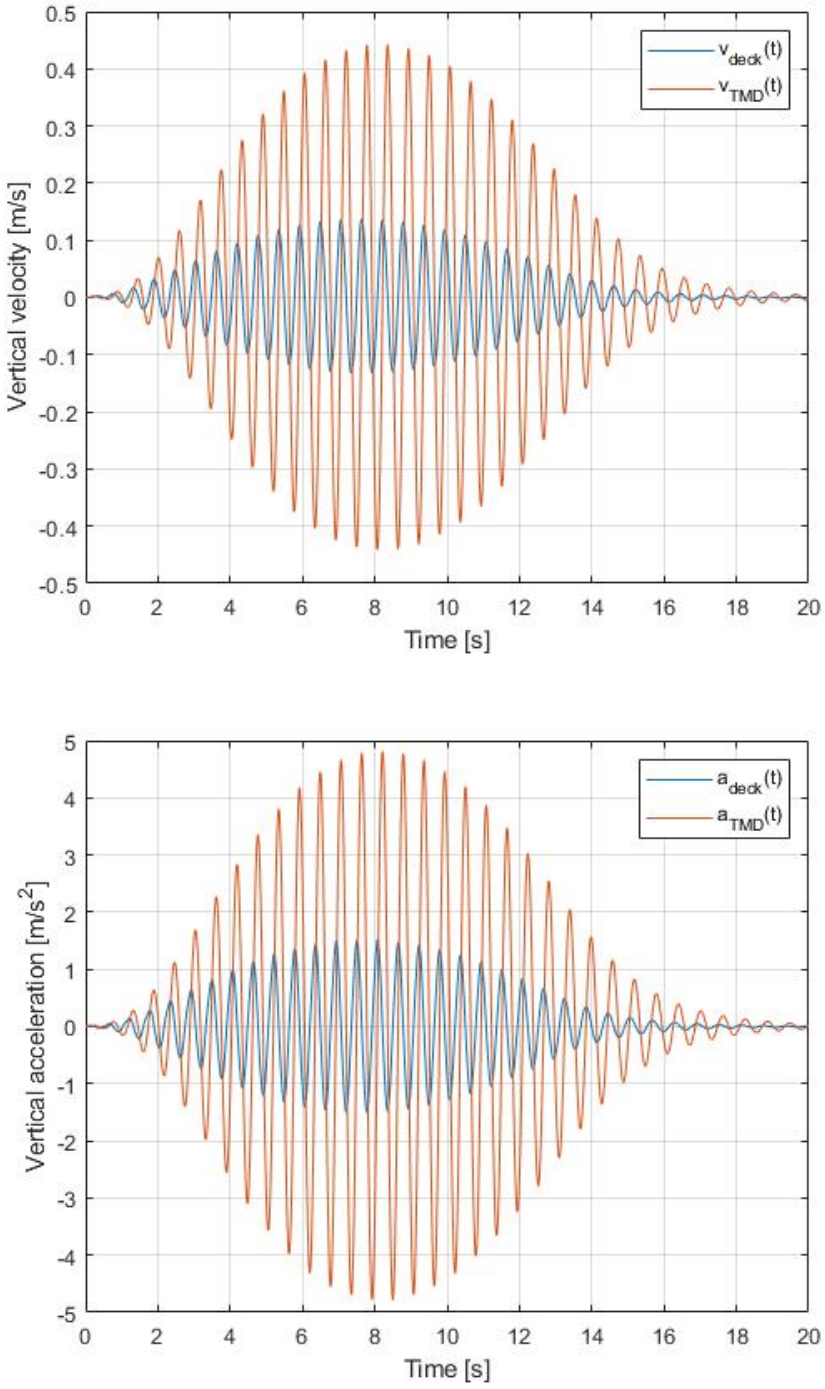

Figure 4.5: The results for Model 3, using $m_{bar} = 0.02$ and $c_h = 100$ kg/s

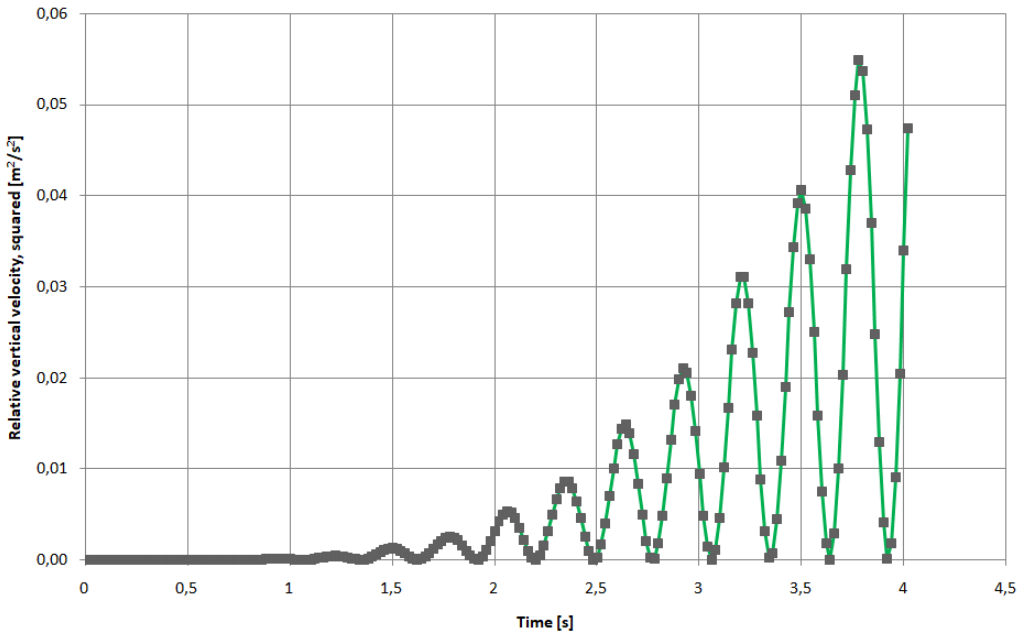

Figure 4.6: The squared relative velocity of the bridge deck w.r.t. the damper for Model 6, using $m_{bar} = 0.02$ and $c_h = 100$ kg/s

Chapter 5

Design Choices

Up until this point, as many parameters and design choices as possible have been kept open, in order to retain flexibility. In this chapter, a final design will be chosen, and some optimization will be done. The final design should be in the form of a continuous system, rather than in SDOF or 2-DOF form. This way, a direct, one-on-one translation to a real-world design can be made as easily as possible.

The first section of this chapter simply lists all the models that have been developed thus far, and briefly mentions aspects that are important to remember or to recall. Secondly, the pros and cons of both the 'extra-dashpot'-variants and the TMD-variants will be discussed, and a choice will be made regarding the final design type. In the third section, certain constraints and requirements on the design are formulated and decided upon. This includes the maximum allowable acceleration of the bridge deck. In section 5.4, the chosen final design is optimized, while respecting the aforementioned constraints. Also, as a demonstration of further possibilities, a system with two TMD's is modelled, and the results are analysed. Finally, the chapter is concluded by a table, showing the analysis results for different models and configurations, for ease of comparison.

5.1 Model Overview

For clarity's sake, a brief overview of all the models up till this point is provided in the following table. For more details about each model, including relevant assumptions that were made, please refer to its respective section (see Table of Contents or table 1.1 to locate those sections).

Table 5.1: Recap of all models used so far

Model	Type	Description
1	SDOF; analytical	Basic bridge deck
2	SDOF; analytical	Deck + extra dashpot
3	2-DOF; numerical	Deck + TMD
4	Continuous; analytical	Deck + extra dashpots
5	Continuous; FEM	Deck + extra dashpots
6	Continuous; FEM	Deck + TMD at midspan

5.2 Choosing a design type

The two main design options that have been investigated in multiple ways are as follows:

- Option 1 - Adding two dashpots, to the left- and to the right-hand side of the midspan point
- Option 2 - Adding a TMD at midspan

It should be noted that these two options are by no means the *only* two options available. For example, adding n TMD's to the bridge deck along the span might yield even better results. Unfortunately, the number of theoretical options is infinite. That is why in this thesis, proper investigation was limited to two simple designs, that would be relatively practical and cheap to implement in reality. we The two aforementioned design options each have their pros and cons, both from a theoretical and a practical perspective. These will be discussed next.

5.2.1 Option 1: Two-dashpot design

First, let us consider the design featuring two dashpots. As discussed before, a practical limitation is the fact that these dashpots have to be supported, at least in vertical direction. This is not always possible.

Another downside is the inability to influence the bridge's eigenfrequency after the dashpots have been placed. Even if the dashpots could be 'tuned' in-situ, such that their damping coefficient goes up or down, this will not have too much of an effect on the natural frequency of the system as a whole. This means that the design is not very adaptable, which might prove problematic. For example, if after installing the bridge the pedestrian loading frequency turned out to be higher than expected, there is not much that can be done to solve the issue. This would not lead to excessive deck acceleration, but it would undermine the bridge's ability to harvest energy optimally.

The most critical downside, however, is the fact that the damper's vertical velocity cannot be more than the velocity that occurs at midspan on the bridge deck. This is a practical upper limit that severely reduces the amount of energy that can be harvested. After all, the harvested energy is a function of the square of the relative velocity.

An advantage of the two-dashpot approach is that the required open space underneath the bridge is not compromised at all. Also, a land-based support for the dashpots means easy access for maintenance work when required. Furthermore, placing the dashpots halfway along the *width* of the bridge deck, they would be neigh invisible. Considering that one of the reasons for this project is the desire for slender, aesthetically pleasing bridges, this definitely counts as an upside.

5.2.2 Option 2: TMD design

Next, we consider the centralized tuned-mass damper design. A major advantage of such a design is that there is no longer a need for vertical support for the dashpot. The aforementioned scenario where a bridge connects two vertical quay walls would no longer be an issue.

Another advantage of this design is the possibility for easy tuning after installation of the TMD. In practice, fine-tuning is almost always done, no matter how good or accurate the initial design was. Since the spring stiffness is the thing being tuned, rather than the damping coefficient, this is quite effective. In fact, even the mass ratio can be modified after testing, if so desired. Simply adding or subtracting some of the metal plates that make up the TMD's weight is very possible as well.

Maybe the largest advantage is the fact that because the TMD and the bridge deck can move (more or less) separately, the *relative* velocity between the deck and the damper may very well exceed the deck's velocity at midspan. This is especially true when considering that the mass of the TMD is allowed to accelerate a lot more than the bridge deck - and thus, its velocity may be higher, too.

A downside of the TMD approach is the space it takes up. Not only does the TMD have some volume of its own, but it requires space to vibrate as well. Note that the exact amount of space needed for such vibrations can be estimated once a final design has been arrived at. The placement options are as follows: either the TMD is located below the bridge deck, which limits the space for boats passing underneath; or it is located (inside and) above the bridge deck, which limits the effective width of the deck at that point, and leaves less space for pedestrians.

If the choice is made to have the TMD be visible to pedestrians crossing the bridge, it could be argued that this is an upside rather than a downside. After all, one of the municipality's desires in this energy-harvesting initiative is to offer pedestrians 'something extra'. Being able to see that their footsteps excite the TMD's mass, for example through a clear plastic bell jar, could be interesting. This, however, is an aesthetic design choice rather than a technical one - technically, the TMD would perform its task equally well, no matter where it is placed.

5.2.3 Conclusion

Taking all of the above considerations into account, it seems like the design featuring a tuned mass damper would be most flexible in practice. It could

be applied to any slender footbridge, regardless of what is underneath the bridge. Furthermore, it allows easy adjustment after in-situ testing. By playing around with the models developed during this thesis, it became clear that especially near-resonance, the behaviour can change drastically with a slightly different excitation frequency. This makes theory-based designing for a real-world application inherently somewhat uncertain.

Because of these reasons, Option 2 will be designed and modelled in full detail.

5.3 Choosing design values

The main design values that will be chosen to go with Option 2 (a TMD added to the middle of the bridge deck) are, as discussed before, the mass ratio $\bar{m}$ and the maximum midspan acceleration of the bridge deck. 'Optimizing' these values means finding the right balance between maximum energy harvesting potential and sufficient damping of the bridge.

5.3.1 Maximum allowable acceleration

As for the maximum allowable bridge deck acceleration, there are a lot of design codes and guidelines specifying values for this. These codes usually ascribe certain values to different comfort classes, ranging from maximum comfort to unacceptable discomfort. For a more in-depth treatise of all different available codes, please refer to [16].

It should be noted that there are *no strict requirements* imposed on vibration levels, since managing these levels is purely a matter of user comfort. As long as the customer agrees, an engineer is perfectly allowed to design a bridge with a larger maximum acceleration value.

For this thesis, the guidelines according to EUR 23984 will be adhered to. The 'unacceptable discomfort' starts at a vertical deck acceleration of 2.50 m/s^2, so that is the value that I will aim for.

A major correction factor needs to be applied to that number, however. The so-called crowd loading enhancement factor m_G relates the occurring bridge deck acceleration under the influence of a single person crossing to the expected acceleration level when multiple people cross the bridge. Many different authors have proposed many different ways to approach this problem. Most authors have proposed enhancement factors that are either a linear or a root function of the number of people N that are on the bridge at the same time.

Complications arise quickly, because this factor depends on things like crowd synchronization and human-structure interactions, as well as the eigenvalue of the specific bridge that is dealt with. In fact, a realistic enhancement factor can only be obtained experimentally, after the bridge has been constructed. For a more detailed discussion of enhancement factors, please refer to [24].

For now, the factor proposed by Grundmann [25] will be used, since it assumed that there is only light traffic on the footbridge. In the case of the Exercitiebrug, this is definitely the case. Grundmann proposes:

$$m_G = 0.135N \tag{5.1}$$

This would mean that even when there are 10 people traversing the bridge simultaneously, a factor of only 1.35 should be taken into account. This seems rather low, especially considering the other options mentioned in [24]. To be on the safe side, an enhancement factor of $m_G = 1.5$ will be assumed for this thesis. This means that the maximum allowable deck acceleration - to still be considered 'allowable discomfort' by EUR 23984 - is:

$$|a_{deck,\,real\,use}| = \frac{|a_{deck,\,single\,person}|}{m_G} = \frac{2.50}{1.5} = 1.67\,m/s^2 \tag{5.2}$$

This value of 1.67 m/s^2 will be used as the maximum allowable deck acceleration when a single person crosses the bridge.

5.3.2 Mass ratio

The mass ratio between the damper and the modal mass of the bridge deck can be theoretically anywhere between 0 and 1 - in fact, it could be even higher if the TMD has a higher mass than the modal mass of the structure. However, in practice, a value of about 0.02 is common [19]. When looking at figures 2.14 and 2.15, which show the expected harvested energy as well as the expected deck acceleration for Model 3, it seems that $\bar{m} = 0.02$ would indeed allow for optimal energy harvesting. Furthermore, the 'penalty' in deck acceleration is not that high for choosing a low $\bar{m}$: even with a mass ratio like 0.02, the aforementioned deck acceleration of 1.67 m/s^2 will most likely not be exceeded. An upside of a relatively low mass ratio is that only a small volume is required to fit the TMD.

For these reasons, a mass ratio of 0.02 will be chosen for the final design.

5.3.3 TMD movement space

Besides the maximum allowable deck acceleration and the mass ratio, there is one other criterion that needs to be mentioned and investigated. Namely, the maximum occurring $|w2-w1|$ should be within reasonable bounds, otherwise the TMD will require too much free space to move up and down relative to the bridge. Figures 2.14 and 2.15 (b) show that this requirement is not too stringent; only for very low values of c_{TMD} at resonance, the 0.10 m threshold is exceeded. This 0.10 m (both above and below the TMD's resting state) seems very well possible to incorporate in the design of the TMD's casing. Higher values might prove problematic; if it turns out the optimal solution exceeds this threshold, a more elaborate evaluation will be performed on whether it is feasible in practice.

5.4 Results of the Optimization

Even though the results obtained by using the the preliminary design values were promising with regards to limiting the deck acceleration to an acceptable

level whilst harvesting energy, there might still be room for improvement. The earlier analysis from Model 3 has helped land at approximately the optimal design point, but fine-tuning the DIANA model might yield even better results.

Now that some more parameters have been fixed in the previous section, and some boundaries are imposed upon the desired solution, Model 6 can be optimized further by adapting the value for c_h. This process has been done by trial-and-error, with the earlier SDOF investigations as a helpful guideline.

After trying various different values, I decided upon using a lower damping coefficient for the TMD than the preliminary value, namely 25 kg/s. The results of this optimization attempt are shown in figure 5.1. Note that an even lower value for c_{TMD} did *not* turn out to lead to better results.

Summarizing the outcomes, we find that $|a_{deck,\,max}| = 1.50\,m/s^2$, and $E_{harvested} =$ 104 J. The optimization with regards to c_{TMD} has worked: a slightly lower deck acceleration has been achieved, as well as an increase in harvested energy. The only 'punishment' for this adaptation is the slightly larger space the TMD needs to move up and down: about 10 cm above and below the moving part of the TMD are required. In practice, some extra space needs to be allotted in case of multiple people crossing in unison, and a form of cushioning should be applied for when the displacement difference exceeds the expected values.

Again, figure 5.2 shows the outcomes from Model 3 that were obtained using the same (new) design values. In this case, MATLAB gives the values $|a_{deck,\,max}| = 1.39\,m/s^2$, and $E_{harvested} = 100$ J. As before, these results match the FEM results quite well, and they have indeed improved with the new values for c_{TMD}.

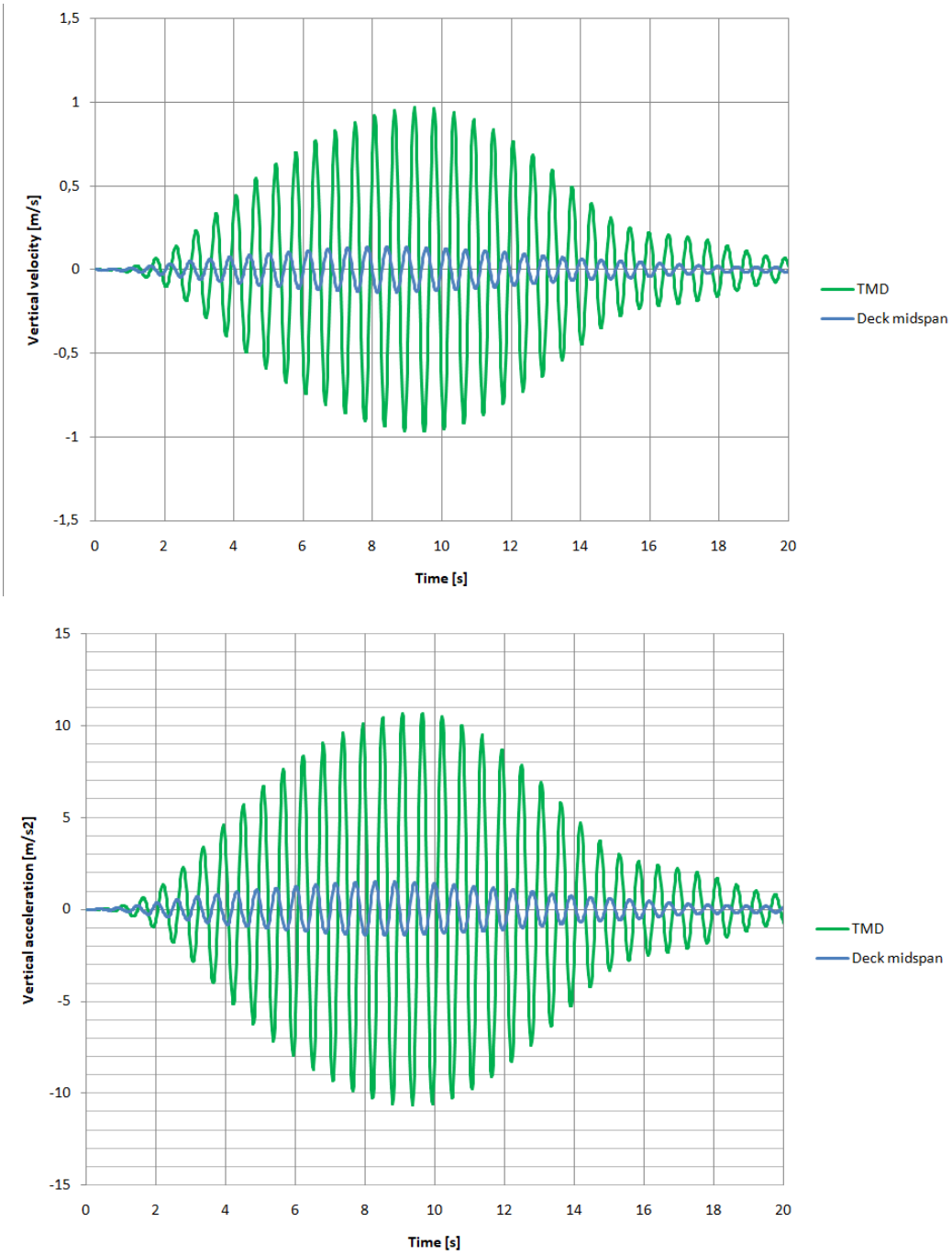

Figure 5.1: The results for Model 6, using $m_{bar} = 0.02$ and $c_h = 25$ kg/s

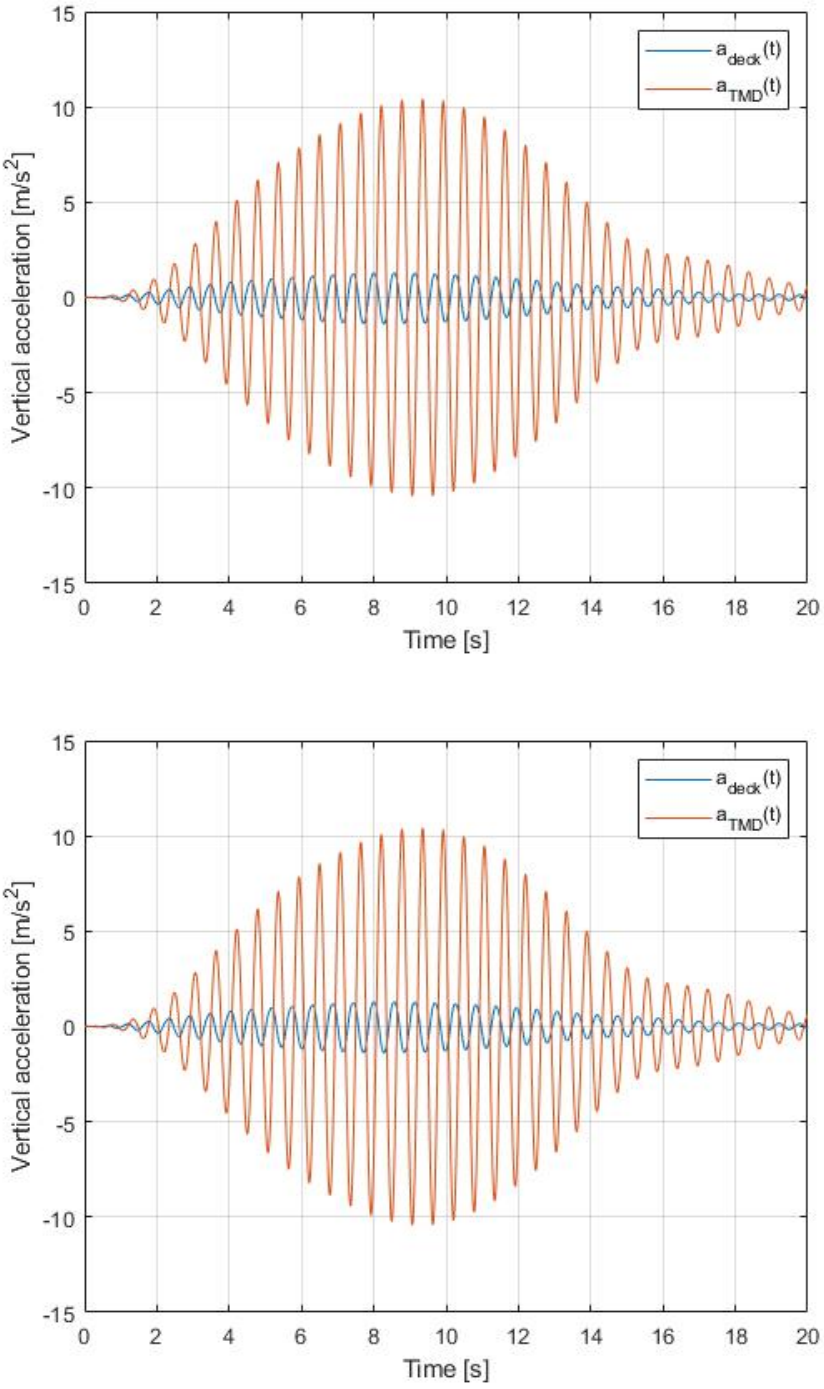

Figure 5.2: The results for Model 3, using $m_{bar} = 0.02$ and $c_h = 25$ kg/s

5.5 Alternate solutions

As already mentioned in section 5.2, the number of possible solutions is infinite if one does not limit the number of TMD's and/or dashpots that can be used. Therefore, in theory, it is not possible to find the 'perfect' solution.

In reality, practical reasons play a role in determining the allowable number of damping devices, of course: each device will cost extra money, so as few as possible should be placed. Normally, these TMD's tend to be positioned at the locations where the eigenmodes that occur most heavily have their peaks. To be more specific: in a simply supported bridge which is loaded at a frequency near the fundamental frequency, the first eigenmode is dominant. This first eigenmode is simply a half-sine, with the largest amplitude at midspan. This is why the one-TMD design placed the TMD exactly at midspan.

As an extra, preliminary investigation - somewhat outside the scope of this thesis - the results will be shown for 'Model 7', which has TMD's at locations $x = L/3$ and $x = 2L/3$, rather than the single TMD at midspan. For now, the parameters of the TMD's are chosen to be the same as the preliminary values that were chosen for Model 6: $\bar{m} = 0.02$ and $c_h = 100$ kg/s. Again, a step frequency of 1.75 Hz is employed.

The maximum deck acceleration that occurs is 1.32 m/s^2, and the gross energy that can be harvested for one crossing is 82 J.

It seems that there is definitely potential for a type of solution with multiple TMD's. Even with these preliminary values, the bridge deck's acceleration is kept well below the maximum allowable value. The amount of energy harvested is quite large as well, already performing better than Model 5. With proper optimization, this design might even outperform the single-TMD solution.

In fact, for large bridges, multiple TMD's are often employed in real-world projects (e.g. the Millennium footbridge in London features 50 vertical TMD's). An advantage is that different TMD's can be tuned to different frequencies, thus providing good performance under a wider range of excitation frequencies. A downside that should be mentioned, however, is that

installing more TMD's (including energy harvesting electronics) will cost more money - even if the individual TMD's can be smaller than a single large one.

Considering the scope of this thesis, suffice it to say that employing more than a single TMD is definitely worth looking into for larger bridges.

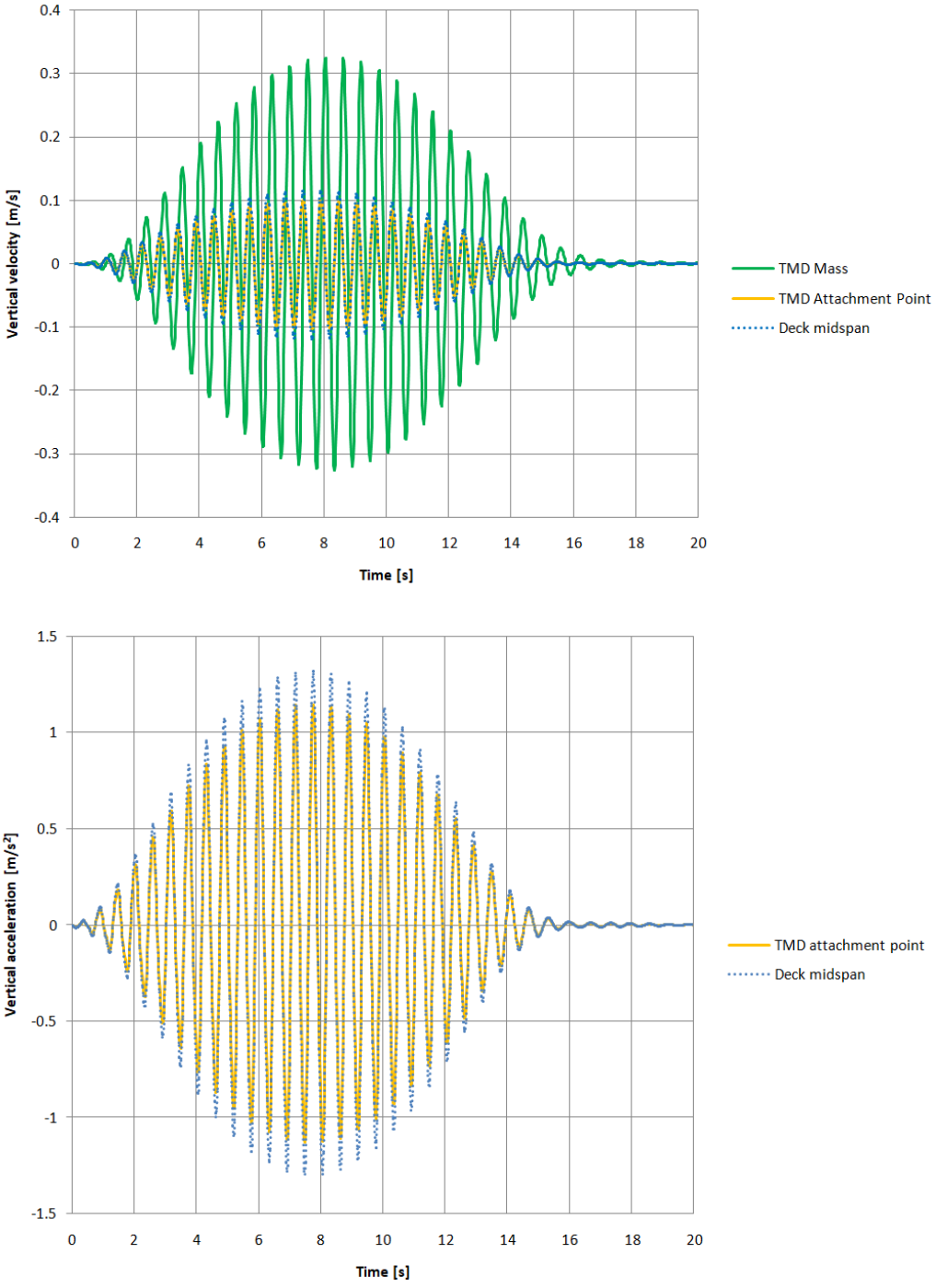

Figure 5.3: The results for Model 7, using $m_{bar} = 0.02$ and $c_h = 100$ kg/s

5.6 Comparison: Results Overview

For comparison's sake, the main results that were obtained using the FEM models are shown in the following table. This includes both the gross energy harvested per crossing (GEPC) and the maximum deck acceleration that occurred.

					Analytical		Numerical	
Model	f_{step} [Hz]	x0 [m]	$\bar{m}$ [−]	c_{harv} [kg/s]	$a_{deck,max}$ $[m/s^2]$	GEPC [J]	$a_{deck,max}$ $[m/s^2]$	GEPC [J]
5	1.75	3	-	100	-	-	2.75	12
5	1.75	3	-	1500	-	-	1.77	77
3 and 6	1.75	-	0.02	100	1.52	74	1.62	83
3 and 6	1.75	-	0.02	25	1.39	100	1.50	104
7	1.75	6.35	0.02	100	-	-	1.32	82

Table 5.2: Overview of all relevant FEM results

Chapter 6

Energy Harvesting System Design

In this chapter, the step from a theoretical solution back to the real world will be made. The simple, idealized dashpot that is present in both analytical and numerical calculations is a lot more complex in practice. Not only does it consist of a damper - which has to be carefully designed to closely match the theoretical damping properties - but it also involves several other electrical components. The term 'energy harvesting system' will be adopted to indicate this real-life combination of components.

This chapter starts with a brief introduction of all the relevant components of an energy harvesting system, starting from a typical electrical diagram. Next, two of these components will be elaborated upon a bit further: the (electromagnetic) damper and the energy storage device. For these two components, several options, requirements, and possibilities are discussed. Finally, some of the differences and similarities between a theoretical dashpot and a real-life energy harvesting system will be discussed, based on two research papers. This will provide insight into the real-world feasibility of the design from Chapter 5

6.1 Energy Harvesting System Lay-out

Energy harvesting systems have already been developed and tested by many different scientists and engineers. Most of the designed systems share approximately the same components. An example of a basic electrical circuit for a (passive) energy harvesting system is shown in the figure below.

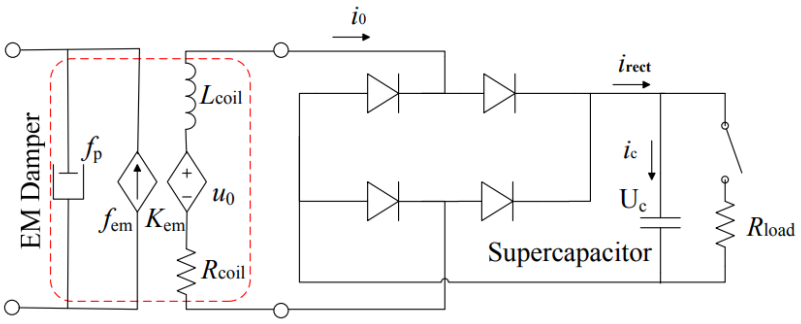

Figure 6.1: A basic configuration for an energy harvesting circuit [7]

As we can see, the basic circuit consists of:

- Electromagnetic (EM) Damper
- Wiring
- Rectifier (AC-DC converter; shown in the figure as four diode symbols)
- Power storage (such as the supercapacitor indicated in figure 6.1)
- A device utilizing the harvested energy (not necessarily always active), shown as R_{load}

Designing the actual energy harvesting system and circuitry is not a trivial task. In fact, there are many papers and studies dedicated exclusively to this design process (e.g. [9], [7], [8]). In this thesis, no such system will be designed in detail. Rather, a short discussion will be present for each key component, highlighting several realistic options. This will be followed by a discussion of theory versus reality with regard to energy harvesters.

6.2 EM Damper design

When performing calculations, it is very convenient and straightforward to include dashpots. However, some thought should be given to how these theoretical dashpots can most accurately be realized in practice. The two main characteristics that should be looked for in a real-world component fulfilling this role are:

- A (near-)linear relation between the damping force exerted on the structure and the velocity of the structure at that point (or, in case of a rotary damper, a linear relation between damping moment and rotational velocity)
- A non-zero hysteresis cycle, i.e. a way for energy to leave the main system (the bridge, in this case)

For this specific project, another requirement is that the energy that is taken out of the main system should not simply be dissipated into heat, but rather in a different form of energy. This eliminates the (commonly used) fluid-based viscous damper as an option, as well as lesser-used alternatives such as friction-dampers [26].

The most obvious - and likely the most practical - solution would be to employ an electromagnetic damper, which is able to convert mechanical energy to electrical energy. An intuitive way to think about this kind of damper is as a reversed electrical motor, i.e. an electrical generator. The basic principle employed by all types of electromagnetic dampers is that of Faraday's Law. Simply put, this law states that:

"The electromotive force around a closed path is equal to the negative of the time rate of change of the magnetic flux enclosed by the path." [27]

The most straightforward application of this law can be found in a so-called Faraday Flashlight. This is a simple flashlight that is powered by shaking a small magnet back and forth in the hollow handle, each time passing it through a coil of electrical wire. This induces a current in the wire, which powers a light bulb or LED.

More advanced devices that use the same principle are legion. We are interested specifically in a damper, however. Three different possible lay-outs of such a damper can be seen in figure 6.2. These images are somewhat simplified, but not by much. Note that while all these designs convert linear motion into electrical energy, (b) and (c) employ rotary generators and a means to convert linear motion into angular motion. An advantage of this conversion is the possibility to achieve higher frequencies than the excitation frequency, for example by means of a gearbox. This could improved the generator efficiency, since generators are optimized for a certain range of 'input' frequencies.

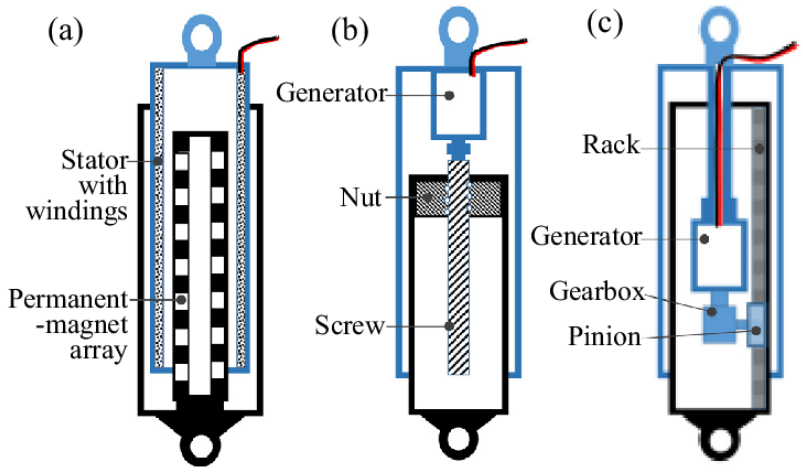

Figure 6.2: Three possible basic layouts for an electromagnetic damper [8]

Electromagnetic dampers are already being used in practice, for example in regenerative shock absorption in cars [28]. As mentioned before, they do not differ much from electromagnetic generators. It might very well be possible to find an existing EM damper that meets the requirements for a particular bridge.

6.3 Energy storage

In order to optimally make use of the energy that is harvested from the vibrating bridge deck, it is desirable that it does not have to be used imme-

diately. Being able to store this energy allows for a wider range of possible applications, as well as the option to provide a steady, averaged power output for a certain time. Such flexibility is provided by including an energy storage device in the energy harvesting system.

As discussed in the previous section, the electromagnetic damper converts mechanical energy intro electrical energy. Electrical energy, unfortunately, is not convenient to store. The only way to do so without converting to a different kind of energy - which always leads to losses - is by using a capacitor. Indeed, even a battery does not store electrical energy, but rather temporarily converts it into chemical energy. Note that since the final output of the system has to be electrical energy for most useful applications, a one-way conversion is not a valid option.

Besides capacitors and batteries, there are of course other methods of storing energy. For this particular application, however, these are a bit more far-fetched. For example, constructing an elaborate system where the electrical energy drives a pump, which pumps up water to a reservoir for potential energy storage, will likely lead to some practical issues. In general, the more components, moving parts and intermediate steps there are, the lower the final system efficiency will be. In other words, more energy will be lost. Because of this, only (super)capacitors and batteries will be considered in this section, which is in line with other research and projects involving energy harvesting (e.g. for Rome's energy harvesting backpack [29]). For an explanation of what supercapacitors are and how they work, please refer to [30].

The most important characteristics of a suitable energy storage device to use in the energy harvesting system are as follows:

- The device should be able to handle partial charging and discharging without suffering damage
- The cycle life of the device should be quite high, considering the long design lifespan of a bridge
- The device should be able to operate (both charge and discharge) at a wide temperature range - roughly from -10 °C to 40 °C

- The device should have a near-constant output voltage and power, for convenient and predictable use
- The device should be able to store energy for several hours (days, preferably) without too much leakage

The following common characteristics of energy storage devices are (nearly) irrelevant in this particular application, and should therefore **not** play a decisive role:

- The weight of the device: compared to the rest of the bridge, the weight of the energy storage device is negligible
- The charge time: there is no hurry to fully charge the device - the limiting factor will be the power harvested, not the maximum power intake
- The cost: compared to the total cost of a bridge, the cost of a suitable energy storage device will be negligible
- The voltage and current range: only low voltage and currents are applicable in this system

A battery would be able to fulfill most of the important requirements mentioned above. The most crucial consideration would be the limited cycle life. A typical cycle life for batteries is around 500 to 1,000 [31], which might not be enough to function for decades without needing a replacement. However, it should be kept in mind that a 'full cycle' will not occur in practice. Rather, the battery would be constantly slightly charged and slightly discharged. The effect of this kind of use on the lifetime is uncertain. Another possible downside is the required temperature range. For example, a standard Lithium-ion battery will not charge at temperatures below 0 °C [30]. This will either have to be accepted as a downside of the bridge, or a fitting battery will have to be found.

A supercapacitor, on the other hand, performs very well when it comes to serviceable temperature range and life cycles. Unfortunately, it runs into the

major issue of charge-dependent output voltage and power. This makes it far less suitable for a role as a power-source. Another downside - although not quite as critical - is increase leakage when compared to a battery. Some of the major selling points of a supercapacitor are, unfortunately, not relevant for this purpose: it boasts a very quick charge time and supports large voltages and power levels.

Summarizing, it seems like a battery would be the best option for storing energy in this particular energy harvesting system. Further investigation will be necessary to determine the effect of partial charging and discharging on the cycle life, so that the required cycle life to match the bridge's lifespan can be determined. Also, it should be investigated whether a type of battery can be selected that still functions at freezing temperatures.

6.4 Real-life Design and Performance.

As mentioned earlier in this chapter, the design of an energy harvesting system is not a simple process. Besides selecting the proper lay-out, there are many different parameters that influence performance and characteristics. Many of these design choices, in turn, influence each other. Because of this, building and testing one or multiple prototypes seems to be the norm. For this thesis, a discussion of some of the main results of several papers will have to suffice. This should be enough to get a feeling for what is - and what is not - within the realm of possibilities.

6.4.1 Jung

As a first example, we consider the paper by Jung [9]. In this paper, an energy harvesting system for cable structures is designed in detail. Such a design process is outside the scope of this thesis, and therefore some of the main findings of [9] will be used to decide upon the *feasibility* of using an electromagnetic damper for energy harvesting. Summarizing: for now it should suffice to determine whether realizing the desired damper is *possible*, rather than actually designing one.

An important result from Jung is shown in figure 6.3. This figure is based on testing the fabricated damper, so it shows the real-world behaviour of such a damper. It appears that there is an almost linear relation between the oscillation amplitude and the maximum damping force. The relation between the maximum damping force and the oscillation frequency, however, is not quite linear. Rather, it seems like there is a minimum required frequency for the damper to be effective. Also, above a certain frequency there are diminishing returns on the damping force. As Jung puts it: "When the excitation frequency exceeded 5 Hz, the change in the magnet flux reached saturation". [9]

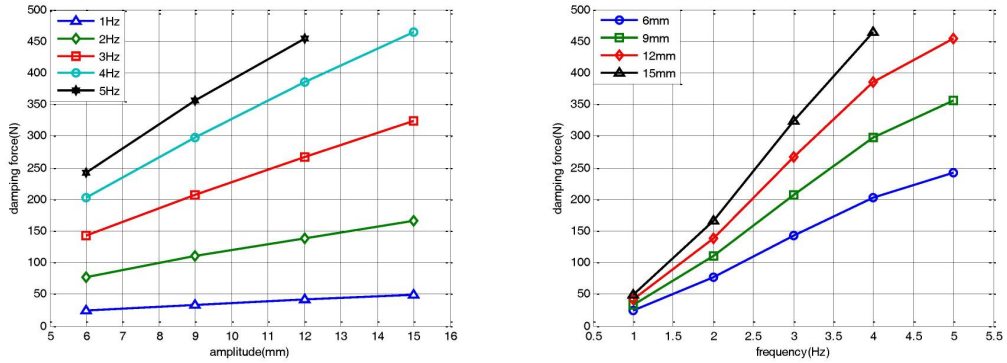

(**a**) Maximum damping force (amplitude change) (**b**) Maximum damping force (frequency change)

Figure 6.3: Experimental results for the fabricated EM damper subjected to an external harmonic load [9]

Another important figure from this paper is shown in figure 6.4. Here, we can see that the experimental hysteresis cycle is in fact very similar to what is expected based on theory (see for example figure 2.10). This is crucial, since the hysteresis is what makes a damper 'work', as explained earlier in this section. The plot of the displacement versus the damping force shows a near-linear relationship, which justifies the assumption made earlier in this thesis that we are dealing with linear viscous damping.

Summarizing: in the paper by Jung, it is shown that it is possible to build an energy harvesting system that:

- Exhibits a near-linear relation between the damping force and the velocity with which the magnets move through the stator

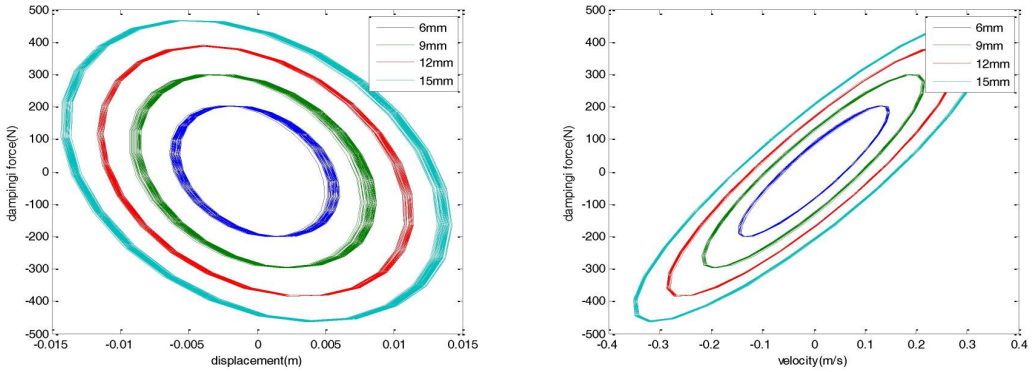

(**a**) Displacement-Damping force plot (4 Hz)

(**b**) Velocity-Damping force plot (4 Hz)

Figure 6.4: Experimental results for the fabricated EM damper subjected to an external harmonic load [9]

- Shows a hysteresis cycle very similar to what is expected based on theory (see for example figure 2.10)
- Is able to handle a sizeable range of excitation frequencies

Such a damper would have to be designed and built based on the theoretical requirements for the energy harvester, if this system were to be implemented in practice. This warrants, however, an entirely different project or thesis. For now, suffice it to say that it should be very well possible to realize such a thing.

6.4.2 Shen

In an earlier section, the basic lay-out of an energy harvesting system was discussed (see figure 6.1). This basic lay-out causes several issues in practice, though. Shen [7] explains that in almost every aspect, the system behaves non-linearly. For example, the damping coefficient and the output voltage are both influenced by how full the power storage device is. This makes optimizing the design - as well as predicting the system's behaviour - very difficult. Another major source of non-linearity is that the system will not always be subjected to the exact same excitation frequency. Even relatively

narrow ranges of frequency will cause the system to leave the linear part of the damping force versus velocity graph.

The overall system performance, however, can definitely be improved upon by making use of power electronics. Shen [7] discusses the positive effect of using a 'performance optimization circuit' - in this case a DC-DC converter that stabilizes the output voltage of the EM damper. The harvester circuitry including this DC-DC converter (a so-called buck-boost converter) can be seen in the figure below.

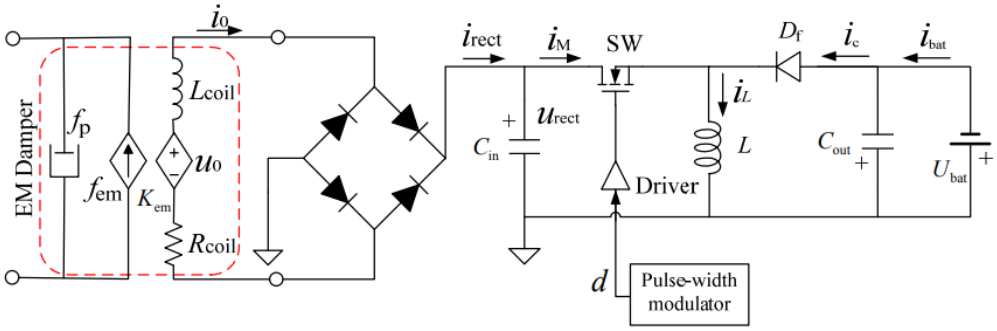

Figure 6.5: A configuration for an energy harvesting circuit, including a buck-boost DC-DC converter [7]

Using experimental results, Shen shows that adding such a converter improves the system efficiency, while also bringing the response of the system closer to that of the ideal linear dashpot that is used in all theoretical models. The experimental plots for the improved circuitry can be seen in the figures below. Judging by these figures, the standard lay-out improved by the proper power electronics does indeed resemble the theoretical dashpot very closely. The hysteresis cycle can be compared to the theoretical cycle shown in figure 2.10, and the damping force is a near-linear function of the damper velocity.

As for the overall energy harvesting system efficiency, Shen shows - using extensive experimental data - that it is highly variable, depending on a lot of factors. The most obvious factor is the excitation load that is applied to the structure, in terms of shape and frequency. Also the exact type of energy harvesting system and how it is fine-tuned has a significant impact. As a rough estimate, an average of 20 to 30% is shown to be reasonable.

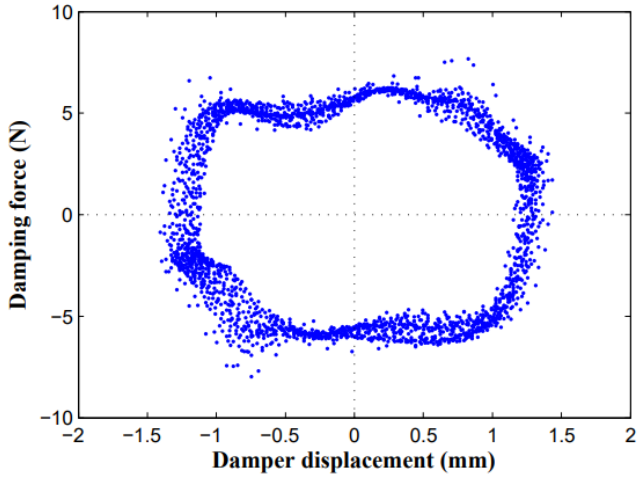

Figure 6.6: The experimental damping force versus displacement plot for the improved circuit [7]

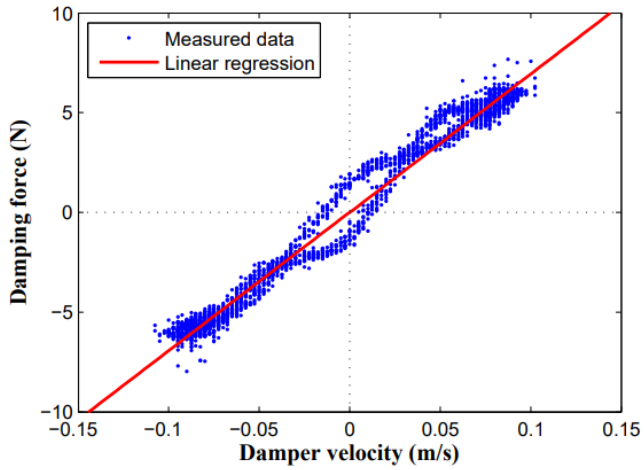

Figure 6.7: The experimental damping force versus damper velocity plot for the improved circuit [7]

6.4.3 Conclusion

Both the papers discussed in this section point in the same direction. It *is* possible, and quite feasible, to design an energy harvester system that

behaves in a way that is close to a perfect theoretical dashpot. However, obtaining such simple (mostly linear) behavior can be quite a challenge. For now, suffice it to say that the possibilities are there, and that achieving the theoretical performance is more than just a pipe dream.

As for the overall efficiency of the energy harvesting system, a very rough estimate will have to suffice. Shen [7] reports highly varying efficiency, but an average value in the order 20 to 30% seems to be the most common. This means that for every Joule of energy that is taken away from the vibrating bridge, about 20 to 30%, will end up in being stored for later use. Overall, Shen's work shows the need for real-life experimentation in the design process.

For this thesis, the following simple rule of thumb will be followed, with $\eta_{system} = 0.25$:

$$E_{harvested\,net} = \eta_{system} E_{harvested\,gross} \tag{6.1}$$

Note that the gross harvested energy is in fact the *theoretical* harvested energy predicted by the models that were used in this thesis.

Chapter 7

Conclusion and Discussion

In this final chapter, conclusions will be drawn about this project's feasibility, and by doing so, the research question will be answered. Also, a discussion will be provided evaluating the process that was followed during this thesis. Finally, a few suggestions for future research and experimentation are given.

7.1 Conclusion

In order to assess the feasibility of harvesting energy from vibrating bridges, we have to consider both the results of the theoretical models (section 5.4) and the outcomes of the investigation into real-world examples (subsection 6.4.3.

In section 5.4, we established that the deck acceleration can (in theory) be limited to acceptable levels. While doing so, about 104 J of (gross) energy can be harvested every time a single person passes the bridges. Note that this remains a rough estimate: no two people walk exactly the same way, let alone the fact that multiple people might be on the bridge at the same time, causing interference. However, let us consider this values of 104 J to be a reasonable estimate.

Based on the conclusions drawn with respect to the real-world application of

energy harvesting systems, we can say that it is definitely possible to design a system that adheres to the theoretical framework that we used for Model 6. Realizing a near-linear relation between dashpot velocity and damping force turns out to be possible by properly designing the electronics. This means that a bridge (including TMD) could be built that behaves as predicted by Model 6, which would then indeed provide the predicted amount of (gross) harvested energy.

Applying the estimate for the overall system efficiency that was discussed in subsection 6.4.3 - namely $\eta_{system} = 0.25$ - we end up with a net value of 26 Joules per person crossing the bridge (let us call this the Net Energy Per Crossing, NEPC).

As a sanity check, we have to ask ourselves whether it makes sense that for a single person crossing the bridge to provide about 2 Watt of net power. According to a study by Starner and Paradiso [32], the power that can be generated using the footfall of an average pedestrian (assuming we utilise the *entire* footfall of about 5 cm) can be calculated to be 67 Watt. Although, as Starner and Paradiso note:

> "The 67W result above is a truly maximum number, in that utilizing the full 5-cm stroke would result in significant additional load on the user (while creating a significant trip hazard); it is like continuously ascending a circa 5° grade, and would result in the feeling of 'walking in sand'. (. . .) A 1-cm stroke, roughly the amount of deflection that one can see in a padded running shoe, can be considered as an upper practical limit that can be tolerated by general users, resulting in maximum of 13W available with full body weight applied."

Note that in this thesis, the loading function $F(t)$ is assumed to be independent of the bridge's response. This implies that the pedestrian does not significantly alter his or her gait while crossing, and thus that he or she is not begin hindered significantly. This assumption is in line with the '1-cm-reasoning' by Starner and Paradiso.

The 13 Watt value mentioned above does *not* take into account the energy efficiency of the harvesting system. Earlier, we assumed $\eta_{system} = 0.25$,

which brings this down to a net value of about 3.2 Watt. Furthermore, the pedestrians would not be walking in-place at midspan, which would be most efficient. Anywhere but at midspan, the reduction factor $\gamma(x)$ has to be applied, reducing the available power even further. Considering these things, the average net harvested power for a person crossing (2 Watt) seems quite realistic.

The total amount of energy that can be harvested in reality, when the bridge is in use, depends on several factors. How often does a 'crossing' occur? And how many people cross the bridge at the same time (on average)?

For a simple order-of-magnitude calculation, some assumptions have to be made. First, let us assume that the bridge is located in a reasonably busy area, where it is in continuous, back-to-back use for 8 hours a day. The crossing time has been estimated earlier as 13.7 seconds; this would mean the bridge is crossed about 2100 times a day. Applying the enhancement factor (EF) of 1.5 assumed earlier means that (as per the definition of this enhancement factor) the accelerations increase by a factor 1.5 as well. Equivalently, we can state that the velocity values - and thus the velocity differential between TMD's mass and the bridge deck - increases by 1.5. Since the amount of energy harvested is proportional to this velocity differential squared, we can apply the following formula to find a rough estimate for the net harvested energy per day (NEPD), given the circumstances described above.

$$\begin{aligned} NEPD &= NEPC \cdot \frac{T_{daily\,use}}{T_{crossing}} \cdot EF^2 \\ &= 1.23 \cdot 10^5 J \end{aligned} \tag{7.1}$$

This value of $1.23 \cdot 10^5$ J can also be written as either 123 kJ, or 0.034 kWh. On a yearly basis, if the assumed foot-traffic is the same every day, this comes down to 12.5 kWh. Using a normal (Dutch, 2019) price of 22 eurocents per kWh, the 'profit' is a rather lackluster €2.75 per year. Unfortunately, we have to conclude that from a purely monetary point of view, there is not a lot to be gained by using an energy harvesting TMD as opposed to a regular TMD.

How can we relate the amount of energy that is being harvested to real-world

applications? An alternative way to look at it is to consider the *power*, rather than the total energy. Under the same assumptions as for equation 7.1, the bridge would be able to provide a continuous 4.3 Watts of power. To get an idea of how much (or how little) that is, consider the following estimations. A small energy-saving LED light-bulb consumes about 4 Watts. A standard fan consumes about 40 Watts. And a standard vacuum cleaner consumes about 1000 Watts. This leaves us with limited options regarding actually utilizing the harvested energy. If the bridge would be averaging a power output of 4.3 Watts while in use, it would be sufficient for some small LEDs being active whenever it is being used. On the other hand, if the power is tapped only 10% of the total usage time, 43 Watts would be available during that time.

The research question that was posed at the beginning of this thesis was the following:

Would it be feasible to build a properly functioning, slender FRP pedestrian bridge that uses energy harvesting techniques to dampen its vibrations?

The answer is that even though damping the vibrations to a suitable level is definitely feasible in practice using a well-designed tuned mass damper, the amount of energy that can be harvested leaves something to be desired. It might serve as an learning example, or a nice novelty, showcasing the omnipresence of energy in all its forms.

The limiting factor turns out to be the relatively low power output of a human that is leisurely walking, as opposed to the much higher energy potential of wind or waves acting on a structure. Especially if the human in question should not feel emburdened by the energy harvesting going on. If the latter were *not* an issue, there would be higher potential. For example, consider the idea of energy-harvesting gym equipment, like the indoor bikes that are being offered by companies such as SportsArt.

Energy harvesting technology has a lot of useful applications. For example, using ambient vibrations can provide plenty of power for sensors and other micro-electronics to function without being connected to the power grid. Or regenerative shock absorption in cars, which can provide reasonable energy savings.

Unfortunately, human power output and power 'intake' (in all of its forms) are simply not in balance. An elite cyclist in the Tour de France might be able to sustain 500 Watts for a few hours. The average person's power consumption when vacuum cleaning is already significantly higher than that - especially when we consider the lights being on, the radio playing, and air conditioning maintaining a comfortable temperature at the same time. Furthermore, in this example we do not even consider the total energy it takes to mine resources, refine them, transport them, make them into a vacuum cleaner, etc. Almost every aspect of modern life requires a lot of energy; a lot more energy than humans could collectively produce using just their bodies.

While initiatives that aim to harness human power that would otherwise be wasted are admirable, we should not overestimate the results of these efforts when compared with society's overall energy demands. Maybe more important than the power regeneration itself is the message that is being sent to consumers: we need to live in a more sustainable way, and this is something *you* can do as well. Hopefully, people will heed this message, but also realize that such initiatives *by themselves* are not sufficient to make our society fully sustainable.

7.2 Discussion

When first planning out this project, I made some assumptions about what would have to be done, and how doable it would be. In this section, I will reflect upon what went according to plan - or even better than expected - and what did not quite work out as well.

Overall, I believe the approach taken was suitable. Starting out with modelling the bridge based on experimental data still seems like the right thing to do. Unfortunately, the limited availability of data proved to be a challenge. For example, the acceleration data was available for 'a person crossing the bridge'. However, what was the exact walking frequency? And how fast did the person move? Solving this required some reverse engineering, which did in fact work out quite well. Unfortunately, this was not possible for the case of multiple people crossing at the same time. Therefore, no conclusive

validation could be provided in that regard.

The SDOF models turned out to be very useful, because they were indeed suited to handle the relatively complicated loading function. Using parametric software (Maple, in this case) allowed for purely analytical solutions for the system's behavior. In hindsight, one could argue that the extremely long analytical expressions that were obtained are no more useful than purely numerical results obtained by, for example, using the state-space approach used for Model 3. However, studying SDOF models and the theory behind it has helped me a lot in getting a feeling for the subject matter, and becoming more familiar with dynamic analysis of systems.

As for the validity of models, it turns out that the usefulness of Model 2 and Model 4 left something to be desired. Model 2 was able to optimize the design in terms of the *equivalent* damping at midspan when adding extra dashpots to the left and the right of the center. However, translating this to a continuous solution was problematic. No one-on-one correspondence was found between Model 2 and Model 4, even with a set value of $x0$.

Model 4 showed the major influence of the distance that the dashpots were placed from both endpoints of the bridge. This added yet another parameter to the optimization process, which became practically speaking very difficult. Another downside of Model 4 was the inability to cope with loading functions other than simple sine functions. All in all, I would conclude that analytical continuous models have limited real-world application: even slight deviations from the simplest case can be tough to deal with. The value such an analysis has over a simple finite element model is questionable.

Models 5 and 6 performed well. They provided flexibility to incorporate the complicated loading function, despite DIANA's lack of moving-load feature for beam elements. I did, however, run into practical problems while modelling. For example, every now and then the license could suddenly not be found, in some cases leading to unsaved work. The MIDAS-FX+ extension, that I had planned on using for pre- and post-processing, turned out to be less user-friendly than one would want - not to mention poorly documented - and in the end I did not use it. Also, extracting the raw data from DIANA was a bit of an issue as well; apparently, only the latest version supports this properly, and the TU Delft version is the second-to-latest. I definitely

underestimated the setbacks that such technical difficulties could have on this project.

As for the optimization process, this turned out to be doable. However, I was forced to make a few more assumptions than I would have liked. Looking back at this project, I am not sure whether that could have been avoided. After all, all evidence points towards the importance of real-life, full-scale testing of the proposed improvements to the bridge. No matter how accurate the theoretical models and loading function that one uses are, in the end it is only an approximation of real life. The entire design process yields no more than a likely starting point for fine-tuning in real-life. The lack of full-scale testing possibilities to validate my models along the way was an issue I underestimated.

The chapter about real-world energy harvesters and how they behave was necessary, I feel, but not easy to write. Talking to a professor of Electrical Engineering convinced me that any design of an electronic system I would be able to come up with - without an extensive background in electrical engineering - would be a gross simplification, at best. I feel like the enormous complexity of designing an electromagnetic energy harvester, including all electrical circuitry and subsystems, is something that was overlooked in the assignment. Speaking for myself, I was admittedly surprised to find that making such a system behave in a simple, near-linear way would be so difficult to do. In the end, I am satisfied with the overview of technical difficulties and possibilities I was able to present, albeit far from in-depth. Again, properly designing and testing the energy harvesting system would be worthy of a thesis in and of itself.

Overall, I am quite satisfied with the conclusions I was able to draw from this thesis. I believe it provides a reasonable theoretical framework for further research, and it outlines what is and what is not possible.

7.3 Further research

As mentioned in the previous section, the theoretical recommendations I came up with are but a starting point for realising an efficient energy har-

vesting bridge. If the Rotterdam municipality would want to pursue the possibilities for this, there are several recommendations I can make as to what work still has to be done.

First of all, an electrical engineer with experience in the field of mechanical-electrical conversion should be consulted. This person could be asked to design all the subsystems mentioned in Chapter 6, and ensure that the desired real-life behaviour is achieved. The scope of such an undertaking is not to be underestimated, however. There is no quick and easy solution.

Once that is done, the bridge and the energy harvesting system could be manufactured. This would require collaboration between the design team and the bridge deck manufacturers. After all, the TMD and all the wiring have to be incorporated into the bridge deck. This should, however, not be too much of an issue; in this case, simply leaving a hole with a diameter of around 10 cm in at midspan should be sufficient to fit the TMD.

Thirdly, the manufactured bridge - including railings and the TMD - should be tested in a controlled environment. Ideally, the bridge should be loaded by means of a force-controlled actuator in the middle, emulating the footfall loads in the manner described in this thesis. Once it has been determined that the bridge is safe, it can be tested in practice. This could either be done by experimentation with volunteers - as described in [16], for example - or by placing the bridge in its intended location and attaching an accelerometer to the midspan deck and the TMD. After a few weeks of use, those data could be collected and used to validate and/or improve the theoretical model. If needed, the TMD could then be fine-tuned to improve the bridge's behaviour. In case in-situ testing over a couple of weeks is chosen, care should be taken to find a way to evaluate not only the deck's acceleration levels over that time, but also the subjective experiences of people using the bridge.

Finally, another person should be asked to come up with a nice and/or useful way of actually using the energy that is being harvested. This should not be too difficult engineering-wise, but it would require experience in a field that also focuses on human perception of technology.

As for future possibilities; energy harvesting from 'useless' mechanical energy is a relatively new field, that is still being developed by scientists and

engineers all over the world. More and more real-life applications are being developed, at scales both small (e.g. sensors) and medium (e.g. regenerative breaking in cars). Larger scale options are currently being investigated. For example, using a regenerative tuned-mass damper system in high-rise buildings or in suspension cables of large bridges seems very promising. Over the lifetime of a skyscraper, a large amount of energy could be harvested this way.

Bibliography

[1] Wikipedia. https://upload.wikimedia.org/wikipedia/commons/f/f5/Rotterdam_noordsingel_burg_roosbrug.jpg. Accessed: 04-06-2019.

[2] "Made in mechelen." http://www.madeinmechelen.be/wp-content/uploads/2017/08/brug-759x500.jpg. Accessed: 04-06-2019.

[3] "Bws berleburger." https://www.berleburger.com/fileadmin/contents/bilder/portal_trittschalldaemmung-schwingi/inhaltsbilder/schwingungsisolierung_maschine/single-degree-of-freedom-system1.jpg. Accessed: 05-06-2019.

[4] Wikipedia. https://upload.wikimedia.org/wikipedia/commons/thumb/f/fd/Damping_1.svg/1280px-Damping_1.svg.png. Accessed: 22-05-2019.

[5] "Diana fea user manual, 4.8.2 - l6ben." https://dianafea.com/manuals/d944/ElmLib/node80.html. Accessed: 14-09-2019.

[6] "Diana fea user manual, 7.8.1.2 - sp2tr." https://dianafea.com/manuals/d96/Theory/node82.html. Accessed: 15-09-2019.

[7] W. Shen, "Electromagnetic damping and energy harvesting devices in civil structures." PhD thesis, Hong Kong Polytechnic University, 2014.

[8] e. a. Zhang, Y., "Electro-hydraulic damper for energy harvesting suspension: Modeling, prototyping and experimental validation." https://www.researchgate.net/publication/316818311_Electro-hydraulic_damper_for_energy_harvesting_suspension_

Modeling_prototyping_and_experimental_validation, 2017. Accessed: 26-11-2019.

[9] K. I. Jung, H. and H. Jung, "Feasibility study of the electromagnetic damper for cable structures using real-time hybrid simulation." https://www.ncbi.nlm.nih.gov/pmc/articles/PMC5713016/, 2017. Accessed: 26-11-2019.

[10] C. Heinemeyer and M. Feldmann, "European design guide for footbridge vibration." Footbridge Conference, 2008. Accessed: 05-06-2019.

[11] K. Blom and W. Schutte, *Test evaluation Exercitiebrug*. Rotterdam municipality internal report, 2016.

[12] C. Heinemeyer, "Design of lightweight footbridges for human induced vibrations." JRC Scientific and Technical Reports, 2009.

[13] H. Bachmann, "Vibration problems in structures: practical guidelines." Birkhäuser Verlag, 1995.

[14] J. Spijkers, A. Vrouwenvelder, and E. Klaver, "Structural dynamics ct 4140, part 1 - structural vibrations." TU Delft course material, 2005. Accessed: 05-06-2019.

[15] D. Inman, *Engineering Vibrations*. Pearson Education, 2009.

[16] M. Sousamli, "Dynamic behavior of slender footbridges due to human-induced vibrations." Master Thesis, TU Delft, Civil Engineering, 2016.

[17] J. Bertram, "Constrained optimization in human walking: cost minimization and gait plasticity." The Journal of Experimental Biology 208, 979-991, Published by The Company of Biologists, 2005. Accessed: 05-06-2019.

[18] NPTEL, "Energy dissipated by damping." https://nptel.ac.in/courses/101105022/m8l14.pdf. Online lecture series on Aerospace Structural Dynamics. Accessed: 05-06-2019.

[19] J. Connor and S. Laflamme, *Structural Motion Engineering*. Springer International Publishing, 2014.

[20] "Wikipedia - state space representation." https://en.wikipedia.org/wiki/State-space_representation. Accessed: 10-09-2019.

[21] "Diana fea user manual, 13.4.1 - pt3t." https://dianafea.com/manuals/d944/ElmLib/node439.html. Accessed: 15-09-2019.

[22] "Prince engineering - fiber reinforced polymers characteristics and behaviors." https://www.build-on-prince.com/fiber-reinforced-polymers.html. Accessed: 15-09-2019.

[23] F. Europe, "Infracore inside - ontwerp en eigenschappen." Customer information, 2014.

[24] C. e. a. Caprani, "Enhancement factors for the vertical response of footbridges subjected to stochastic crowd loading." https://arrow.tudublin.ie/cgi/viewcontent.cgi?article=1032&context=engschcivart, 2012. Accessed: 8-2-2020.

[25] S. M. Grundmann H, Kreuzinger H, "Dynamic calculations of footbridges." Bauingenieur 68, 215–225, 1993.

[26] "Seismic dampers – types, working mechanism, and components." https://theconstructor.org/earthquake/seismic-dampers/8332/. Accessed: 26-11-2019.

[27] Wikipedia, "Faraday's law of induction." https://en.wikipedia.org/wiki/Faraday\%27s_law_of_induction. Accessed: 26-11-2019.

[28] S. Edelstein, "Audi regenerative shock absorber recaptures energy." https://www.greencarreports.com/news/1105548_audi-regenerative-shock-absorber-recaptures-energy, 2016. Accessed: 26-11-2019.

[29] e. a. Rome, L.C., "Generating electricity while walking with loads." http://courses.washington.edu/biomechs/homework/Rome.pdf, 2005.

[30] "Battery university - how does a supercapacitor work?." https://batteryuniversity.com/learn/article/whats_the_role_of_the_supercapacitor, 2019. Accessed: 3-12-2019.

[31] "Battery universe blog - how long should batteries last?." https://www.batteryuniverse.com/blog/tags/cycle-life/, 2017. Accessed: 3-12-2019.

[32] T. Starner and J. Paradiso, "Human generated power for mobile electronics." https://www.researchgate.net/publication/239722229_Human_Generated_Power_for_Mobile_Electronics, 2003. Accessed: 19-04-2020.

Appendix A

Verification Process and Results

This appendix shows the verification results for all the models that were used.

In the following table, an overview of all the models that were developed is shown. This includes the limitations on loading conditions, which made verification more tricky.

Table A.1: Overview of all models, including loading limitations

Model	Type	Description	Loading conditions
1	SDOF; analytical	Basic bridge deck	Any
2	SDOF; analytical	Deck + extra dashpot	Any
3	2-DOF; numerical	Deck + TMD	Any
4	Cont.; analytical	Deck + extra dashpots	Sine at mid-span
5	Cont.; FEM	Deck + extra dashpots	Any (stationary) load
6	Cont.; FEM	Deck + TMD at midspan	Any (stationary) load

Verification – part 1

Modelling just the bridge deck, with the following properties:

c_deck=340
m_deck=1606
f_walk=11/(2*pi)=1.75 Hz
F_static=95*9.81=932 N

Response (acceleration) to Bachmann crossing loading is obtained for different models.

Model 1 (Maple):
a_max=3.9 m/s^2

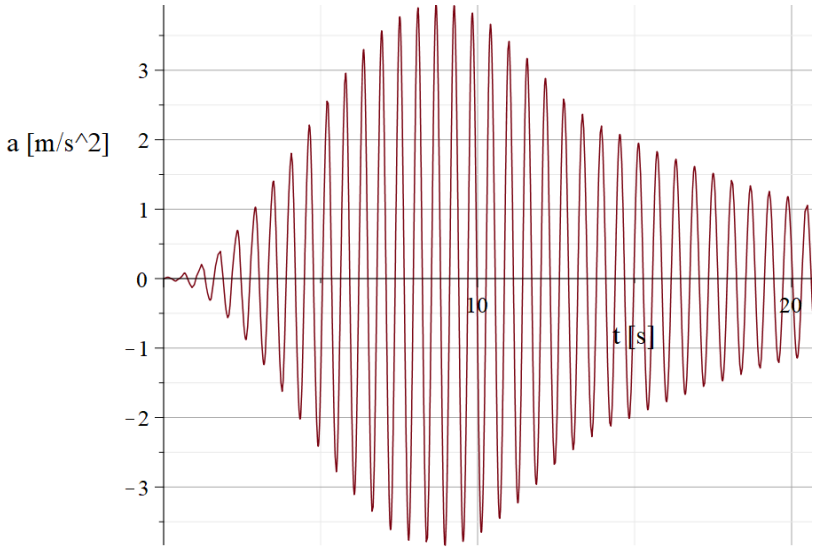

Model 3 (Matlab) – note that for verification purposes, mass ratio is chosen as approaching 0.
a_max=3.8 m/s^2

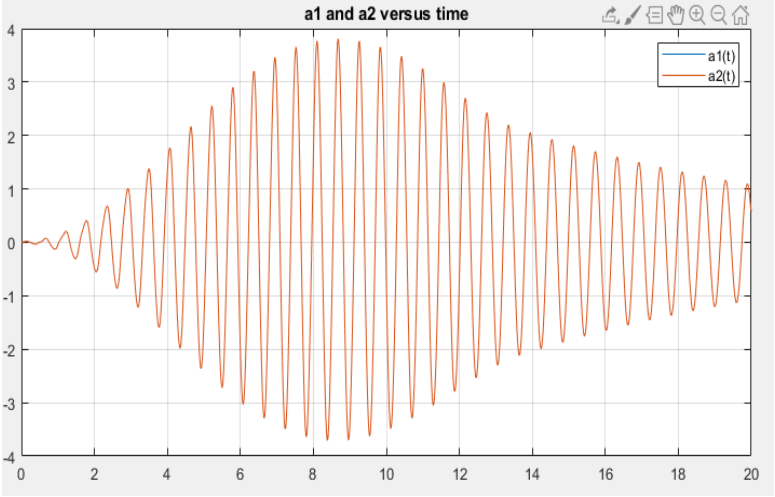

Model 1 using DIANA:

a_max=3.8 m/s^2

Note: at first, the wrong loading function was used, which gave the wrong a(t). This is fixed now.
Note 2: when using a delta T of 0.05 seconds, the a_max is about 2.3 m/s^2. When using delta T of 0.01 seconds, a_max is correct!

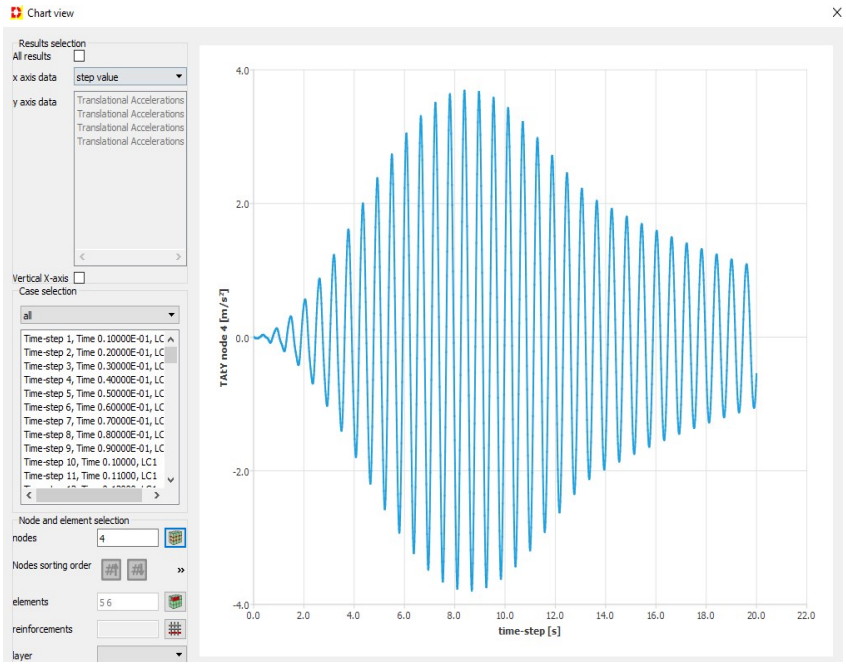

Verification – part 2

Modelling the bridge deck including TMD, with the following properties:

c_deck=340
m_deck=1606
f_walk=11/(2*pi)=1.75 Hz
F_static=95*9.81=932 N ← *note that 95 kg is used here!*

mass_ratio=0.02
c_TMD=200

Response (acceleration) to Bachmann crossing loading is obtained for different models. Note that "a1" is the acceleration of the bridge deck.

Model 3 (Matlab):
a1_max= 2.4 m/s^2
a2_max= 4.4 m/s^2

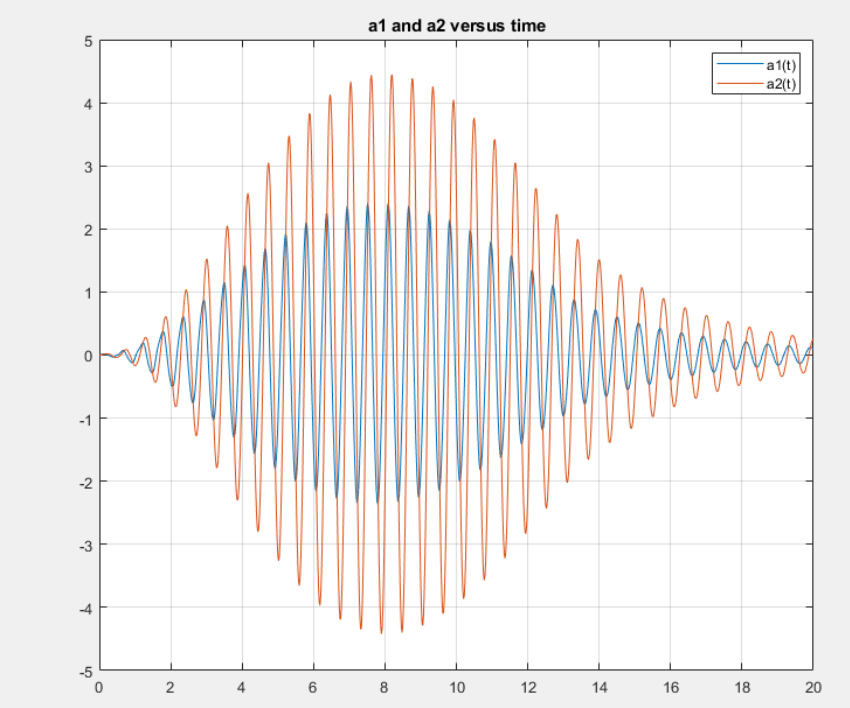

Model 3 (using DIANA):

a1_max= 2.4 m/s^2

a2_max= 4.4 m/s^2

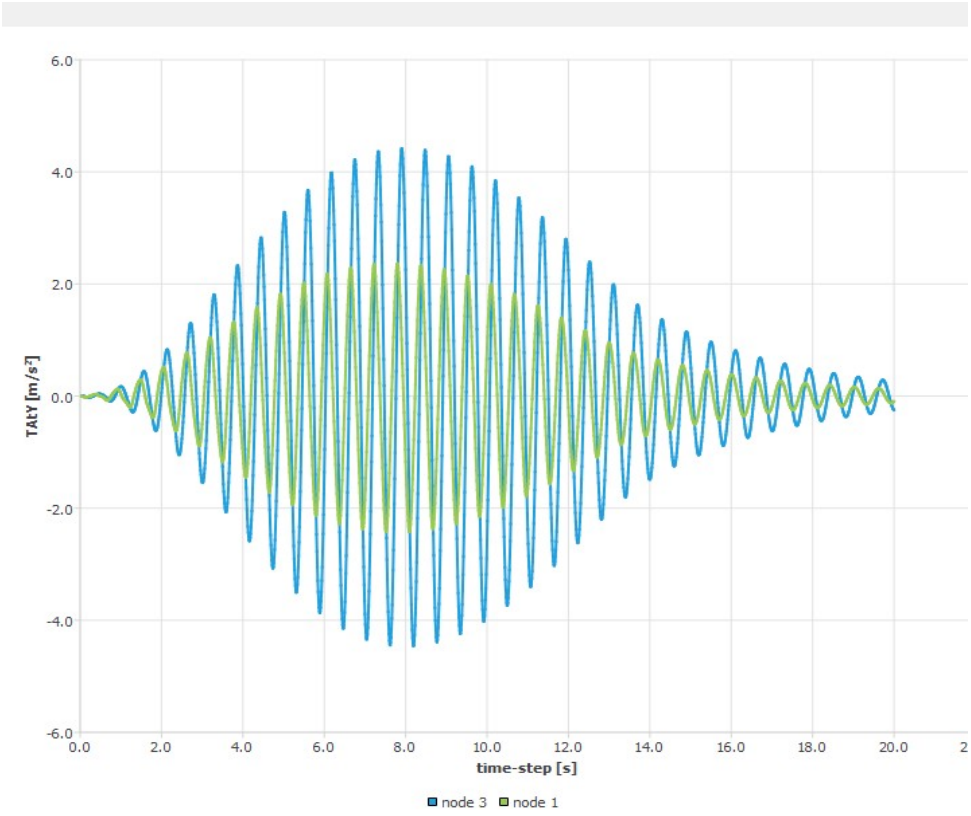

Verification – part 3

Modelling the bridge as a continuous system, consisting of the deck and added dashpots to the left and right. The following properties are used:

omega_walk=11 rad/s
f_walk=11/(2*pi)=1.75 Hz
F_static (= P0) = 75*9.81=736 N ← *note that 75 kg is used here!*
*P(t)=P0*sin(omega_walk*t)*

x0 =3 m
*EI = 2.58*10^7 Nm^2*
m_bar=182 kg/m
k_dashpot=0
c_dashpot=1000

Response (acceleration) to a simple sine load P(t) is obtained for different models. Maximum acceleration in steady state is considered in the FEA model (i.e. $t \rightarrow \infty$)

Model 4 – continuous model using Maple
a_max(x=x0) = 1.5 m/s^2
a_max(x=L/2) = 3.1 m/s^2

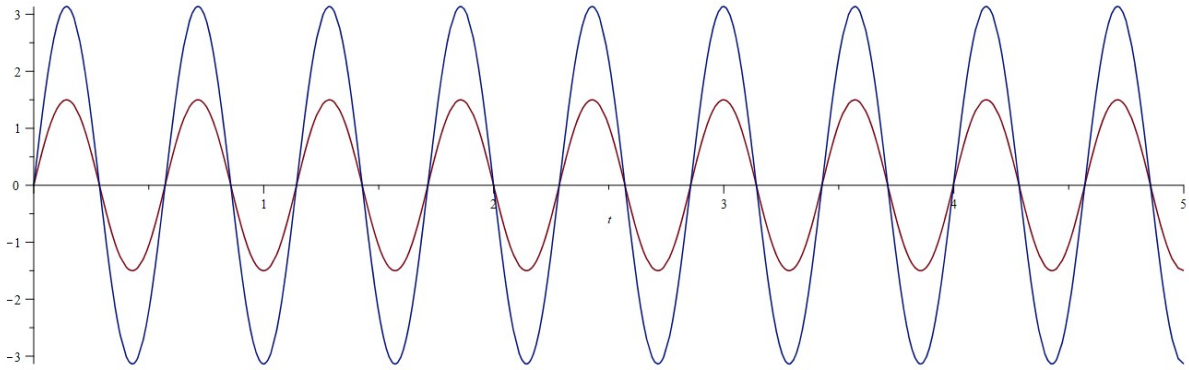

Model 5 – continuous model using DIANA

a_max(x=x0) = 1.4 m/s^2 ← once steady state has been reached!
a_max(x=L/2) = 3.0 m/s^2 ← ,, ,, ,, ,, ,,

Full solution (including transient response):

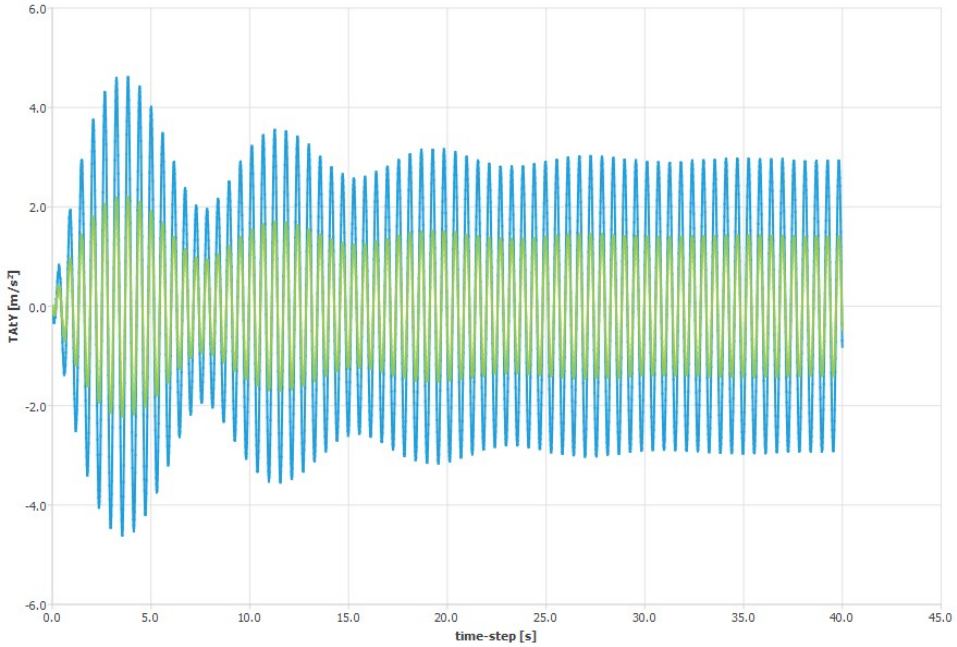

Steady-state part:

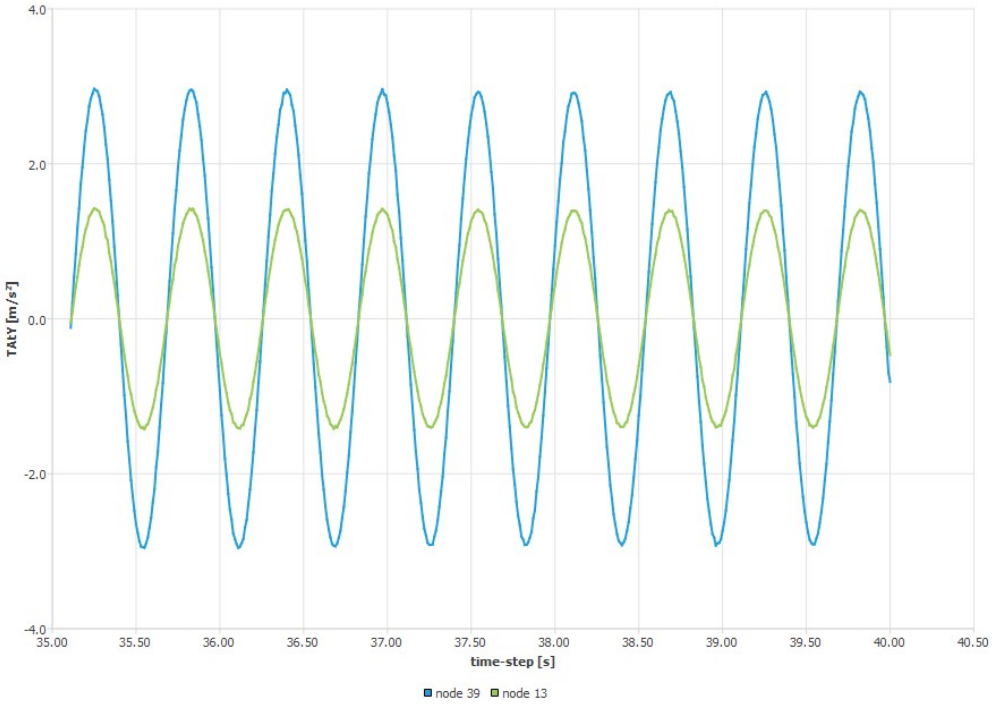

Verification – Conclusions

Model	Type	Software	How was it verified?	Verification ok?
1	SDOF; analytical	Maple	Compared to DIANA SDOF, and to experimental data	Near-perfect match with DIANA SDOF. Good match with experimental results.
2	SDOF; analytical	Maple	Compared to Model 1. Expect lower acceleration for non-zero c_harv.	Only compared to Model 1. Behaves as expected.
3	2-DOF; numerical	Matlab	Compared to DIANA 2-DOF.	Near-perfect match.
4	Continuous; analytical	Maple	Compared to DIANA (Model 5)	Very good match – slight difference may be caused by the curved deck in DIANA.
5	Continuous; numerical	DIANA	Compared to analytical (Model 4) using a simple sine load.	Very good match.
6	Continuous; numerical	DIANA	-	-

Model 1: ok!
Model 2: ok? Doesn't seem to warrant separate verification.
Model 3: ok!
Model 4: ok!
Model 5: no way to verify for complex loading. Do I need to address this? And if so, how? Ideally, this could be done using a prototype.
Model 6: no way to verify this, as far as I can tell.

Appendix B

DIANA Command File

The following shows the DIANA command file (`.dcf`) for the structural non-linear analysis that was performed on the final design (Model 6). This includes (amongst others) defining the desired time step size and the sources of non-linearity, as well as specifying the desired output.

```
*NONLIN LABEL="Structural nonlinear"
  BEGIN TYPE
    PHYSIC OFF
    GEOMET
    BEGIN TRANSI
      METHOD NEWMAR
      DYNAMI DAMPIN
      TIMEDE
    END TRANSI
  END TYPE
  BEGIN EXECUT
    TIME STEPS EXPLIC SIZES 0.0200000(1000)
    ITERAT METHOD NEWTON
  END EXECUT
  SOLVE PARDIS
  BEGIN OUTPUT
```

```
    TEXT "Output"
    BINARY
    SELECT STEPS ALL /
    DISPLA TOTAL TRANSL GLOBAL
    VELOCI TOTAL TRANSL GLOBAL
    ACCELE TOTAL TRANSL GLOBAL
    ELMFOR DAMPIN TRANSL
  END OUTPUT
*END
```

Appendix C

DIANA Input File

The following shows the DIANA input data file (`.dat`) that was used for the final model. This includes (amongst other things) element types, overall geometry, and material properties. The list of load factors for each time-step has been omitted, since it would be 15 pages of numbers representing the proper loading function.

```
: Diana Datafile written by Diana 10.2
'DIRECTIONS'
   1   1.00000E+00   0.00000E+00   0.00000E+00
   2   0.00000E+00   1.00000E+00   0.00000E+00
   3   0.00000E+00   0.00000E+00   1.00000E+00
'MODEL'
DIMENS "2D"
GRAVDI 2
GRAVAC  -9.81000E+00
'COORDINATES'
   1   9.52000E+00   0.00000E+00   0.00000E+00
   2   9.52000E+00   4.16000E-01   0.00000E+00
   3   1.90400E+01   0.00000E+00   0.00000E+00
   4   0.00000E+00   0.00000E+00   0.00000E+00
   5   2.49917E-01   2.15548E-02   0.00000E+00
```

6	4.99882E-01	4.25402E-02	0.00000E+00
7	7.49895E-01	6.29559E-02	0.00000E+00
8	9.99954E-01	8.28013E-02	0.00000E+00
9	1.25006E+00	1.02076E-01	0.00000E+00
10	1.50020E+00	1.20780E-01	0.00000E+00
11	1.75039E+00	1.38912E-01	0.00000E+00
12	2.00062E+00	1.56473E-01	0.00000E+00
13	2.25089E+00	1.73461E-01	0.00000E+00
14	2.50120E+00	1.89877E-01	0.00000E+00
15	2.75154E+00	2.05720E-01	0.00000E+00
16	3.00192E+00	2.20989E-01	0.00000E+00
17	3.25233E+00	2.35685E-01	0.00000E+00
18	3.50278E+00	2.49808E-01	0.00000E+00
19	3.75326E+00	2.63356E-01	0.00000E+00
20	4.00377E+00	2.76330E-01	0.00000E+00
21	4.25431E+00	2.88729E-01	0.00000E+00
22	4.50487E+00	3.00553E-01	0.00000E+00
23	4.75547E+00	3.11802E-01	0.00000E+00
24	5.00608E+00	3.22475E-01	0.00000E+00
25	5.25673E+00	3.32573E-01	0.00000E+00
26	5.50739E+00	3.42095E-01	0.00000E+00
27	5.75807E+00	3.51041E-01	0.00000E+00
28	6.00878E+00	3.59411E-01	0.00000E+00
29	6.25950E+00	3.67204E-01	0.00000E+00
30	6.51024E+00	3.74420E-01	0.00000E+00
31	6.76100E+00	3.81060E-01	0.00000E+00
32	7.01177E+00	3.87123E-01	0.00000E+00
33	7.26256E+00	3.92609E-01	0.00000E+00
34	7.51335E+00	3.97517E-01	0.00000E+00
35	7.76416E+00	4.01849E-01	0.00000E+00
36	8.01498E+00	4.05603E-01	0.00000E+00
37	8.26580E+00	4.08780E-01	0.00000E+00
38	8.51663E+00	4.11379E-01	0.00000E+00
39	8.76747E+00	4.13401E-01	0.00000E+00
40	9.01831E+00	4.14845E-01	0.00000E+00
41	9.26916E+00	4.15711E-01	0.00000E+00
42	9.77084E+00	4.15711E-01	0.00000E+00
43	1.00217E+01	4.14845E-01	0.00000E+00

```
  44   1.02725E+01   4.13401E-01   0.00000E+00
  45   1.05234E+01   4.11379E-01   0.00000E+00
  46   1.07742E+01   4.08780E-01   0.00000E+00
  47   1.10250E+01   4.05603E-01   0.00000E+00
  48   1.12758E+01   4.01849E-01   0.00000E+00
  49   1.15266E+01   3.97517E-01   0.00000E+00
  50   1.17774E+01   3.92609E-01   0.00000E+00
  51   1.20282E+01   3.87123E-01   0.00000E+00
  52   1.22790E+01   3.81060E-01   0.00000E+00
  53   1.25298E+01   3.74420E-01   0.00000E+00
  54   1.27805E+01   3.67204E-01   0.00000E+00
  55   1.30312E+01   3.59411E-01   0.00000E+00
  56   1.32819E+01   3.51041E-01   0.00000E+00
  57   1.35326E+01   3.42095E-01   0.00000E+00
  58   1.37833E+01   3.32573E-01   0.00000E+00
  59   1.40339E+01   3.22475E-01   0.00000E+00
  60   1.42845E+01   3.11802E-01   0.00000E+00
  61   1.45351E+01   3.00553E-01   0.00000E+00
  62   1.47857E+01   2.88729E-01   0.00000E+00
  63   1.50362E+01   2.76330E-01   0.00000E+00
  64   1.52867E+01   2.63356E-01   0.00000E+00
  65   1.55372E+01   2.49808E-01   0.00000E+00
  66   1.57877E+01   2.35685E-01   0.00000E+00
  67   1.60381E+01   2.20989E-01   0.00000E+00
  68   1.62885E+01   2.05720E-01   0.00000E+00
  69   1.65388E+01   1.89877E-01   0.00000E+00
  70   1.67891E+01   1.73461E-01   0.00000E+00
  71   1.70394E+01   1.56473E-01   0.00000E+00
  72   1.72896E+01   1.38912E-01   0.00000E+00
  73   1.75398E+01   1.20780E-01   0.00000E+00
  74   1.77899E+01   1.02076E-01   0.00000E+00
  75   1.80400E+01   8.28013E-02   0.00000E+00
  76   1.82901E+01   6.29559E-02   0.00000E+00
  77   1.85401E+01   4.25402E-02   0.00000E+00
  78   1.87901E+01   2.15548E-02   0.00000E+00
'MATERI'
   1 NAME   "FRP_bridge_deck_incl_rayleigh"
     MCNAME MCSTEL
```

```
     MATMDL ISOTRO
     ASPECT RAYDAM
     POISON   2.00000E-01
     YOUNG    4.00000E+10
     DENSIT   1.67000E+03
     RAYLEI   1.63000E-01   3.92000E-04
   3 NAME   "TMD_dummy_material_5"
     RAYLEI   0.00000E+00   0.00000E+00
     MCNAME MASSEL
     MATMDL POINTM
     MASS     3.25000E+01   3.25000E+01   3.25000E+01
   4 NAME   "dashpot_material_new"
     MCNAME SPRING
     MATMDL LINETR
     DAMP     2.50000E+01
     SPRING   3.58000E+03
'GEOMET'
   1 NAME   "deck_geom"
     GCNAME LINE
     GEOMDL CLS1B2
     CROSSE   1.01400E-01
     INERTI   6.45000E-04
'ELEMENTS'
SET  "Point body 4"
CONNECT
   1 PT3T   1
MATERIAL 3
SET  "deck"
CONNECT
   2 L6BEN  4 5
   3 L6BEN  5 6
   4 L6BEN  6 7
   5 L6BEN  7 8
   6 L6BEN  8 9
   7 L6BEN  9 10
   8 L6BEN  10 11
   9 L6BEN  11 12
  10 L6BEN  12 13
```

```
11 L6BEN  13 14
12 L6BEN  14 15
13 L6BEN  15 16
14 L6BEN  16 17
15 L6BEN  17 18
16 L6BEN  18 19
17 L6BEN  19 20
18 L6BEN  20 21
19 L6BEN  21 22
20 L6BEN  22 23
21 L6BEN  23 24
22 L6BEN  24 25
23 L6BEN  25 26
24 L6BEN  26 27
25 L6BEN  27 28
26 L6BEN  28 29
27 L6BEN  29 30
28 L6BEN  30 31
29 L6BEN  31 32
30 L6BEN  32 33
31 L6BEN  33 34
32 L6BEN  34 35
33 L6BEN  35 36
34 L6BEN  36 37
35 L6BEN  37 38
36 L6BEN  38 39
37 L6BEN  39 40
38 L6BEN  40 41
39 L6BEN  41 2
40 L6BEN  2 42
41 L6BEN  42 43
42 L6BEN  43 44
43 L6BEN  44 45
44 L6BEN  45 46
45 L6BEN  46 47
46 L6BEN  47 48
47 L6BEN  48 49
48 L6BEN  49 50
```

```
  49 L6BEN  50 51
  50 L6BEN  51 52
  51 L6BEN  52 53
  52 L6BEN  53 54
  53 L6BEN  54 55
  54 L6BEN  55 56
  55 L6BEN  56 57
  56 L6BEN  57 58
  57 L6BEN  58 59
  58 L6BEN  59 60
  59 L6BEN  60 61
  60 L6BEN  61 62
  61 L6BEN  62 63
  62 L6BEN  63 64
  63 L6BEN  64 65
  64 L6BEN  65 66
  65 L6BEN  66 67
  66 L6BEN  67 68
  67 L6BEN  68 69
  68 L6BEN  69 70
  69 L6BEN  70 71
  70 L6BEN  71 72
  71 L6BEN  72 73
  72 L6BEN  73 74
  73 L6BEN  74 75
  74 L6BEN  75 76
  75 L6BEN  76 77
  76 L6BEN  77 78
  77 L6BEN  78 3
MATERIAL 1
GEOMETRY 1
SET  "TMD_spring_dashpot"
CONNECT
  78 SP2TR  2 1
MATERIAL 4
'LOADS'
CASE 1
NAME "Geometry load case 1"
```

```
NODAL
2    FORCE  2  -7.36000E+02
'SUPPOR'
NAME "Geometry support set 1"
/ 3 4 / TR 2
4    TR 1
'TIMELO'
LOAD 1

[Omitted table of load factor for every single timestep]

'END'
```